Imperial College London

Centre for Doctoral Training in
Theory and Simulation of Materials
&
Department of Materials

Instabilities of High Speed Dislocations

Jonas Verschueren

December 2018

Supervisors

Prof. Daniele Dini

Dr. Daniel S. Balint

Prof. Adrian P. Sutton FRS

Submitted in part fulfilment of the requirements for the
degree of Doctor of Philosophy of Imperial College London
and the Diploma of Imperial College

The copyright of this thesis rests with the author. Unless otherwise indicated, its contents are licensed under a Creative Commons Attribution-Non Commercial 4.0 International Licence (CC BY-NC).

Under this licence, you may copy and redistribute the material in any medium or format. You may also create and distribute modified versions of the work. This is on the condition that: you credit the author and do not use it, or any derivative works, for a commercial purpose.

When reusing or sharing this work, ensure you make the licence terms clear to others by naming the licence and linking to the licence text. Where a work has been adapted, you should indicate that the work has been changed and describe those changes.

Please seek permission from the copyright holder for uses of this work that are not included in this licence or permitted under UK Copyright Law.

I hereby declare that this thesis and the ideas reported herein are original work. Information derived from the published and unpublished work of others has been acknowledged appropriately and references are given in the bibliography.

Jonas Verschueren,

December 2018

Acknowledgements

First and foremost I would like to thank my supervisors Daniele, Daniel and Adrian for their invaluable support and guidance throughout my PhD research project. The balance they struck between letting me run with wild ideas and keeping me on a path that would one day allow me to write this thesis was an absolutely crucial part of the process.

A special mention should go to my collaborator and colleague Beñat. His insights, founded on an understanding of the relevant and wider literature second to none, were extremely valuable to me. Thank you for being so generous with your time.

Finally, I would like to thank all my friends and family for their unwavering support, encouragement and patience.

To Elle, the absolute best.

Abstract

Despite numerous theoretical and computational works, a clear understanding of dislocations travelling at speeds comparable to those of the speed of sound of the material is lacking. In this thesis, a lattice dynamics model of uniformly moving dislocations is derived and used to uncover the existence of mechanical instabilities at characteristic dislocation speeds. These instabilities are shown to emanate from resonances in the atomic interactions between the dislocation and the lattice vibrations at material-dependent dislocation velocities. We then go on to explain how these resonances may be the onset for an atomistic kinematic generation mechanism, applicable to gliding edges as well as screws. The existence of these instabilities and subsequent kinematic generation mechanism are confirmed in equivalent molecular dynamics simulations of realistic metals. Since resonances are observed to be excited at dislocation speeds far below the shear wave speed of the material, kinematic generation may be more important than previously assumed in moderate and high strain rate phenomena including adiabatic shear banding and industrially relevant processes such as machining, forging and wear.

Contents

Abstract **6**

1 Introduction **10**

2 Literature review **16**

2.1 Historical perspective 19

2.2 Continuum models of gliding dislocations 21

2.2.1 The uniformly moving Volterra dislocation 21

2.2.2 Dynamics of dislocations and special relativity 23

2.2.3 Breakdown of the small strain approximation 25

2.2.4 Kinematic generation 27

2.2.5 Introducing atomic effects 29

2.2.6 Beyond the Peierls-Nabarro model 33

2.2.7 Elastodynamic models 34

2.2.8 Continuum models of gliding dislocations: the verdict . 37

2.3 Dislocation Mobility 38

2.4 Atomistic models of gliding dislocation 41

2.4.1 Lattice dynamics models 41

2.4.2 Molecular dynamics simulations 44

2.4.3 Atomistic models of gliding dislocations: the verdict . . 49
2.5 Conclusion 50

3 The lattice dynamics method 52
3.1 Elements of Green's function theory 52
3.1.1 Time-independent theory 53
3.1.2 Time-dependent Green's functions 54
3.1.3 Green's functions as fundamental solutions 56
3.2 The lattice Green's function 58
3.2.1 Lattice periodicity and Fourier series 58
3.2.2 The harmonic approximation 61
3.2.3 The lattice Green's function 62
3.3 The Kanzaki force 65
3.4 Uniformly moving dislocations in lattice dynamics models . . . 69

4 Modern lattice models 73
4.1 Evaluating the lattice dispersion relation 73
4.1.1 Force evaluations for tabulated EAM potentials 76
4.2 The Kanzaki force distribution 77

5 Results 80
5.1 The simple cubic lattice 81
5.2 Uniformly moving dislocations in real crystals. 87
5.2.1 Gliding dislocations in tungsten 87

5.2.2 Gliding dislocations in aluminium 95
5.3 Revisiting kinematic generation and supersonic dislocations . . 96

6 Conclusions & future work **101**

Bibliography **107**

List of Figures **126**

A Publications resulting from this work **132**

B Copyright permissions **133**

1 Introduction

By and large, materials research is the scientific pursuit for better or completely new materials that enable new technologies and applications. Throughout history, progress in materials technologies has proven to be instrumental in advancing human development and civilisation: From the early steps in metallurgy that catapulted humanity into the bronze and iron ages to the silicon technologies that brought us into the digital age. Today, materials research remains a key part in solving some of the biggest problems of our time such as climate change [1, 2] or providing potable water for the ever increasing human population [3].

Although metallurgy is one of the oldest fields in materials science, it remains very much a key topic in modern science and engineering for two reasons; Firstly, there is a huge industrial interest to develop newer and better applications such as next generation jet engines [4]. Secondly, metals physics is a highly active research field as fundamental questions, such as the famous work hardening problem [5, 6], remain unanswered. The two go hand in hand as a better fundamental understanding of the physical laws governing a material's property may eventually lead to ways of fine-tuning the material or even design novel ones to suit one's needs.

One of the most interesting properties of metals, from both a fundamen-

tal research as well as an industrial perspective, is their ability to be shaped and worked, i.e. their plastic behaviour [7, 8]. This plastic deformation of metals is achieved through the movement and propagation of defects through the crystal [5]. These lattice defects are irregularities, where the atoms occupy positions different from the lattice sites, and include point defects, grain boundaries and dislocations [5, 6]. Although they all play their role in material deformation, dislocations are the key actors and carriers of plasticity in metals [6, 9]. They are therefore of great interest in the metallurgy industry as well academic fundamental research.

Driven by a common desire for a better understanding of the physical processes that govern metal plasticity, many experimental, theoretical and computational investigations into the dynamic properties of dislocations have been carried out since their discovery in 1934 [10–12] (cf. chapter 2). Broadly speaking, the field that occupies itself with investigating the movement of dislocations is subdivided into two research areas. When dislocations travel slowly their motion is governed by their ability to overcome a finite potential barrier, the Peierls barrier [13]. This is achieved through statistical fluctuations in the kinetic energy of the constituent atoms which are ultimately determined by the materials' temperature [6]. This regime is therefore called the *thermally activated regime* [14, 15]. On the other hand, when dislocations travel at speeds which are a significant fraction of the speeds of sound in a material and above, the Peierls barrier is overcome with ease and is no longer a significant obstacle [6]. These high speed dislocations can propagate

through the material freely - in the absence of other obstacles - and this regime is therefore called the *pure glide regime*. In this thesis we will only concern ourselves with the latter.

However, even though research into high speed dislocation dynamics has been ongoing for almost 70 years, we still can not unequivocally answer the rather fundamental question:

How do high speed dislocations move through a crystalline material?

Two questions in particular have tormented researchers in the field since its inception. Debate on the possibility that dislocations may travel faster than the speed of sound in a material has been ongoing ever since the question was first put forward in 1949 [16, 17]. Although this topic may seem rather abstract, it demonstrates clearly the uncertainty surrounding the phenomenology associated with gliding dislocations that persists to this day. The second question that researchers in the field have attempted to answer is: What is relationship between the force on a gliding dislocation and its resulting velocity? This relationship, called the *dislocation mobility* [18], not only captures our quantitative understanding of the dynamic properties of dislocations but is also a key part of *discrete dislocation dynamics* simulations [18, 19]. It may rightfully be asked whether the formulation of mobility laws is not premature given that there is no qualitative agreement in the field on how a dislocation should behave at these velocities, as the aforementioned debate surrounding limiting velocities for dislocations illustrates.

Despite numerous research endeavours to provide answers to these two questions and advance our understanding of the dynamics of gliding dislocations, uncertainty is rife. This will be discussed at length in chapter 2. This is first and foremost due to an absence of clear experimental observation of dislocations at these velocities. It may be undrstood that generating and tracking dislocations at speeds of kilometres per second in samples is technically challenging. This has left progress in the field at the mercy of theoretical models and computational simulations. However, as will be made abundantly clear in chapter 2, these works are both flawed in their own way. Ultimately, this has hampered high speed dislocation research to the extent that questions that were posed when the field was established in 1949 [16, 17] remain open up to this day.

Finding answers to these rather fundamental open issues is more than just a matter of scientific pride. These high speed dislocations may actually be found in many real-life and industrial applications in which the loading and strain rates a material will be subjected to are high enough to generate gliding dislocations. Examples of such processes are wear [20], forging [8] and machining [7]. They may also play an important role in moderate and high strain rate phenomena such as adiabatic shear banding [21], dynamic fracture [22, 23], and in describing the Hugoniot state under ramp and shock loading [24, 25].

In this work I will defend the thesis that instabilities of high speed dislocations, caused by resonances in the interaction between lattice vibrations and

gliding dislocations, may be much more relevant than previously thought. To set the scene, a comprehensive literature study of the field of the dynamics of gliding dislocations will be offered in the next chapter. In this review, possible reasons will be offered to explain why so much uncertainty remains around rather fundamental questions in the field. More specifically, continuum and atomic scale works will be discussed and their respective merits and flaws constrasted in detail. This will lead to the conclusion that the works which account for the atomic nature of the dislocation's core and the lattice in which it propagates seem to capture the relevant physical phenomena more accurately than their continuum scale counterparts. Furthermore, it will be argued that lattice dynamics models are more appropriate to address general qualitative questions than their more modern counterpart, the molecular dynamics method. This will naturally lead into chapter 3, where the theoretical foundations of the lattice dynamics method will be derived. Then, it will be shown that it may be employed to model the dynamics of uniformly moving dislocations in realistic crystals using a Kanzaki force formalism [26, 27]. Following a short methodology chapter, chapter 5 will present the results derived from this lattice model. Ultimately, these demonstrate the existence of resonant velocities at which dislocation motion may become unstable in real crystals. The lattice model observations are then confirmed in molecular dynamics simulations of uniformly moving dislocations in tungsten and aluminium. Finally, we will discuss how these findings may improve our understanding of the interactions between a dislocation and the lattice in which

it moves and what they imply with regards to the existence of faster-than-sound dislocations. A concluding chapter will summarise our findings and suggest further works that may one day lead to a complete phenomenological picture of the dynamics of dislocations in the pure glide regime.

2 Literature review

What happens to a dislocation when it travels at velocities of the order of magnitude of the wave speeds of the material in which it propagates? This deceptively straightforward and seemingly obvious question has been at the centre of debates and controversies since it was first posed in 1949. More generally, the field of high speed dislocation dynamics remains a research area with many mysteries and a salient absence of physical consensus. This fogginess is most certainly not due to a lack of effort. As will become apparent in this chapter, this problem has been addressed from various viewpoints employing many different methodologies. However, none of them have been able to provide a definitive, undisputed answer to the question posed above due to two reasons. The first and foremost one is the absence of experimental evidence caused by the technical challenges involved in generating and tracking dislocations at speeds of the order of kilometres per second. Admittedly, some related empirical results exist, such as the observation of supersonic cracks [28], twins [29] and dislocations in plasma crystals [30]. Notwithstanding these results, the direct experimental observations of fast moving dislocations in metals have been limited to velocities below about one third of the shear wave speed of the material [31–37], the lower boundary of the velocity regime of interest.

The second reason for the enduring physical uncertainty in our field is the ambiguous results emanating from the multiplicity of theoretical and computational methods that have been employed to study fast moving dislocations. Without the guidance of unambiguous experimental evidence, advances in the field were necessarily left to theoretical models and computer simulations. Generally speaking, the former take the form of linearly elastic continuum models at microsecond and micrometer time and length scales in which the atomic nature of matter is assumed to be of secondary importance. These were some of the oldest and most successful models in micro- and defect mechanics [6, 38]. However, as will be shown in section 2.2, it quickly became apparent that the assumed description of the dislocation core, which needs to be added explicitly in these models, had significant impact on the derived results. This made it particularly evident that accounting for the atomic nature of the dislocation core only in an approximate fashion may not be justifiable.

This motivated the atomistic[1] modelling of gliding dislocations which will be discussed in section 2.4. These captured the interaction between the dislocation and the lattice explicitly and as such complemented their continuum counterparts. Initially these models were not given much consideration as they were limited to arguably oversimplified systems due to computational cost limitations. Furthermore, they contained instabilities at speeds below about half of the shear wave speed of the material which remained unex-

[1]The term *atomistic* is used as a shorthand for "on the atomic scale" throughout.

plained. This reduced the physical credibility of these atomistic models even further as these instabilities were interpreted to mean that low velocity dislocation motion was impossible (cf. section 2.4.1). With the advent of the non-equilibrium molecular dynamics method, more realistic atomistic simulations were performed. Nowadays, computational resources are such that these simulations can be performed with realistic interaction potentials and adequate system sizes. However, they have so far not provided the field with the conclusive phenomenological understanding it yearns for because observations in these computer experiments showed little transferability to seemingly equivalent simulations, as will be explained in section 2.4.2.

For these reasons we lack an uncontested qualitative understanding of the dynamics of high speed dislocations. Many hypotheses have been suggested and subsequently been proved or disproved depending on one's point of view, but many of these arguments have remained open by lack of tools to construct decisive arguments for or against them. In this literature review, I will argue that the state of the field is such that we are still debating how fast moving dislocations should behave on a qualitative level. Hence, I hope to convince the reader that quantitative results should be treated with a healthy dose of scepticism as they are largely unverifiable due to the aforementioned challenges.

This literature study is structured as follows. In the first section, the reader will be given the historical context within which dislocation dynamics first emerged. Then, I will go on to describe advances in continuum scale

models of high speed dislocation dynamics in the last 70 years. Then I will contrast and draw parallels between these works and equivalent atomistic models. These two distinct perspectives will be pitted against each other throughout in discussions of three important topics associated with fast moving dislocations: dislocation mobility, the existence of a limiting velocity and finally other exotic phenomena that have been hypothesised or observed in continuum and/or atomic scale models.

2.1 Historical perspective

Dislocations were first introduced in the scientific literature in 1907 by Volterra [39]. Building on previous work by Weingarten [40], Volterra [39] proved 2 related theorems. Firstly, he showed that a finite simply-connected elastic body - i.e. containing no displacement discontinuities - on which no forces act must find itself in its natural, undeformed state [39]. In contrast, he demonstrated that finite multiply connected elastic bodies, containing at least one displacement discontinuity, may find themselves in a state different from their natural state in the absence of external forces [39]. He named the defect that remains in the elastic body following a cutting and reconnecting procedure to introduce such a displacement discontinuity "une distortion" [39]. However, it took almost three more decades of further physical insights for these mathematical theorems, conjectures and continuum defect to be recognised as their real-world counterpart in crystalline materials: the dislocation.

In the first quarter of the 20$^{\text{th}}$ century, the concepts of the atomicity of matter and the crystalline structure of solids established themselves in the physical sciences. This quickly sparked the insight that the plastic deformation of materials may occur through rearrangements of their constituting atoms. Early mechanisms put forward entailed the en-masse sliding of one entire lattice plane over an adjacent one, the so-called file (or saw) model [41]. However, the yield stresses calculated from these models were comparable to the shear modulus of the material μ, orders of magnitude above the experimentally observed values 10^{-4} - $10^{-3}\mu$ [6]. Famously, this discrepancy was resolved independently by Orowan, Taylor and Polanyi who realised that plastic slip may occur through the rearrangement of only a small number atoms near a crystal defect: the edge dislocation [10–12]. This localised lattice distortion reduced the barrier to motion by stretching and compressing the atomic bonds around it, thus allowing them to move through the lattice driven by applied stresses of magnitudes in agreement with experiment [6]. Burgers followed up these early works and considered dislocations with more general geometries and proposed screw and mixed dislocations [42, 43].

2.2 Continuum models of gliding dislocations

2.2.1 The uniformly moving Volterra dislocation

As dislocations increasingly established themselves as the main carriers of plastic deformation in crystalline materials in the subsequent decade, it was only natural that their associated dynamic properties quickly became of interest. The equation of motion for the displacement field of the uniformly moving Volterra screw dislocation in an isotropic continuum was first formulated in 1949 by Frank [16]. The solution was obtained by observing that the equation of motion was invariant under a Lorentz transform with the transverse speed of sound of the medium (c_t) replacing the speed of light [16]. This allowed Frank [16] to simply write down the solution to the dynamic problem by applying a Lorentz transform to the previously known displacement field due to a stationary screw dislocation [42]. Unsurprisingly, this solution methodology introduced a whole host of phenomena usually associated with special relativity into the field of dislocation dynamics. Famously, Frank's displacement field solution u_z for a screw dislocation with Burgers vector $(0, 0, B)$ travelling along the x-axis with speed v_d was subject to Lorentz contraction [16]:

$$u_z(t) = \frac{B}{2\pi} \arctan\left[\frac{y}{\gamma(x - v_d t)}\right] \tag{2.1}$$

where $\gamma = (1 - v_d^2/c_t^2)^{-1/2}$. This inevitably resulted in divergences in the elastic fields as the dislocation's velocity approached that of the speed of

sound of the elastic continuum [16] completely analogous to the divergences that arise in the fundamental equations of special relativity as a particle's velocity approaches the speed of light. For example, Frank demonstrated the existence of divergences in the elastic energy E associated with this uniformly moving screw dislocation [16]

$$E = \gamma E_0 \tag{2.2}$$

where E_0 is the elastic energy of the static screw dislocation. This naturally led to the conclusion that screw dislocations could not travel faster than this limiting velocity due to an infinite increase in its inertia [16].

In the same year, Frank's study was followed up by Eshelby who published the equivalent solution for the uniformly moving Volterra edge dislocation [17]. Ultimately, he arrived at a solution which showed relativistic effects comparable with those hypothesised by Frank for uniformly moving screws [16]: Divergences in the displacement field of the uniformly moving edge dislocation appeared at both the transverse (c_t) and longitudinal (c_l) speeds of sound [17]. Again, this naturally led to the conclusion that the former had to be a limiting velocity for uniformly moving edge dislocations as it would require an infinitely large driving force to accelerate dislocations beyond these points of infinite inertia [17]. In addition, Eshelby also discovered a curiosity associated to the edge case that was not observed for the uniformly moving screw dislocation: a "radiation free state" was revealed to

exist at a dislocation velocity of $\sqrt{2}c_t$ for which the required driving force to maintain uniform motion of the dislocation was zero [17]. However, Eshelby was quick to draw attention to the fact that its existence was far from clear as the route to this state seemed to be obstructed by the hard barrier for gliding edges at c_t.

Together, these early results for the uniformly moving edge and screw Volterra dislocations founded the field of high-velocity dislocation dynamics. Furthermore, the early insights and ideas laid out in these two seminal 1949 articles provided the frame in which further developments in this area have been viewed and assessed ever since, giving their findings an exceptional longevity. By way of illustration, the question around limiting velocities of dislocations remains at the heart of many discussions up to this day (e.g. [44, 45]) and the search for Eshelby's "radiation free state" is still ongoing (e.g. [46, 47]).

2.2.2 Dynamics of dislocations and special relativity

It is worth pausing for a minute to shed light on the seemingly intimate connection between the dynamics of dislocations and the theory of special relativity. It is surprising to say the least that the theory of uniformly moving dislocations is so closely related to the physics of light, an especially fundamental theory underpinning modern physics.

The relativistic picture of dislocation dynamics was definitely more than just a curiosity in the field. An "electromagnetic analogy" was formally laid

out by Eshelby in 1953 which attempted to describe the dynamics of dislocations in the language of electrodynamics[2] [49]. However, it was shown later that the equivalent Lorentz force was irrelevant for moving dislocations [38, 50]. Only then was it accepted that the analogy between electromagnetism and dislocation theory was imprecise. Subsequently, the electromagnetic analogy went out of fashion. One relativistic issue that famously survived was the one surrounding the mass of a dislocation. Sparked by Frank and Eshelby's early works, attempts to re-establish the connection between the dynamics of gliding dislocations and special relativity were made by Hirth *et al.* [18, 51]. More specifically, they tried to derive physical expressions for the relativistic mass of a dislocation by bringing together Frank's expression for the elastic energy of a uniformly moving screw dislocation (cf. Eqn.(2.2)) and special relativity's $E = \gamma mc^2$ [18, 51].

Despite its initial popularity, there are good reasons to have reservations about the seemingly close connection between special relativity and dislocation dynamics as there seems to be little physical motivation behind it. The fact that the equation of motion of a uniformly moving screw dislocation could be solved by applying a Lorentz transform to the static equation is not surprising as the dynamic equation took the form of a wave equation [16], which are Lorentz invariant [52, 53]. However, this solution methodol-

[2]Interestingly, this is reminiscent of the discovery of special relativity, but in reverse. Special relativity was found within Maxwell's theory of electromagnetism and then postulated to be more generally valid [48]. Here, special relativistic elements were found in the theory of uniformly moving dislocations sparking attempts to construct an electromagnetic analogy from it.

ogy endows the dynamic solution with some peculiar relativistic assumptions and results in addition to the limiting velocity alluded to above. Firstly, it ascribes the same physical importance to the speed of sound in a medium as to the speed of light has in vacuum. This would lead one to conclude that the speed of sound in any medium would be an insurmountable barrier, a conclusion which we know is false.

These rather unphysical predictions seem to suggest that the fundamental equations of motion of the uniformly moving edge and screw Volterra dislocations can not be Lorentz invariant. In other words, the equations of motion as written down by Frank [16] and Eshelby [17] are incomplete. This disconcerting conclusion does not only put into question the results derived from any analogy with special relativity. The fact that terms seem to be missing in the equations of motion also highlights the most fragile assumption underpinning continuum models of high speed dislocations: the small strain approximation.

2.2.3 Breakdown of the small strain approximation

The small strain approximation is a cornerstone of linear elasticity theory. It entails that the strain tensor ϵ_{ij} can be described using only the first order gradients of the displacement field u_i in the body [6]:

$$\epsilon_{ij} = \frac{1}{2}\left(\frac{\partial u_i}{\partial x_j} + \frac{\partial u_j}{\partial x_i}\right) \tag{2.3}$$

This requires that the deformation gradients are small everywhere in the elastic continuum [54]. If this approximation holds, the deformation gradient tensor in elasticity theory can be linearised which simplifies the equations of linear elasticity considerably [6, 38].

Another perspective on this requirement is that the disturbances in the body should be slowly varying in space such that the homogeneity of the elastic continuum is a good approximation to the underlying atomic displacements it represents [55]. The breakdown of the small strain approximation is more prominent for moving than for static dislocations due the relativistic contraction of the displacement field solution as derived by Frank [16] and Eshelby [17]. Furthermore, it can be understood that the radiation emanating from the dislocation as it moves causes disturbances around the dislocation core which are naturally on atomic length and time scales. This implies that the small strain approximation may be rightfully questioned in this regime as higher order strain gradients are required to describe the deformation tensor accurately [38].

This breakdown of one of the key approximations of linear elasticity in continuum treatments of gliding dislocation was pointed out by Eshelby himself very early on [17]. From this, he did not explicitly conclude that his and Frank's [16] equations of motion were incomplete. However, it is not unreasonable to assume that this may have been implied as acknowledging the breakdown of the small strain approximation and admitting that higher order (beyond linear) elasticity theories [56] are required to address this problem

are two sides of the same coin.

2.2.4 Kinematic generation

Before moving the discussion away from the uniformly moving Volterra dislocation altogether, this review would not be complete without introducing the concept of *kinematic generation*. This is a dislocation reaction in which a fast moving dislocation spawns new dislocations in the absence of traditional sources such as Frank-Read sources or grain boundaries [6]. Kinematic generation was first proposed by Frank who realised that dislocations may multiply in this fashion near a boundary or free surface [57]. Later, it was suggested that if the kinetic energy of a moving dislocation is large enough, it may nucleate 2 dislocations of opposite sign [50] as illustrated schematically in Fig(2.1). In other words, a mechanism may exist which facilitates the reaction

$$B \longrightarrow (B) + (B) + (-B) \tag{2.4}$$

for fast moving dislocations with Burgers vector magnitude B. This may therefore be an important source of dislocations in high strain rate (upwards of $\sim 10^6 s^{-1}$) experiments and simulations [58]. At these strain rates, *homogeneous nucleation* - the generation of dislocations in complete absence of other defects or sources - was demonstrated to play an important role in both real [59, 60] and simulated shock experiments [60–63].

An exact onset mechanism for the kinematic generation reaction repre-

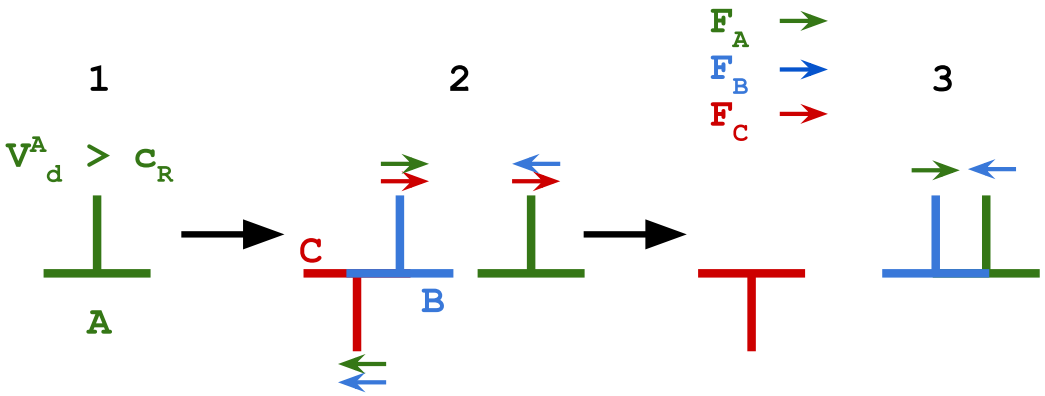


Figure 2.1: Schematic representation in three steps of the kinematic generation of edge dislocations as accounted for by continuum works [6]. The coloured arrows represent the forces the dislocations exert on one another where the directions are key and magnitudes approximate. The vectors labelled F_A represent the forces on B and C due to A, and similarly for F_B and F_C. Step 1 shows an edge dislocation A travelling with a speed above the Rayleigh wave speed of the material which may generate two nascent edge dislocations of opposite sign (B and C), shown in step 2. From the mutual interactions between the dislocations represented in stage 2, it can be seen that this results in the final configuration consisting of a single dislocation and a bound dislocation pair travelling in opposite directions.

sented in Eqn.(2.4) was proposed from Frank and Eshelby's 1949 works on uniformly moving Volterra dislocations. Investigations of the interactions between gliding Volterra edge dislocations found that above the Rayleigh wave speed - the speed of surface waves in a material [64] - dislocations of like sign attracted and dislocations of opposite sign repelled each other [6, 50, 65–68]. Now, it is plausible that a fluctuation in the core of a fast moving edge dislocation may result in 2 nascent edge dislocations of opposite sign in close proximity [6] (cf. Fig.(2.1) step 2). Then, rather than attracting, they would repel each other above the Rayleigh wave speed and ultimately

produce the dislocation reaction from Eqn.(2.4), sketched in Fig.(2.1). This reasoning led to the conclusion that the Rayleigh wave speed may be the limiting velocity for edge dislocations as they would dissociate following this kinematic generation mechanism at higher speeds [6]. Interestingly, the deduction that c_R should be the limiting velocity for edge dislocations was also reached from completely different argument. Namely, an edge travelling at the Rayleigh wave speed would resonate with any free surface in the body inducing a divergence in the elastic energy of this system [6, 69]. Since no real body is infinitely extended, edge dislocations may never surpass this limiting velocity.

Although the kinematic generation mechanism explained above seems sound, it might immediately bring an obvious question to the forefront of the reader's mind: Is it physically reasonable that no equivalent kinematic generation mechanism exists for screw dislocations? We will return to this issue in the results chapter of this thesis.

2.2.5 Introducing atomic effects

It may be surprising to read that work following the two seminal 1949 articles concerning themselves with the uniformly moving screw and edge Volterra dislocation did not dedicate itself to the search for higher order theories that might address the concerns alluded to in section 2.2.3. In stead, Eshelby realised very quickly that the Volterra models were missing one crucial ingredient: lattice wave radiation [49]. So far the work had focused on changes in the

elastic fields and in particular the velocity dependence of the energy stored in them, the so-called *inertial* effects. However, energy loss mechanisms due to the emission of lattice waves from the dislocation, collectively resulting in a dissipation mechanism called dislocation *drag*, were missing completely [70]. This resulted in a research endeavour aiming to include atomic scale effects, mainly more intricate core models, in continuum scale models with increasing level of sophistication in order to describe the dislocation–lattice interaction more accurately.

The first to investigate the uniform motion of dislocations including an effort to include some atomic level detail was Eshelby himself who considered the dynamics of straight edge and screw dislocations using Peierls - Nabarro (PN) style core descriptions [13, 71]. In this model, the elastic continuum is divided into two half spaces, separated by a cut plane across which the displacement discontinuity associated with the dislocation lies [6]. The two half spaces interact across the cut plane through a simple force law mimicking the atomic interactions across the cut plane. This provides a driving force to confine the region of misfit of atoms across the glide plane to the smallest possible area as it attaches an energetic penalty for misalignment of atoms across the glide plane. However, these atoms also interact with the elastic half-spaces away from the cut plane. This in turn favours a uniform distribution of the misfit along the glide plane and hence drives a widening of the misalignment region. The competition between these two establishes the core width [13, 71].

As alluded to above, Eshelby was the first to introduce some atomic detail into continuum models when he studied the uniform motion of these PN dislocations [17]. He made two interesting observations. Firstly, he concluded that the core width contracted in relativistic fashion. For the screw, the dislocation's width vanished as its velocity approached c_t [17, 70]. However, for the PN edge dislocation the equivalent contraction of the core happened as the dislocation approached the Rayleigh wave speed c_R of the material. This led to the conclusion that the latter may be a limiting velocity of edge dislocations [17].

A couple years later Eshelby came to the insight that this PN model could be modified to include even more atomic scale detail by including a more realistic dispersion for the lattice waves [70]. As described in section 2.2.1, Frank and Eshelby started a discussion surrounding limiting velocities for gliding dislocations that remains undecided up to this day. In an attempt to circumvent this discussion altogether, Eshelby hoped that adding this more realistic lattice dispersion relation may provide a dissipative damping force strong enough so that dislocations may never reach their respective limiting velocities [70]. In particular, he demonstrated that his solution for the subsonic[3] PN screw dislocation did not dissipate any energy away from the core meaning that they would move indefinitely in the absence of any driving

[3]Screw dislocations are deemed to be subsonic when travelling at speeds below c_t and supersonic otherwise. Edge dislocations are subsonic, supersonic and transonic when their speed is below c_t, above c_l and in between c_t and c_l respectively. Terminology taken from [72].

force [70]. However, their supersonic counterparts did radiate energy away from the glide plane [70]. He argued that improving the dispersion relation from the elastic continuum ($\omega = ck$) may provide a dissipation mechanism or drag force on subsonic dislocations as this would make a subsonic dislocation supersonic with respect to some lattice waves. He tried to quantify the amount of energy dissipation this dispersion mechanism could provide [70]. However, definitive quantitative results eluded him as the strength of the energy dissipation was highly sensitive to the assumed force law in the PN model, i.e. the detail of the assumed core model [70]. Despite this, he did ultimately conclude that it was unlikely that dispersion would provide the main source of energy dissipation for uniformly moving dislocations.

Recently, the idea that a more truthful dispersion relation may provide a drag force that is missing in traditional continuum models of high speed dislocations was reinvigorated [73, 74]. In an attempt to study the interaction between a Volterra dislocation and a lattice explicitly, a model was proposed in which the elastic continuum was linked explicitly to a phononic Hamiltonian [73, 74]. This allowed expressions for the drag experienced by a moving dislocation as it scatters and generates phonons[4] to be obtained [73]. However, this model suffers from relativistic divergences comparable to those of the early works discussed in section 2.2.1. Because of this, it is

[4]The term *phonon* is used frequently in the literature to describe the interaction between a dislocation and the lattice. However, lattice vibration seems more apt as the quantum nature of lattice vibrations does not play a role in the context of high speed dislocation dynamics

debatable whether this line of enquiry may eventually provide us with definitive answers to the key questions that have eluded us so far. Specifically, it remains to be seen whether the improved insights this model offers are worth the considerable added mathematical complexity. Despite this, it is a clear next order improvement over the traditional continuum theories and a valiant attempt to address one of its most obvious flaws: the lack of lattice wave dissipation.

2.2.6 Beyond the Peierls-Nabarro model

A first generalisation of PN models and their consequences for high speed dislocations was put forward by Weertman [72]. He investigated the role of the assumed force law across the cut plane in the PN model for gliding screw and edge dislocations [50, 72, 75]. Particular attention was devoted to what the functional form of different possible force laws meant with regards to the existence of a limiting velocity for these dislocations. For uniformly moving screw dislocations he concluded that they are limited by the shear wave speed of the material, in agreement with Eshelby before him [70]. For the edge case however, Weertman argued that the traditional PN sinusoidal force law used by Eshelby was not physically suited to describe a gliding PN dislocation [72]. Assessing the validity of qualitatively different force laws for the interaction across the cut plane, Weertman concluded that these dislocations could overcome c_t and that the limiting velocity was to be found somewhere in the transonic regime [72]. However, like Eshelby before him

Weertman too had to forgo definitive quantitative results admitting that these would be sensitive to the exact detail of the assumed force law in the PN core model [72].

Since the turn of the millennium, interest renewed in improved core models with a flurry of novel suggestions. P. Rosakis suggested a generalised PN model for dislocation cores in an attempt to account for phonon drag in continuum level models [76]. This allowed him to explicitly derive a relationship between the driving force on a dislocation and its resulting velocity from which he concluded that transonic and supersonic dislocations could exist [76].

2.2.7 Elastodynamic models

So far, all the continuum models have occupied themselves with uniformly moving dislocations. This significantly reduces the mathematical complexity as this problem is amenable to treatment with elastostatic methods in which there is no explicit time dependence of the elastic fields. However, this simplification also implies that the dislocation has been moving with this constant speed for an infinitely long time. This boundary condition, required so that the explicit time dependence of the elastic fields may be dropped, also entails that the problem has reached a steady state. Therefore, these uniformly moving dislocations do not radiate [70]. It is clear that to address this hiatus, the uniform motion requirement has to be dropped. In other words, the time dependence of the elastic fields has to be treated explicitly.

Only then may radiating solutions for possibly nonuniformly moving dislocations be obtained. This *elastodynamic* description [64] of the dynamics of dislocations is necessary to describe their inertia appropriately.

It was not until the late seventies that sufficient progress was made in the field of continuum elastodynamics such that non-uniformly moving dislocations could be modelled [77, 78]. Several related elastodynamic studies appeared of non-uniformly moving edge and screw Volterra dislocations [79–81]. With regards to fast moving dislocations, these concluded that the elastodynamic drag forces, caused by the energy dissipation of elastic waves, would be negligibly small up to around 80% of the shear wave speed of the medium [81]. However, due to a dramatic increase in energy release at speeds beyond this, it was claimed that to overcome this drag, a driving force of such magnitude would be required that material bonds break [81]. Hence, supersonic motion would be highly unlikely [81]. However, Markenscoff and co-authors later concluded that this barrier due to the Mach wavefront may be overcome by introducing a ramp core model [82–84].

Lazar treated the uniformly moving screw dislocation within an elastodynamic gauge theory for dislocations which removed the usual divergences near the Volterra dislocation core [85]. He found no objections to supersonic screw dislocations [85].

Finally, Pellegrini provided the most complete continuum treatment of high speed dislocation up to this day with a fully elastodynamic treatment of the moving PN dislocation [86–90]. Building on previous work by Pillon

et al. [91], he proposed a methodology to solve the dynamic Peierls-Nabarro equations which had been derived previously but never solved due to their inherent mathematical complexity [49]. This so-called collective-variable approach did not constrain the core's dynamics a priori, as was the case for most dynamic PN models before him. In contrast, the dynamics of the core was solved for explicitly as part of the solution scheme [89, 90]. From this highly intricate and mathematically complex model, he ultimately concluded that transient transonic motion for edge dislocations may be possible [90]. However, the model remained inconclusive with regards to the possibility of uniform motion in the transonic and supersonic regimes [90].

Further elastodynamic models aimed at regularising the dislocation's core were proposed [92, 93] . However, the conclusions from these works as well were found to be dependent on the assumed core model properties. Finally, some works took one further step and studied elastostatic and elastodynamic models of dislocations in anisotropic continua [93–97]. Given how many fundamental questions remain surrounding the dynamics of gliding dislocations in isotropic media, we will not discuss the additional complications that arise with the introduction of anisotropy here.

2.2.8 Continuum models of gliding dislocations: the verdict

At this point it is sensible to step back for a moment and assess what 70 years of continuum modelling of high speed dislocations has brought us. More specifically, have we answered the most salient question posed by Frank and Eshelby in 1949: Do supersonic dislocations exist? Unfortunately, from section 2.2 we can only conclude that continuum models so far have not been able to provide the conclusive answer. It seems that even the qualitative predictions made from these models are highly dependent on the specific choices of parameters and mainly the choice of core description. This has led to the peculiar situation that many possible phenomena associated with high speed dislocations have been suggested in the literature but without decisive evidence to accept or refute one continuum model over another, discussion surrounding them can not be put to bed. This is a further reason why Frank and Eshelby's early insights are still largely speaking the consensus in the field, despite the obvious physical flaws that undermine their model as explained in section 2.2.3.

The one major exception is that it is now widely accepted that supersonic dislocation motion is possible. However, as we will see in section 2.4, this was an insight driven by atomistic works and models. It can be rightfully questioned whether continuum level models will ever be able to capture the relevant core effects in enough detail to be conclusive beyond reasonable

doubt. Furthermore, it has to be considered whether the ever increasing mathematical complexity that this brings along with it is justified in the light of the improvements they bring.

2.3 Dislocation Mobility

Dislocation mobility is the relationship between the Peach-Koehler force on a dislocation [6] and its resulting velocity [98]. Alternatively called a *mobility law*, it is defined in this rather vague fashion as it has to capture a broad spectrum of physical phenomena in dislocation dynamics. The reason for bringing it up here is that it forms the perfect bridge between the continuum models discussed in the previous section and the atomistic works that will be presented in the next.

As well as being an interesting physical concept in its own right, the mobility law is particularly important in discrete dislocation dynamics methods [19, 99]. In this continuum scale simulation technique, the mobility law - along with dislocation injection [100] - is a physical quantity through which atomic scale information is transferred (for an excellent review see [18]). It is usually built up of two parts. On the one hand it consists of an *inertial* term which captures the changes in self-energy of a dislocation as it changes its velocity. This is naturally described in continuum models in which the elastic energy of a dislocation is most easily described. On the other hand, a phenomenological *drag* term is added to mobility laws to ac-

count for the interactions between the lattice and the dislocation and the energy loss mechanisms they entail. This term is mainly atomistic in origin and at best only described in an approximate fashion in the continuum models discussed above.

Recently, Gurrutxaga-Lerma showed that the two halves that make up a mobility law, do not contribute equally [18]. Notably, he showed that for dislocations accelerating from rest in aluminium, the inertial contribution vanished in less than 10 ps as the dislocations approached their terminal velocity [18]. This is shown in Fig.(2.2) and highlights the importance of the drag term. Unfortunately, as described in the previous section, the dislocation–lattice interactions which are the cause of this "phonon drag" is not easily captured in continuum models. Therefore, the drag terms currently in use (e.g. [76, 101, 102]) are most often phenomenological [18].

This emphasises very clearly the need for improvements in our understanding of the atomic scale interactions that occur between gliding dislocations and the lattice. One could even argue that a paradigm shift may be in order: Rather than attempting to introduce atomic effects in continuum models with more and more detail at the cost of more and more mathematical complexity, it may be worth approaching the modelling of high speed dislocations from an atomistic point of view from the outset.

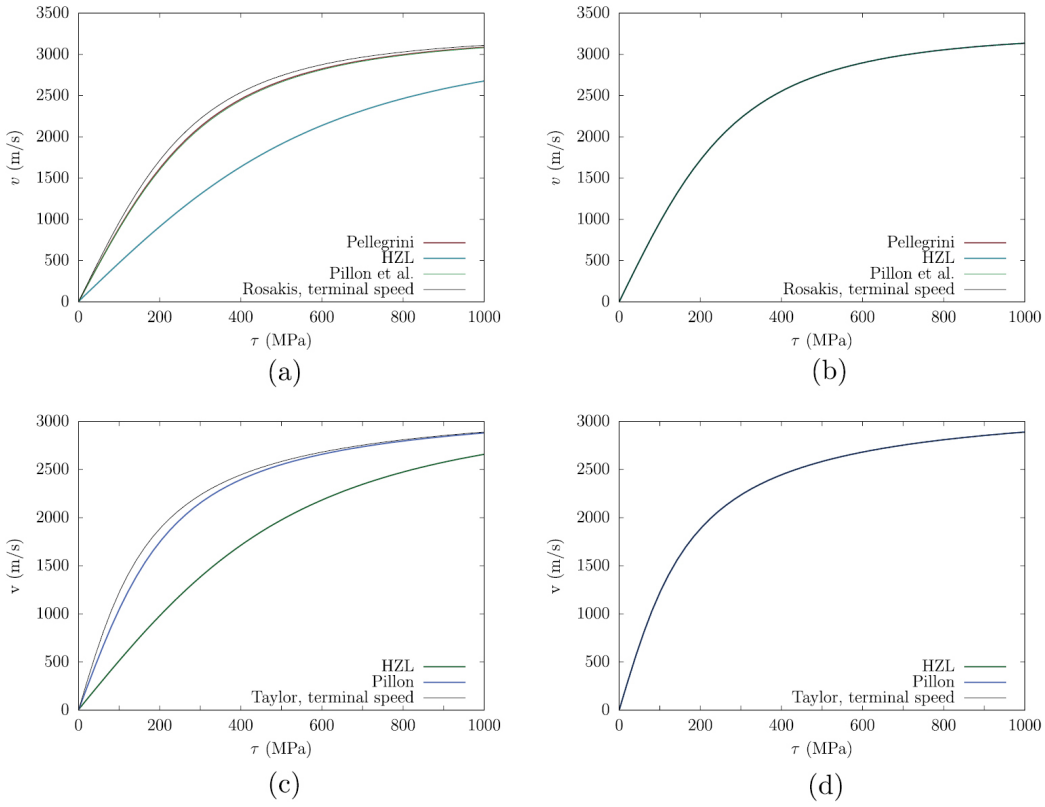


Figure 2.2: Comparison of various inertial terms in mobility laws with a Rosakis [76] (a and b) or Taylor [101, 102] (c and d) drag force for an edge dislocation accelerating from rest in aluminium. 1 ps (a and c) later, the difference in mobility due to the differnt intertial terms can still be distinguished but at 10 ps (b and d) the dislocation's mobility is completely dominated by its drag component. *Reproduced with permission (CC3.0) from [18].*

2.4 Atomistic models of gliding dislocation

2.4.1 Lattice dynamics models

The first atomic scale models of uniformly moving dislocations that appeared were lattice dynamics models. These describe the reaction of a crystalline lattice, treated within the harmonic approximation, to a prescribed driving force [103, 104]. Lattice models first emerged in atomic scale investigations of point defects [26, 27, 105], and this methodology was successfully extended to treat dislocations [55, 106, 107]. A detailed explanation and the theoretical foundations of the lattice dynamics method are described in chapter 3.

The oldest lattice dynamics studies of gliding dislocations that appeared were a family of related models called *snapping bond models* [108–110]. These generated the required dislocation displacement jump, with magnitude equal to the Burgers vector, by explicitly breaking and restoring atomic bonds across the glide plane [108–113]. Hence the name. However, these were often simple models of Frenkel-Kontorova (FK) [114] type or of gliding dislocations in square or simple cubic lattices. These were the first tools that allowed the dislocation–lattice interactions to be investigated directly [115, 116]. Furthermore, they allowed two atomistic and distinct drag mechanisms to be separated. On the one hand, a gliding dislocation suffers drag from the scattering of pre-existing thermal lattice vibrations [15, 117], a phenomenon referred to as *phonon wind*. On the other hand, a dislocation generates lattice

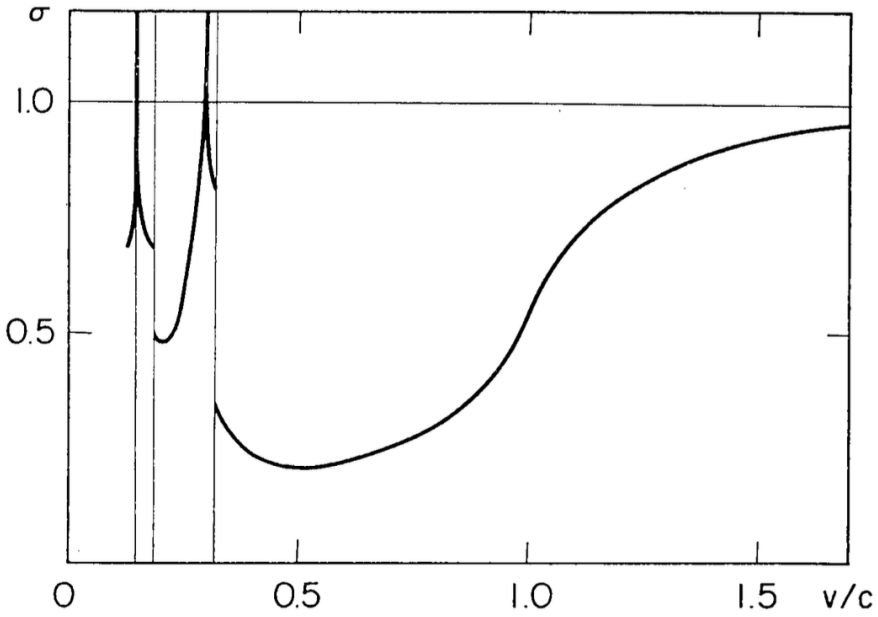


Figure 2.3: Dislocation mobility law derived for uniformly moving screw dislocation in a simple cubic lattice dynamics model with nearest neighbour interactions. *Reproduced with permission, (c) (1971) The Physical Society of Japan* [110].

wave radiation as it glides through the lattice [108–110, 112, 113]. Together, these two effects constitute the *phonon drag* [118] that eluded contemporary continuum models. Moreover, being able to quantify these energy dissipation mechanisms also allowed the explicit derivation of precise relationships between the dislocation's velocity and the force required to maintain uniform motion. A representative example of such a *mobility law* derived from a lattice dynamics model of a uniformly moving screw dislocation in a square lattice is shown in Fig.(2.3) [110].

With the struggles of continuum models to prove or disprove the existence

of supersonic dislocations in mind (cf. section 2.2), one feature of Fig.(2.3) jumps out immediately: Nothing of note occurs at the shear wave speed. As far as lattice models were concerned, this was the end of the discussion as all related works were in complete agreement on this [108–113]. This seems to suggest that the shear wave speed is given a particular status within continuum models of gliding dislocations due to the oversimplified dispersion relation ($\omega = ck$) they subsume [55].

However, the second obvious feature of Fig.(2.3) turned out to be an Achilles heel for lattice dynamics models of uniformly moving dislocations. At velocities below approximately $c_t/3$, these models contained clear instabilities. These were investigated prior in great mathematical detail [119–121] and found to occur at dislocation velocities where both phase and group velocities of the excited lattice vibrations were equal to the dislocation's velocity. These resonances were problematic for two reasons. Firstly, they implied that for dislocations travelling at speeds below $c_t/3$, their displacement field should diverge or at least contain regions with very large displacements. This contradicts the small displacement assumption, in the form of the harmonic approximation, at the heart of lattice models [122]. Secondly, these resonances were not found in computer experiments [123, 124]. This sparked some high-profile criticism, most notably in Refs. [122] and [6] p. 208.

These critiques added to the pressure on lattice models that already faced scrutiny due to their apparent simplicity. The FK and simple cubic systems under consideration raised the question whether these models were at all

representative of dislocations propagating in real crystals. In particular, it was questioned whether the simple assumed atomic interactions in these early lattice models were justified [111, 123, 125] and whether the a priori assumed uniform motion was internally consistent within them [122, 123, 126–129]. Employing equivalent computer simulations, it was demonstrated that at velocities just below c_t, uniform dislocation motion seemed no longer possible [126, 128], a feature missed completely in lattice models. In addition, they suggested that these *breakdown velocities* could be critical points and provide onset mechanisms for kinematic generation and twin formation [111, 128]. Of course, these studies brought the inescapable issue around the existence of supersonic dislocations to the fore once more, though for reasons very different from the inertial arguments presented by continuum theories [126].

These two shortcomings ultimately resulted in the rejection of these early lattice models as they were deemed to be too simple to be physical. Their conclusions were subsequently largely discarded. The continuum perspective that dislocations were relatively free up to around $c_t/2$ beyond which inertial effects were thought to dominate remained consensus within the community [6].

2.4.2 Molecular dynamics simulations

A second wave of atomic scale dislocation models was driven by the advent of the molecular dynamics (MD) method [130] and more specifically the availability of the required computing power to simulate adequately sized systems.

MD simulations possess the same same advantages as the lattice dynamics models compared to continuum models: it allows detailed investigations of the dislocation–lattice interaction. However, it also constituted a vast improvement over the relatively simple lattice models: In MD simulations, one is no longer limited by the harmonic approximation and most importantly realistic interatomic potentials can be used to capture the core–lattice interaction with physical realistic detail [131, 132]. All these elements, combined with the development of adequate atomic interaction potentials for metals [133–136], reinvigorated atomistic models of gliding dislocations in the mid to late 1990s.

Before proceeding, an important general remark with regards to the use of MD simulations to study fast moving dislocations should be made. Namely, the MD method is fundamentally a statistical tool that samples the paths of many individual particles through phase space [130]. Therefore, MD simulations of phenomena that are highly dependent on the exact paths of only a small number of the particles under consideration should be appropriately scrutinised. This is clearly the case for non-equilibrium MD simulations of gliding dislocations through a crystal as only a relatively small number of particles localised around the dislocation core ultimately determine its characteristics. This does not mean that simulations of fast moving dislocations are inherently untrustworthy. However, care should be taken to respect the inherent statistical nature of the MD method when presenting simulation results. This caveat should be kept in the back of the reader's mind for what

follows.

The seminal 1999 paper by Gumbsch and Gao [44] in particular provided the spark that inspired a flurry of subsequent MD studies of fast moving dislocations [45, 63, 137–149]. This was the first MD simulation that clearly demonstrated the existence of supersonic dislocations [44] as shown in Fig.(2.4). This simulation result was in perfect agreement with lattice model results and subsequently confirmed in equivalent MD simulations of dislocations in other materials [45, 137, 143, 145, 146, 148]. This also opened up a whole new perspective on the issue of supersonic dislocations. At this point in time it was widely accepted that the speed of sound was indeed a hard barrier for dislocation motion as the main counterarguments came from lattice dynamics models that were perceived in a bad light (cf. section 2.4.1). Hence, it is not surprising that this first observation of supersonic edge dislocations in computer experiments caused a stir in the field. So much so that it also drove a flare-up in continuum studies, the majority of which now allowed for trans- and supersonic dislocations in some way or another as can be seen upon close inspection of sections 2.2.6 and 2.2.7 and the references therein.

The second driver behind MD studies of high speed dislocations was the need for dislocation mobility laws in the pure glide regime in discrete dislocation dynamics (DD) simulations [18, 99]. As explained in section 2.3, this mobility law is one of the main quantities through which this atomic - continuum gap is bridged. An obvious strategy to obtain such a relation is

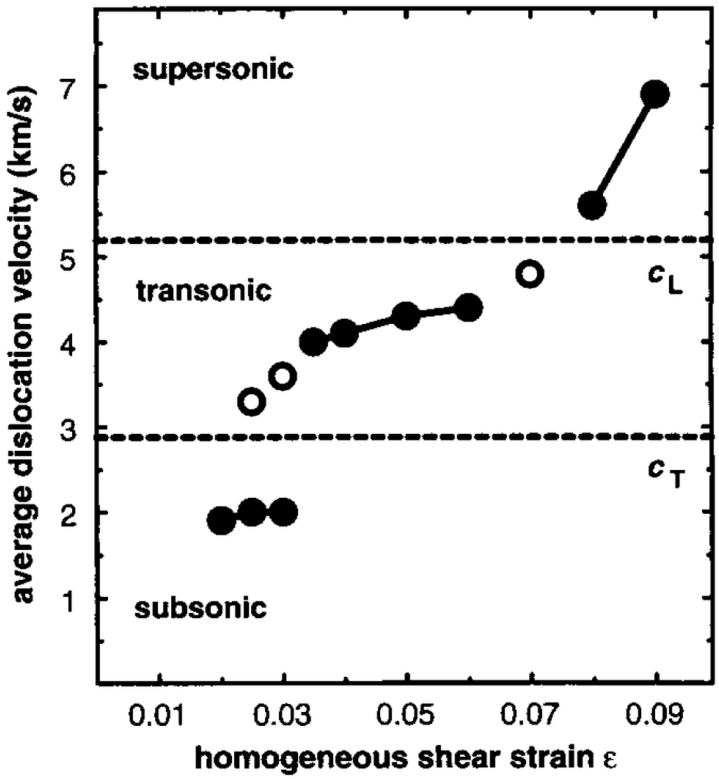


Figure 2.4: Observed average dislocation velocity for edge dislocations in MD simulations of tungsten [134, 135]. Solid circles indicate stable dislocation motion whereas open circles mark the average velocities at which the observed motion was unstable varied significantly throughout the simulation. *From [44]. Reprinted with permission from AAAS.*

to perform MD simulations of gliding dislocations from which a quantitative mobility relation to be used in DD simulations may be obtained [45, 143, 149, 150].

Finally, a third group of MD dislocation dynamics studies existed that were united in their aim to understand the physics of the dislocation–lattice interaction at fundamental level [124, 140, 142, 151]. In many ways these works took up the mantle and spirit of the out of fashion lattice dynamics models (cf. section 2.4.1). However, despite the physical richness inherent to modern MD simulations it proved difficult to extract transferable, generally applicable, qualitative results from these [140, 142, 151]. So much so that some took a step back and performed much simpler MD simulations, reminiscent of the lattice models discussed above [124, 139]. The most notable result coming out of these was the observation of kinematic generation of screw dislocations in square and hexagonal lattices, a process that can not be accounted for within linear elasticity [124]. The kinematic generation of edge dislocations, allowed in elastic continuum theories as discussed in section 2.2.4, was confirmed previously in MD simulations [152]. This raises the question whether there may be a more general mechanism, different to the one mentioned above, driving kinematic generation.

2.4.3 Atomistic models of gliding dislocations: the verdict

In many ways it is challenging to understand why MD simulations have not been able to resolve the outstanding issues left by continuum theories. Today's computational resources allow the simulation of systems containing hundreds of millions of atoms [153] with interaction potentials with near density functional theory level accuracy that describe dislocation core structures truthfully [136, 154, 155]. Yet nowadays, we still don't talk about *the* mobility law for a given dislocation topology in a material [18]. This is because so far an unequivocal picture of the phenomenology of gliding dislocations has not emerged from the multitude of MD studies that have been undertaken ([45, 63, 137–149] i. a.). Assuming that the vast majority of the MD simulations in the literature have been performed adequately, it is not at all obvious why this is the case.

It may be possible that these MD simulations are so physically rich that they are the forest through which we do not see the trees any more. This may explain why some chose to go back to much simpler toy MD systems [124], rather than looking at more and more complex MD potentials, in an attempt to reduce the complexity of the system to pinpoint exactly which bits of physics are the key to understanding dislocation mobility.

2.5 Conclusion

In summary, it is fair but though to conclude that after almost 70 years of research into the phenomenology associated with fast moving dislocations, definitive conclusions remain elusive. The search for a common ground in the results derived from continuum and atomistic models is inhibited by the fact that both are flawed. Continuum models of fast moving dislocations are hampered since dislocations fundamentally and inextricably link the atomistic and continuum length and time scales. So far attempts of marrying the two starting from a continuum perspective seem to be too dependent on model parameters to be definitively conclusive.

Atomistic models seem to circumvent this issue by taking an a priori atomic scale point of view. Lattice dynamics models however seem to be too simplistic to be realistic and contain features that so far have gone unexplained, most notably the low velocity instabilities. MD simulations on the other hand, although upon first sight contain all the right physical ingredients to address the problems encountered by both continuum and lattice models, have been unable to unequivocally provide us with a fundamental understanding of dislocation mobility.

Therefore, this has left the field in a state where discussion clearly finds itself on the qualitative plane. Only after issues around limiting velocities of dislocations or which components contribute to dislocation drag have been decided and agreed upon on a phenomenological level does it make sense to

start investigating these issues in further quantitative detail that MD models provide. Only continuum and lattice dynamics models possess a natural transferability and generality which is not material specific. Given that the drag dominates the inertial component in mobility laws, it seems sensible to take an atomistic approach. Therefore, lattice dynamics models seem to provide the middle-of-the-road tool that may provide general qualitative insights into the dislocation–lattice interaction that has so far eluded the more physically rich MD models. Provided, of course, they are improved to be more realistic and their known outstanding issues are addressed.

I believe that bringing the lattice dynamics models of the 1970s and 80s into the 21st century is the most promising route so we may one day be able to provide answers to the questions that were raised when this field was founded in 1949.

3 The lattice dynamics method

Sections 3.3 and 3.4 of this chapter were partly published in [25] under a CC BY 4.0 license.

Lattice dynamics models are a natural choice when modelling high speed dislocations as they capture the interaction between the dislocation and the lattice and all ensuing dissipative effects explicitly. In this section, the theoretical foundations associated with the lattice dynamics method will first be presented. Then, it will be shown that these models may be employed to describe uniformly moving dislocations using Kanzaki forces [26].

3.1 Elements of Green's function theory

Green's function theory is a widely used tool in most disciplines in the physical sciences. Therefore, many excellent textbooks on this topic exist (e.g. [156]) and no attempt will be made here to discuss the topic in full. Only the specific elements of Green's function theory of relevance to lattice dynamics will be highlighted and derived[1] below.

[1] in the physicists' sense

3.1.1 Time-independent theory

The Green's function $G(\boldsymbol{x}, \boldsymbol{y})$ for a time-independent linear operator $\mathcal{L}(\boldsymbol{x})$ is defined by

$$\mathcal{L}(\boldsymbol{x})G(\boldsymbol{x}, \boldsymbol{y}) = \delta(\boldsymbol{x} - \boldsymbol{y}) \tag{3.1}$$

where $\delta(\boldsymbol{x})$ is the multi-dimensional generalisation of the Dirac delta distribution. Furthermore, the Green's function as defined in Eqn.(3.1) should satisfy the boundary conditions of the problem at hand. From Eqn.(3.1) it can be seen immediately that $G(\boldsymbol{x}, \boldsymbol{y}) = G(\boldsymbol{x} - \boldsymbol{y})$ by symmetry. We will assume that $\mathcal{L}$ is Hermitian and therefore possesses a spectrum of real eigenvalues $\{\lambda_n\}$ and orthogonal eigenstates $\{|\phi_n\rangle\}$ [157]

$$\mathcal{L}\,|\phi_n\rangle = \lambda_{\hat{n}}\,|\phi_n\rangle \tag{3.2}$$

where n and $\hat{n}$ have the same numeric value but the hat superscript indicates that summation is not triggered[2]. As this index notation suggests, we will explicitly treat the Green's function of an operator $\mathcal{L}$ with a discrete spectrum. However, these results can readily be generalised to operators with associated continuous spectra [157]. Additionally, it will be assumed without loss of generality that the eigenstates $|\phi_n\rangle$ are orthonormal, i.e.

$$\langle\phi_n|\phi_m\rangle = \delta_{nm} \tag{3.3}$$

[2]In this section, Einstein summation convention will be assumed.

where δ_{nm} is the Kronecker delta function. In the basis of these eigenstates we can rewrite Eqn.(3.1) as

$$\begin{aligned}(\mathcal{L}G)_{nl} &= \langle\phi_n|\,\mathcal{L}\,|\phi_m\rangle\,\langle\phi_m|\,G\,|\phi_l\rangle \\ &= \lambda_{\hat{n}} G_{nl} \\ &= \delta_{nl}\end{aligned} \tag{3.4}$$

where we have used the completeness of the eigenstates $|\phi_n\rangle\,\langle\phi_n| = \mathbb{1}$ with $\mathbb{1}$ being the identity. Hence, we can solve Eqn.(3.1) formally in the basis of eigenstates $\{|\phi_n\rangle\}$ of $\mathcal{L}$ from Eqn.(3.4) as

$$G_{nl} = \frac{\delta_{nl}}{\lambda_{\hat{n}}} \tag{3.5}$$

In an arbitrary complete basis $\{|\psi_\alpha\rangle\}$ we can write

$$\begin{aligned}G_{\alpha\beta} &= \langle\psi_\alpha|\,G\,|\psi_\beta\rangle \\ &= \langle\psi_\alpha|\phi_n\rangle\,G_{nm}\,\langle\phi_m|\psi_\beta\rangle \\ &= \frac{\langle\psi_\alpha|\phi_n\rangle\,\langle\phi_n|\psi_\beta\rangle}{\lambda_{\hat{n}}}\end{aligned} \tag{3.6}$$

3.1.2 Time-dependent Green's functions

When the time evolution of a system is of interest, a time-dependent operator $\mathcal{M}(t)$ may be introduced in the Green's function machinery. We can define

the time-dependent Green's function as

$$[\mathcal{M}(t) - \mathcal{L}(\boldsymbol{x})]\, G(\boldsymbol{x}-\boldsymbol{y}; t-t') = \delta(\boldsymbol{x}-\boldsymbol{y})\delta(t-t') \tag{3.7}$$

by analogy with the equivalent time-independent definition from Eqn.(3.1). When $\mathcal{M}(t)$ is a differential operator it is convenient to proceed in Fourier space and find the frequency domain Green's function $G'(\boldsymbol{x}-\boldsymbol{y};\omega)$ satisfying

$$[\mathcal{M}(\omega) - \mathcal{L}(\boldsymbol{x})]\, G'(\boldsymbol{x}-\boldsymbol{y};\omega) = \delta(\boldsymbol{x}-\boldsymbol{y}) \tag{3.8}$$

since $\mathcal{M}(\omega)$ will reduce to a polynomial expression in the frequency domain. Hence, the time-dependent Green's function can be found by a Fourier transform of $\mathcal{M}(t)$, provided the time-independent part of the Green's function was previously calculated from Eqn.(3.5). From Eqn.(3.8), it can be seen by inspection that

$$G'_{nl}(\omega) = \frac{\delta_{nl}}{\mathcal{M}(\omega) - \lambda_{\hat{n}}} \tag{3.9}$$

in the basis of the eigenstates of $\mathcal{L}$. Note that this Green's function possesses poles in the complex ω-plane where $\mathcal{M}(\omega) = \lambda_n$. If these lie on the real ω-axis a contour prescription must be provided to uniquely define the real space Green's function

$$G(\boldsymbol{x}-\boldsymbol{y}; t-t') = \int \frac{\mathrm{d}\omega}{2\pi}\; e^{i\omega(t-t')} G'(\boldsymbol{x}-\boldsymbol{y};\omega) \tag{3.10}$$

i.e., the inverse Fourier transform of Eqn.(3.9). In section 3.2.3 we will see that the appropriate choice of contour is provided by causality considerations.

3.1.3 Green's functions as fundamental solutions

The defining property of the Green's function expressed in Eqn.(3.1) is particularly useful when solving inhomogeneous equations of the form

$$\mathcal{L}u(\boldsymbol{x}) = f(\boldsymbol{x}) \tag{3.11}$$

Knowledge of the Green's function for $\mathcal{L}$ which satisfies the boundary conditions associated with the particular problem, allows us to solve for $u(\boldsymbol{x})$. Convolving the left-hand side (LHS) of Eqn.(3.11) with the Green's function yields[3]

$$\int \mathrm{d}^{\mathrm{n}}y'\ G(\boldsymbol{x}-\boldsymbol{y'})\mathcal{L}u(\boldsymbol{y'}) = \int \mathrm{d}^{\mathrm{n}}y'\ \mathcal{L}G(\boldsymbol{x}-\boldsymbol{y'})u(\boldsymbol{y'}) \tag{3.12}$$

$$= \int \mathrm{d}^{\mathrm{n}}y'\ \delta(\boldsymbol{x}-\boldsymbol{y'})u(\boldsymbol{y'}) \tag{3.13}$$

$$= u(\boldsymbol{x}) \tag{3.14}$$

[3] $\int \mathrm{d}^{\mathrm{n}}x\ f(\boldsymbol{x})$ denotes integration over the entire n-dimensional domain on which the integrand is defined.

where we exploited the Hermitian property of the Green's function and the so-called "sifting-property" of the Dirac delta distribution:

$$\int_{\boldsymbol{a}-\boldsymbol{\epsilon}}^{\boldsymbol{a}+\boldsymbol{\zeta}} \mathrm{d}^{\mathrm{n}}x\, f(\boldsymbol{x})\delta(\boldsymbol{x}-\boldsymbol{a}) = f(\boldsymbol{a}) \tag{3.15}$$

where ϵ and ζ are arbitrary positive constants. Combined with the convolution of the right-hand side (RHS) of Eqn.(3.11) we obtain

$$u(\boldsymbol{x}) = \int \mathrm{d}^{\mathrm{n}}y\; G(\boldsymbol{x}-\boldsymbol{y})f(\boldsymbol{y}) + \phi(\boldsymbol{x}) \tag{3.16}$$

where $\phi(\boldsymbol{x})$ is a solution to the homogeneous equation associated with Eqn.(3.11). Thus, the Green's function is the fundamental solution of the operator $\mathcal{L}$ and can be used as an integral kernel to obtain inhomogeneous solutions.

The equivalent of Eqn.(3.16) for a Green's function in Fourier space can be easily written down because the first term on the RHS of Eqn.(3.16) is a convolution. From the Fourier transform convolution theorem for two functions f and g we have

$$f * g = \mathcal{F}^{-1}\left[\mathcal{F}(f)\mathcal{F}(g)\right] \tag{3.17}$$

where $*$ denotes the convolution operator. In this thesis, the forward Fourier transform is taken to be

$$\mathcal{F}(f) = \tilde{f}(\boldsymbol{k}) = \int \mathrm{d}^{\mathrm{n}}x\; e^{-i\boldsymbol{k}\cdot\boldsymbol{x}} f(\boldsymbol{x}) \tag{3.18}$$

and $\mathcal{F}^{-}1$ denotes its inverse. Subsequently, from Eqn.(3.16) we can write down

$$u(\boldsymbol{x}) = \mathcal{F}^{-1}\left[\mathcal{F}(G)\mathcal{F}(f)\right] + \phi(\boldsymbol{x}) \tag{3.19}$$

This alternative form will be particularly useful in deriving the time-dependent Green's functions for periodic lattices in the next section.

3.2 The lattice Green's function

3.2.1 Lattice periodicity and Fourier series

Consider a perfect monatomic crystal consisting of N lattice points $\{\boldsymbol{r}_i\}$[4]

$$\boldsymbol{r}_i = r'_{i\alpha}\boldsymbol{a}_\alpha = r_{i\alpha}\hat{\boldsymbol{x}}_\alpha \tag{3.20}$$

where $\boldsymbol{a}_\alpha$ are the basis vectors of the primitive unit cell such that $r'_{i\alpha} \in \mathbb{Z}$ and $\hat{\boldsymbol{x}}_\alpha$ are the usual Cartesian unit vectors. We will be interested in bulk properties of crystalline materials, without surface effects. In order to do so, we assume Born-von Karman periodic boundary conditions [104]

$$g(\boldsymbol{r}_i) = g(\boldsymbol{r}_i + N'_{\hat{\alpha}}\boldsymbol{a}_\alpha) \tag{3.21}$$

[4]Roman indices run over all particles in a lattice, Greek indices run over the basis set axes.

where $g(\boldsymbol{r}_i)$ is an arbitrary function, N'_α is the number of primitive cells in direction $\boldsymbol{a}_\alpha$ and $N = N'_1 N'_2 N'_3$. The reciprocal lattice is defined as the set of points $\{\boldsymbol{k}_{i'}\}$ which obey [104]

$$e^{i\boldsymbol{k}_{i'}\cdot\boldsymbol{r}_j} = 1 \tag{3.22}$$

This defining condition is satisfied by construction if the reciprocal lattice points are generated by the dual basis vectors $\boldsymbol{b}_{\alpha'}$

$$\boldsymbol{k}_{i'} = k'_{i'\alpha}\boldsymbol{b}_\alpha \tag{3.23}$$

where the dual basis vectors $\boldsymbol{b}_\alpha$ satisfy

$$\boldsymbol{a}_\alpha \cdot \boldsymbol{b}_\beta = 2\pi\delta_{\alpha\beta} \tag{3.24}$$

From Eqns.(3.21) and (3.22) we can express the Born-von Karman boundary condition in reciprocal space as

$$\begin{aligned} e^{i\boldsymbol{k}_{i'}\cdot\boldsymbol{r}_j} &= e^{i\boldsymbol{k}_{i'}\cdot\boldsymbol{r}_j} e^{2\pi i k'_{i'\alpha} N'_\alpha} \\ \implies k'_{i'\alpha} &= \frac{n}{N'_\alpha} \quad n \in \mathbb{Z} \end{aligned} \tag{3.25}$$

Eqn.(3.22) expresses the fact that the reciprocal lattice is built up of points in k-space which represent plane waves with the periodicity of the lattice. This can be used to represent functions which are periodic with the

lattice as a Fourier series

$$\widetilde{f}(\boldsymbol{k}_{i'}) = \sum_{j=1}^{N} f(\boldsymbol{r_j}) e^{-i\boldsymbol{k}_{i'}\cdot\boldsymbol{r}_j} = \sum_{j} f(\boldsymbol{r}_j) e^{-2\pi i k'_{i'\alpha} r'_{j\alpha}} \tag{3.26}$$

where we have used Eqns.(3.20, 3.22) and (3.24). Furthermore, Eqn.(3.26) shows that

$$\widetilde{f}(\boldsymbol{k}_{i'}) = \widetilde{f}(\boldsymbol{k}_{i'} + \boldsymbol{b}_\beta) \tag{3.27}$$

such that $f(\boldsymbol{k}_{i'})$ is uniquely defined on the domain for which $k'_{i'\alpha} \in [0, N'_\alpha]$ with all other points in k-space related by the translation symmetry from Eqn.(3.27). This particular choice of values for $k_{i'\alpha}$ spans a domain in k-space referred to as the first Brillouin zone (BZ) [104]. Now, because we are interested in bulk properties without size effects, let us impose lattice periodicity at infinity, taking $N'_\alpha \to \infty$. As a result, the points that make up the reciprocal lattice are infinitessimally close together and therefore can justifiably be approximated using a continuous variable $\boldsymbol{k}$. Then, we can write the inverse of the Fourier transform from Eqn.(3.26) as

$$g(\boldsymbol{r}_i) = \int_{BZ} \frac{\mathrm{d}^3\boldsymbol{k}}{\Omega_{\boldsymbol{k}}}\, \widetilde{g}(\boldsymbol{k}) e^{i\boldsymbol{k}\cdot\boldsymbol{r}_i} \tag{3.28}$$

where the BZ subscript denotes the integral is performed over the Brillouin zone with volume $\Omega_{\boldsymbol{k}} = \boldsymbol{b}_1 \cdot (\boldsymbol{b}_2 \times \boldsymbol{b}_3)$.

3.2.2 The harmonic approximation

Let the total energy of a collection of atoms U be determined by

$$U = \sum_i \phi_i(\boldsymbol{r}_1, \boldsymbol{r}_2, ..., \boldsymbol{r}_N) = \sum_i \phi_i\left(\{\boldsymbol{r}_j\}\right) \tag{3.29}$$

where ϕ_i is the the binding energy of particle i. Consider a crystalline structure in which all atoms are in mechanical equilibrium. Then we may expand Eqn.(3.29) around this minimum energy configuration consisting of the set of atomic positions $\{\boldsymbol{r}_n^0\}$

$$\begin{aligned} U = &\sum_i \phi_i|_{\{\boldsymbol{r}_n^0\}} + \sum_i \left.\frac{\partial \phi_i}{\partial r_{j\alpha}}\right|_{\{\boldsymbol{r}_n^0\}} u_{j\alpha} \\ &+ \sum_i \left.\frac{\partial^2 \phi_i}{\partial r_{j\alpha} \partial r_{k\beta}}\right|_{\{\boldsymbol{r}_n^0\}} u_{j\alpha} u_{k\beta} + \text{h.o.t.} \end{aligned} \tag{3.30}$$

where $\boldsymbol{u}_i$ is the atomic displacement of particle i with respect to its equilibrium positions[5]. Firstly, note that the first term in the expansion may be dropped as this constant energy term will not contribute to the dynamics of the system. Secondly, the second term vanishes due to the equilibrium assumption. Then, the harmonic approximation entails that the higher order terms (h.o.t.) in Eqn.(3.30) may be dropped [104]. This is justified if atomic displacements are small [104].

The second derivatives of the interaction potential with respect to atomic

[5]Again, Roman indices run over all particles in a lattice, Greek indices run over the basis set axes.

positions yields the force constants matrix

$$D_{\alpha\beta}(\boldsymbol{r}_i^0, \boldsymbol{r}_j^0) = D_{i\alpha,j\beta} = \left.\frac{\partial^2 U}{\partial r_{i\alpha}\partial r_{j\beta}}\right|_{\{\boldsymbol{r}_n^0\}} \tag{3.31}$$

Due to the translation symmetry a perfect lattice possesses we can write

$$D_{i\alpha,j\beta} = D_{\alpha\beta}(\boldsymbol{r}_i^0 - \boldsymbol{r}_j^0) \tag{3.32}$$

for defect free crystals. Note that the lattice Green's function derived here is one for the perfect lattice as we required translation invariance from the very onset (cf. Eqn.(3.1)). From Eqns.(3.29, 3.30, 3.31) and (3.32), the force on a particular atom in the lattice within the harmonic approximation is given by

$$f_{i\alpha} = -\frac{\partial U}{\partial r_{i\alpha}} \tag{3.33}$$

$$= -D_{i\alpha,j\beta}u_{j\beta} \tag{3.34}$$

3.2.3 The lattice Green's function

Now, we are in a position to derive the equation of motion of a monatomic lattice within the harmonic approximation. From Eqn.(3.34) we can simply write down the fundamental equation of motion of the lattice

$$M\frac{\partial^2 u_{i\alpha}(t)}{\partial t^2} = -D_{i\alpha,j\beta}u_{j\beta}(t) - 2M\Gamma\frac{\partial u_{i\alpha}(t)}{\partial t} \tag{3.35}$$

where M is the mass of all particles in the lattice. Here we added the final term in Eqn.(3.35) which is a viscous damping term that is applied on every atom in the lattice with strength Γ. The simplifications that led to the harmonic approximation (cf. Eqn.(3.30)) also removed interactions between lattice vibrations such that they survive indefinitely [156]. The viscous damping term represents these anharmonic interactions that would cause disturbances to decay over time. Furthermore, the sign of this term is such that it pushes the poles in the lattice Green's function of the real axis in such a way as to preserve causality in the system.

As discussed in section 3.1.2, finding the Green's function of Eqn.(3.35) consists of solving the static and dynamic parts separately. So, let us consider the time-independent part of Eqn.(3.35) first. The natural way to employ the lattice periodicity to our advantage is to solve the problem in k-space as outlined in section 3.2.1. By analogy with Eqn.(3.26) we have

$$\widetilde{D}_{\alpha\beta}(\boldsymbol{k}) = \sum_{(i-j)} D_{i\alpha,j\beta} e^{-i\boldsymbol{k}\cdot(\boldsymbol{r}_i - \boldsymbol{r}_j)} \tag{3.36}$$

where the sum runs over all pairs $(\boldsymbol{r}_i - \boldsymbol{r}_j)$. Taking into account the translation invariance of the lattice Eqn.(3.36) may be rewritten as [104]

$$\widetilde{D}_{\alpha\beta}(\boldsymbol{k}) = -2 \sum_{(i-j)} D_{i\alpha,j\beta} \sin^2\left(\frac{1}{2}\boldsymbol{k}\cdot(\boldsymbol{r}_i - \boldsymbol{r}_j)\right) \tag{3.37}$$

The eigenvalue equation of interest to obtain the time-independent lattice

Green's function becomes

$$\widetilde{D}_{\alpha\beta}(\boldsymbol{k})\tilde{u}_{\beta}(\boldsymbol{k},b) = M\omega^2(\boldsymbol{k},b)\tilde{u}_{\alpha}(\boldsymbol{k},b) \tag{3.38}$$

where $\omega(\boldsymbol{k},b)$ are the frequencies of the lattice vibrations with wavevector $\boldsymbol{k}$ and normalised polarisation $\tilde{u}_{\beta}(\boldsymbol{k},b)$ and b is the index enumerating all possible solutions called the *branch index*. From these equations it is clear that the big advantage of transforming the problem to Fourier space is that it has simplified from a coupled system of $3N$ equations in real space to a system of only 3 coupled equations at at N points in k-space [104]. Now, we can write down the static lattice Green's function from Eqns.(3.6) and (3.38) as

$$\widetilde{G}_{\alpha\beta}(\boldsymbol{k}) = \frac{\tilde{u}_{\alpha}(\boldsymbol{k},b)\tilde{u}^{*}_{\beta}(\boldsymbol{k},b)}{M\omega^2(\boldsymbol{k},b)} \tag{3.39}$$

where indices α and β may refer to any arbitrary basis set (cf. section 3.1.1).

Now we turn our attention to the dynamic part of Eqn.(3.35). We are interested in the the time-dependent operator

$$T(t) = M\frac{\partial^2 u_{i\alpha}(t)}{\partial t^2} + 2M\Gamma\frac{\partial u_{i\alpha}(t)}{\partial t} \tag{3.40}$$

whose Fourier transform is given by

$$\mathcal{F}\left[T\right](\omega) = -M\omega^2 + 2iM\Gamma\omega \tag{3.41}$$

So, finally we can write down the *dynamic lattice Green's function* from Eqns.(3.9, 3.39) and (3.41) as [25]

$$\widetilde{G}_{\alpha\beta}(\boldsymbol{k},\omega) = \frac{1}{M}\sum_{b}\frac{\tilde{u}_{\alpha}(\boldsymbol{k},b)\,\tilde{u}^{*}_{\beta}(\boldsymbol{k},b)}{\omega^{2}(\boldsymbol{k},b)-\omega^{2}+2i\Gamma\omega} \tag{3.42}$$

3.3 The Kanzaki force

Now that we have derived the appropriate Green's function, all we need to model a uniformly moving dislocation in a lattice is a driving force which represents the dislocation appropriately. This is given by a Kanzaki type driving force which was first devised for point defects [26, 27] but has been extended to dislocations [25, 55, 107, 113].

Kanzaki forces are fictitious forces which when applied on a perfect harmonic lattice give rise to a displacement field associated with a particular defect [26, 27]. It is important to note that these forces are in no way real. They are merely a source term that introduces dislocations into a perfect harmonic lattice and should not be confused with the real forces required to inject a dislocation in a real crystal [55, 100]. For dislocations, they are the direct atomic equivalent of the body forces that may be derived from the Burridge - Knopoff (BK) representation theorem to represent any internal displacement or traction field discontinuity in a defect-free continuum [55, 158]. As such, these BK forces are an alternative to the popular *eigenstrain* method [38, 159] for the mathematical modelling of dislocations [55]. How-

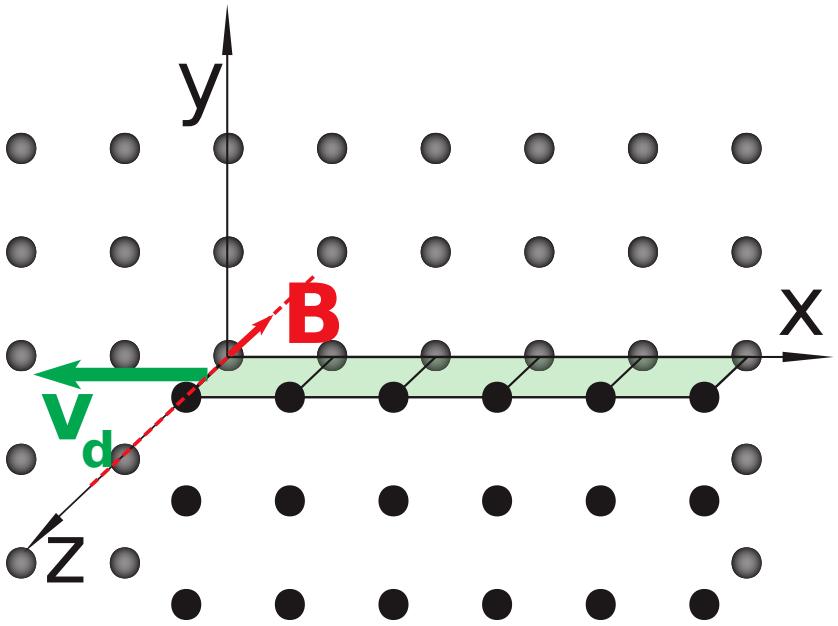


Figure 3.1: Schematic representing a uniformly moving screw dislocation propagating in a simple cubic lattice with velocity v_d. *Reproduced with permission (CC4.0) from [25].*

ever, the latter do not have a straightforward atomic equivalent [55] and as such are not suited to act as source forces in lattice models. Furthermore, due to the Kanzaki - BK forces correspondence, it is straightforward to construct atomistically informed elastic models of dislocations with realistic core descriptions [55].

We consider the case of a uniformly moving dislocation with Burgers vector $\boldsymbol{B}$, propagating with velocity v_d along the x axis passing $x = 0$ at $t = 0$. Furthermore, we will assume that the dislocation line is parallel with $\hat{\boldsymbol{z}}$-axis and remains straight throughout, effectively reducing the dimensionality of the problem from 3 to 2. The glide plane is defined to lie halfway between

2 lattice planes with normal $\hat{\boldsymbol{y}}$, a schematic of which is shown in Fig.(3.1). Then, a moving dislocation is generated in a perfect lattice by the Kanzaki forces [55, 107, 113]

$$\boldsymbol{F}_K(\boldsymbol{r_i}) = F_{i\alpha} = \sum_{j,\beta} B_\beta \Psi_{ij} D_{i\alpha,j\beta} \times \Theta\left(v_d t - x_i\right) \tag{3.43}$$

where $\Theta(x)$ is the step function and $\Psi_{ij} = \pm 1$ if the particle i is above (below) the glide plane and j below (above), and 0 otherwise. We see from Eqn.(3.43) that this Kanzaki force distribution is non-zero only in a finite region centred on the glide plane equal to the range of the force constants [25, 55]. The lattice symmetry in the z direction is retained and the crystal is treated as a 2D arrangement of infinitely long, rigid atomic rows. The Kanzaki forces, Eqn.(3.43), introduce a relative displacement of atomic rows on either side of the slip plane equal to $\boldsymbol{B}$ in the harmonic lattice. One could interpret this as a paradox as this violates the small displacement requirement on which the harmonic approximation relies (cf. section 3.2.2). However, the Kanzaki forces merely shift the equilibrium of relative displacement between particles on either side of the cut plane from 0 to B [110].

As outlined above, lattice dynamics is most naturally formulated in Fourier

space. Therefore, in reciprocal space, Eqn.(3.43) yields

$$\begin{aligned}\widetilde{F}_\alpha(\boldsymbol{k},t) &= \sum_{i,j,\beta} B_\beta \Psi_{ij} D_{i\alpha,j\beta} \times \Theta\left(v_d t - x_i\right) e^{-i\boldsymbol{k}\cdot\boldsymbol{r}_i} \\ &= 2\sum_{l'>0} F_{l'\alpha} \sin\left(k_y y_{l'}\right) \frac{e^{-iv_d t k_x}}{k_x + i\epsilon}\end{aligned} \tag{3.44}$$

where the index l' refers to the l^{th} lattice plane above and parallel with the cut plane with

$$\boldsymbol{F}_{l'} = \sum_{j,\beta} B_\beta \Psi_{l'j} D_{l'\alpha,j\beta} \tag{3.45}$$

being the Kanzaki force acting on every atomic row in this plane, and where $\lim \epsilon \to 0^+$ is implied whenever ϵ appears in an expression. Furthermore, to obtain Eqn.(3.44) we used

$$\begin{aligned}&\lim_{\epsilon\to 0^+} \int_{-\infty}^{\infty} \frac{\mathrm{d}k_x}{2\pi} \frac{e^{ik_x x_i}}{k_x + i\epsilon} = -i\Theta(-x_i) \\ \implies &\sum_i \Theta(v_d t - x_i) e^{-ik_x x_i} = i\frac{e^{-iv_d t k_x}}{k_x + i\epsilon}\end{aligned} \tag{3.46}$$

The domain on which Eqn.(3.44) is uniquely defined is $k_x \in [-\infty, \infty], k_y \in [-k_y^b, k_y^b]$, where k_y^b is the maximum value of k_y found in the lattice Brillouin zone [25]. This is because the Kanzaki force distribution as defined in Eqn.(3.43) breaks the crystal symmetry in the x-direction only, leaving the y-direction translation symmetry intact. Finally, using the standard identity

$$\int_{-\infty}^{\infty} \mathrm{d}t\ e^{-i\omega t} = 2\pi\delta(\omega) \tag{3.47}$$

we obtain

$$\widetilde{F}_\alpha(\boldsymbol{k},\omega) = 4\pi \sum_{l'>0} F_{l'\alpha} \sin\left(k_y y_{l'}\right) \frac{\delta\left(\omega + v_d k_x\right)}{k_x + i\epsilon} \tag{3.48}$$

from Eqn.(3.44). Note that we have recovered the usual dislocation–lattice interaction selection rule $\omega = -v_d k_x$ as derived in similar models previously [108–110, 121].

3.4 Uniformly moving dislocations in lattice dynamics models

In order to represent a uniformly moving dislocation in a lattice, all that remains is to plug the driving force and the lattice Green's function in Eqn.(3.19). Hence, from Eqns.(3.19, 3.42, 3.48) we have

$$u_{i\alpha}(t) = \int_{-\infty}^{\infty} \frac{\mathrm{d}\omega}{2\pi} \int_{-\infty}^{\infty} \frac{\mathrm{d}k_x}{2\pi} \int_{-k_y^b}^{k_y^b} \frac{\mathrm{d}k_y}{2k_y^b}\; e^{i(\boldsymbol{k}\cdot\boldsymbol{r}_i + \omega t)} \widetilde{F}_\beta(\boldsymbol{k},\omega) \widetilde{G}_{\alpha\beta}(\boldsymbol{k},\omega) \tag{3.49}$$

$$= 2\int_{-\infty}^{\infty} \frac{\mathrm{d}k_x}{2\pi} \int_{-k_y^b}^{k_y^b} \frac{\mathrm{d}k_y}{2k_y^b}\; e^{i(\boldsymbol{k}\cdot\boldsymbol{r}_i - v_d k_x t)} \sum_{l'>0} F_{l'\beta} \frac{\sin(k_y y_{l'})}{k_x + i\epsilon} \widetilde{G}_{\alpha\beta}(\boldsymbol{k}, -v_d k_x) \tag{3.50}$$

The particular quantity of interest in the case of dislocations is the magnitude of the displacement jump caused by a moving dislocation as it passes a particular point in the lattice. Let's define this displacement jump as the relative displacement between the rows immediately above ($y = y_1$) and below

($y = y_{-1}$) the glide plane

$$\Delta u_{i\alpha}(t) = u_\alpha(x_i, y_1, t) - u_\alpha(x_i, y_{-1}, t) \tag{3.51}$$

which can be evaluated as

$$\Delta u_{i\alpha}(t) = \frac{4i}{k_y^b \pi M} \sum_{l'>0,b,\beta} \int_0^{k_y^b} \mathrm{d}k_y \int_0^\infty \mathrm{d}k_x F_{\beta l'} \sin(k_y y_{l'}) \sin(k_y y_1) \frac{e^{ik_x(x_i - v_d t)}}{k_x + i\epsilon} \times \frac{\tilde{u}_\alpha(\boldsymbol{k}, b)\, \tilde{u}^*_\beta(\boldsymbol{k}, b)}{\omega^2(\boldsymbol{k}, b) - v_d^2 k_x^2 - 2i\Gamma v_d k_x} \tag{3.52}$$

where the $*$ superscript denotes complex conjugation. After some straightforward algebra and using the Sokhotski - Plemelj formula along the real line [160]

$$\lim_{\epsilon \to 0^+} \int_{-\infty}^{\infty} \mathrm{d}x \, \frac{f(x)}{x \pm i\epsilon} = \mp i\pi\delta(x) + \mathcal{P} \int_{-\infty}^{\infty} \mathrm{d}x \, \frac{f(x)}{x} \tag{3.53}$$

where $\mathcal{P}$ indicates the Cauchy principal value, we eventually obtain [25]

$$\begin{aligned} \Delta u_{i\alpha}(t) = & \\ & - \frac{4}{k_y^b \pi M} \sum_{l'>0,b,\beta} \int_0^{k_y^b} \mathrm{d}k_y \int_0^\infty \mathrm{d}k_x F_{\beta l'} \sin(k_y y_{l'}) \sin(k_y y_1) \tilde{u}_z(\boldsymbol{k}, b) \tilde{u}^*_\beta(\boldsymbol{k}, b) \\ & \times \left\{ \frac{(\omega^2(\boldsymbol{k}, b) - v_d^2 k_x^2) \sin\left[k_x(x_i - v_d t)\right] + 2\Gamma v_d k_x \cos\left[k_x(x_i - v_d t)\right]}{k_x \left[(\omega^2(\boldsymbol{k}, b) - v_d^2 k_x^2)^2 + 4\Gamma^2 v_d^2 k_x^2\right]} - \frac{\pi\delta(k_x)}{2\omega^2(\boldsymbol{k}, b)} \right\} \end{aligned} \tag{3.54}$$

Note that the cosine term of the integrand in Eqn.(3.54) is ill-defined as $\boldsymbol{k} \to (0,0)$. Let $D(\boldsymbol{k})$ be this offending term

$$\begin{aligned} D(\boldsymbol{k}) =& F_{\beta l'} \sin(k_y y_{l'}) \sin(k_y y_1) \tilde{u}_z(\boldsymbol{k}, b) \tilde{u}^*_\beta(\boldsymbol{k}, b) \\ & \times \left\{ \frac{2\Gamma v_d \cos\left[k_x(x_i - v_d t)\right]}{(\omega^2(\boldsymbol{k}, b) - v_d^2 k_x^2)^2 + 4\Gamma^2 v_d^2 k_x^2} \right\} \end{aligned} \tag{3.55}$$

Keeping leading order terms in k_x and k_y only, taking the limit $\boldsymbol{k} \to (0,0)$ yields

$$\lim_{\boldsymbol{k}\to(0,0)} D(\boldsymbol{k}) \propto \frac{k_y^2}{k_x^2(1+k_y^2)} \tag{3.56}$$

where we have dropped all constants and used [104]

$$\lim_{\boldsymbol{k}\to(0,0)} \omega^2(\boldsymbol{k}) \propto k_x^2 + k_y^2 \tag{3.57}$$

It is clear that limit expressed in Eqn.(3.56) is not defined as its result is path-dependent: for any path with $k_x = 0$, the limit in Eqn.(3.56) diverges. However, this singularity can be avoided using a $k_x = 1/\lambda$ substitution since

$$\begin{aligned} \int_0^\infty \mathrm{d}k_x D(\boldsymbol{k}) = \int_0^\infty & \mathrm{d}\lambda F_{\beta l'} \sin(k_y y_{l'}) \sin(k_y y_1) \tilde{u}_z(\boldsymbol{k'}, b) \tilde{u}^*_\beta(\boldsymbol{k'}, b) \\ & \times \left\{ \frac{2\Gamma v_d \lambda^2 \cos\left[(x_i - v_d t)/\lambda\right]}{(\lambda^2 \omega^2(\boldsymbol{k'}, b) - v_d^2)^2 + 4\Gamma^2 v_d^2 \lambda^2} \right\} \end{aligned} \tag{3.58}$$

is well-defined on the whole domain including the integration limits and where $\boldsymbol{k'} = (1/\lambda, k_y)$. Thus Eqn.(3.54) may be evaluated in $\boldsymbol{k'}$ space.

To summarise, in this chapter an expression for the displacement jump

across the cut plane for a uniformly moving dislocation in an atomic lattice was derived (Eqn.(3.54)). Furthermore, we derived from first principles its constituent parts: the lattice Green's function and the dislocation Kanzaki forces (Eqns.(3.42) & (3.48)). In the next chapter it will be explained how Eqn.(3.54) may be solved numerically to study the uniform motion of screw and edge dislocations in realistic metals.

4 Modern lattice models

This chapter was partly published in [55] under a CC BY 4.0 license.

The rest of this thesis will focus on the solution of Eqn.(3.54) and the conclusions that may be drawn from them. Although it may seem straightforward to perform this integral numerically, it is worth focusing on two terms in particular: the dispersion of lattice waves $\omega(\boldsymbol{k}, b)$ and the Kanzaki forces $\boldsymbol{F}_l$. Namely, the evaluation of these quantities from modern MD interaction potentials is what sets apart this work from the early lattice models discussed in section 2.4.1.

4.1 Evaluating the lattice dispersion relation

It is evident from Eqns.(3.38) and (3.45) that both the dispersion of lattice waves and the Kanzaki forces for dislocations depend on the evaluation of the force constants matrix $D_{i\alpha,j\beta}$. Here, it is computed from MD interaction potentials of the embedded atom method (EAM) variety [133, 154, 155]. However, they may also be obtained from first principles [161, 162] or from phenomenological interatomic potentials such as those available for MD simulations [163]. A lattice statics code[1] was written and employed in a central

[1] https://github.com/jonasverschueren/latstat

difference method with step size h to approximate the force constant matrix as

$$D_{i\alpha,j\beta} = \frac{f_{j\beta}(r_{i\alpha} - h) - f_{j\beta}(r_{i\alpha} + h)}{2h} \tag{4.1}$$

where $\boldsymbol{r_i}$ is the position of particle i in the lattice and Greek indices run over the Cartesian axes as before. Here $\boldsymbol{f}_j$ is the force induced on atom j upon displacing atom i along Cartesian direction α by $\pm h$.

A few details merit further clarification with regards to the force constants of a perfect monatomic crystal. In a computational scheme to derive these from MD interaction potentials one begins with generating a periodic supercell from the lattice's unit cell. This supercell needs to be sufficiently large such that there are no spurious self-interactions of particles with their periodic image. Then one may obtain the force constants for a monatomic lattice from Eqn.(4.1) as shown below in Algorithm 1, expressed in pseudo-code. Once the force constants of the supercell are known, it is trivial to obtain the dynamical matrix from Eqn.(3.37). Subsequently the lattice dispersion relation $\omega(\boldsymbol{k}, b)$ and polarisation vectors $\tilde{u}_\alpha(\boldsymbol{k}, b)$ may be obtained by calculating the eigenvalues and eigenvectors of this dynamical matrix (cf. Eqn.(3.38)).

Result: Force constants matrix $D_{i\alpha,j\beta}$

Generate sufficiently large periodic supercell;

Choose some $i \in [1, 2, \ldots N]$;

forall $\alpha \in [0, 1, 2]$ **do**

  forall $j \in [1, 2, \ldots N]$ **do**

    $r_{i\alpha} += h$;

    Evaluate $\boldsymbol{f}_j(r_{i\alpha} + h)$;

    $r_{i\alpha} -= 2h$;

    Evaluate $\boldsymbol{f}_j(r_{i\alpha} - h)$;

    $r_{i\alpha} += h$;

    forall $\beta \in [0, 1, 2]$ **do**
      $D_{i\alpha,j\beta} = \left[f_{j\beta}(r_{i\alpha} - h) - f_{j\beta}(r_{i\alpha} + h)\right]/(2h)$;

    end

  end

end

Algorithm 1: Algorithm to evaluate all the force constants for a monatomic supercell consisting of N particles. The generated periodic supercell is deemed sufficiently large when there are no spurious interactions across the periodic boundaries. Note that this brute force method yields $3 \times 3N$ force constants values.

4.1.1 Force evaluations for tabulated EAM potentials

In the previous section it was demonstrated how one may obtain the force constants, lattice dispersion and lattice wave polarisations for a monatomic lattice from MD interaction potentials. However, we glossed over the crucial step of evaluating the force on a particle in the lattice. In this section it will be explained how this is achieved for EAM interaction potentials [133, 134]. Interatomic potentials derived from the semi-empirical embedded atom method are a sum of two terms: the N-body term U_N and a pair-potential contribution U_P [133, 134]. For a collection of N particles the total energy takes the functional form

$$E_{tot} = U_N + U_P \tag{4.2}$$

$$U_N = \sum_i F(\rho_i) \tag{4.3}$$

$$\rho_i = \sum_{j \neq i} \phi(r_{ij}) \tag{4.4}$$

$$U_P = \frac{1}{2} \sum_{j \neq i} V(r_{ij}) \tag{4.5}$$

where F is the embedding function, ρ_i represents the local electronic charge density at atomic site i, $\phi(r_{ij})$ and $V(r_{ij})$ are functions provided by the particular EAM potential and $r_{ij} = |\mathbf{r}_i - \mathbf{r}_j|$. To obtain the α component of the force on some particle i $f_{i\alpha}$, the first derivative of the total interaction

energy has to be evaluated. From Eqn.(4.2) it can be seen that [134]

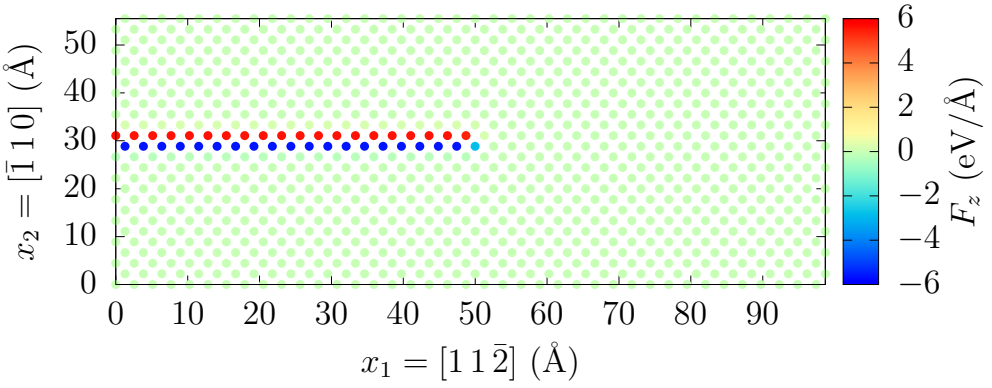
$$f_{i\alpha} = -\frac{\partial E_{tot}}{\partial r_{i\alpha}} \tag{4.6}$$

$$= -\sum_{j\neq i} \left(F'(\rho_i) + F'(\rho_j)\right) \phi' \frac{r_{ij\alpha}}{r_{ij}} - \sum_{j\neq i} V' \frac{r_{ij\alpha}}{r_{ij}} \tag{4.7}$$

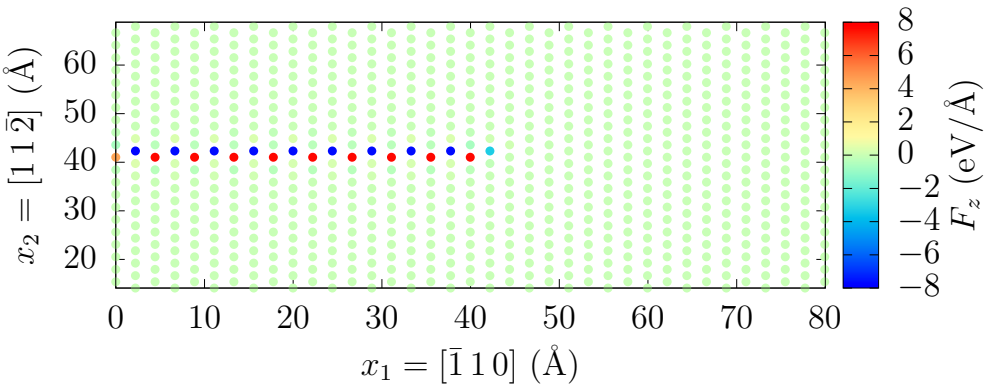
after some simple algebra as shown in [134]. In MD packages such as LAMMPS [164] the particle interactions are evaluated from pre-calculated values for F, ϕ and V at specified values of ρ and r_{ij}. In this work, these tabulated values were interpolated using a standard cubic spline interpolation scheme for the evaluation of the respective terms in Eqn.(4.6) and their first order derivatives.

4.2 The Kanzaki force distribution

Before diving into the results chapter it is worth looking at the static Kanzaki force distribution in more detail. As an illustrative example we will discuss the Kanzaki forces of a screw dislocation in BCC tungsten [155]. In Figs.(4.1) the z-component of the Kanzaki force distribution is plotted for a screw dislocation in tungsten [155]. Away from the core, we observe that along the first atomic row there acts two forces of equal magnitude but opposite sign. If the cut plane is placed along the $x_2 = [1\,1\,\bar{2}]$ direction, the average force at either side of the cut surface is $\pm 5.602\text{eV/Å}$ in the first layer immediately above and below the cut surface, and $\mp 0.22\text{eV/Å}$ along the second layer. In



(a) Cut across $(\bar{1}\,1\,0)$.



(b) Cut across $(1\,1\,\bar{2})$.

Figure 4.1: Magnitude of the F_z Kanzaki forces across the cut surface for a $1/2\langle 1\,1\,1\rangle$ screw dislocation in BCC tungsten [155]. Note that the Kanzaki forces are the fictional forces that generate the required displacement discontinuity across the glide plane in an harmonic lattice. They should not be mistaken for the physical forces between the particles in the real lattice. *Reproduced with permission (CC4.0) from [55].*

the subsequent atomic layers, these forces are negligible. If on the other hand the cut is placed along the $x_2 = [\bar{1}\,1\,0]$ direction instead (see Fig.4.1a), the magnitude of the slip Kanzaki forces is $\pm 7.636\text{eV/Å}$ along the first layer, and $\mp 0.24\text{eV/Å}$ along the second layer. Despite this seeming dependence of the Kanzaki forces on the cut plane orientation, it is in fact irrelevant. The differences in magnitudes are due to the different interatomic spacing between the atoms at either side of the cut. The net distributed force is the same irrespective of where the cut is placed, confirming the well-known feature of the Volterra dislocation that the orientation of the cut surface is irrelevant in generating the dislocation. Thus, the Kanzaki forces across the cut surface appear to be extremely short range, and heavily localised at either side of the slip surface. Although only the Kanzaki forces for a screw in tungsten are shown, this observation is more generally applicable and holds for edge dislocations and different materials as well[2].

[2]B. Gurrutxaga-Lerma and J. Verschueren, *General theory of the Kanzaki force field of extended defects, with applications to the modelling of edge dislocations*, in preparation.

5 Results

This chapter was partly published in [25] under a CC BY 4.0 license.

In this chapter, results for the dynamics of the displacement jump derived fom Eqn.(3.54) will be presented. These will be compared directly to equivalent MD simulations. First, we will study a simplified model of a screw dislocation propagating in a cubic lattice with nearest neighbour interactions. Although arguably oversimplified, it is the only lattice model discussed in the existing literature body (cf. section 2.4.1). Furthermore, this case very clearly demonstrates the atomic mechanism by which resonances in the dislocation–lattice interaction may result in the kinematic generation of screw dislocations. In the second half of this chapter we will extend the validity of these results to realistic materials as we will present equivalent results derived from modern MD interaction potentials as discussed in the previous chapter. The existence of instabilities will be demonstrated in tungsten. This shows explicitly that resonances in the atomic dislocation–lattice interactions may be more relevant to models of gliding dislocations than previously thought. The equivalent aluminium results on the other hand show that the strength of the resonances is highly material dependent.

5.1 The simple cubic lattice

As discussed in chapter 4, an in house lattice statics code[1] was written to evaluate Eqn.(3.54) for MD interaction potentials. This lattice statics code was then coupled to *cubature*[2], a numerical integration library, to perform the inverse Fourier transform expressed in Eqn.(3.54). First, results were obtained for a uniformly moving screw dislocation in a square lattice with lattice constant a and the dislocation line parallel to a cube edge. Atomic rows interact only with their nearest neighbours

$$U^h(u_{z,ij}) = \frac{K}{2} u_{z,ij}^2 \tag{5.1}$$

where K is the harmonic force constant and $u_{z,ij} = u_z(\mathbf{r}_i) - u_z(\mathbf{r}_j)$. This is the lattice as studied by Caro and Glass in [113] and drawn schematically in Fig.(3.1). All results were evaluated with the minimal Γ that ensured convergence of the results. In Fig.(5.2) we make 3 observations. Firstly, a resonance is present for dislocations travelling at $v_d = 0.3c_t$, far below the shear wave speed of the lattice c_t. This is in agreement with previous studies on the mobility of a screw dislocation in comparable lattices [108–110, 113]. These works and others [119–121] also explain in detail why the resonance occurs at this velocity. The focus here is on the physical consequences of this resonance. With increasing velocity, we observe the expected screw

[1] https://github.com/jonasverschueren/latstat
[2] https://github.com/stevengj/cubature

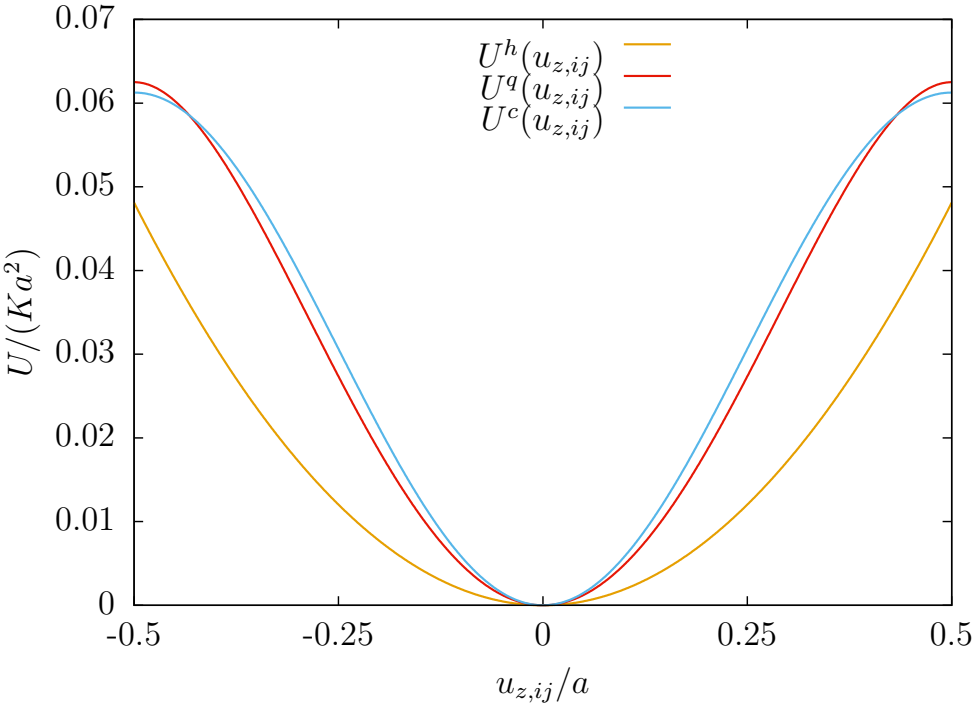


Figure 5.1: The quartic interaction potential U^q from Eqn.(5.2) as used in the square lattice MD simulation. It is compared to the harmonic potential U^h assumed in lattice dynamics models (cf. Eqn.(5.1)) and the cosinusoidal potential $U^c \propto 1 - \cos(2\pi u/a)$ used in [124]. Note that all potentials assume periodic boundary conditions $U(x) = U(x + n)$ for $n \in \mathbb{N}$. Furthermore, the interaction constant K was scaled such that the theoretical shear strengths of all potentials are equal.

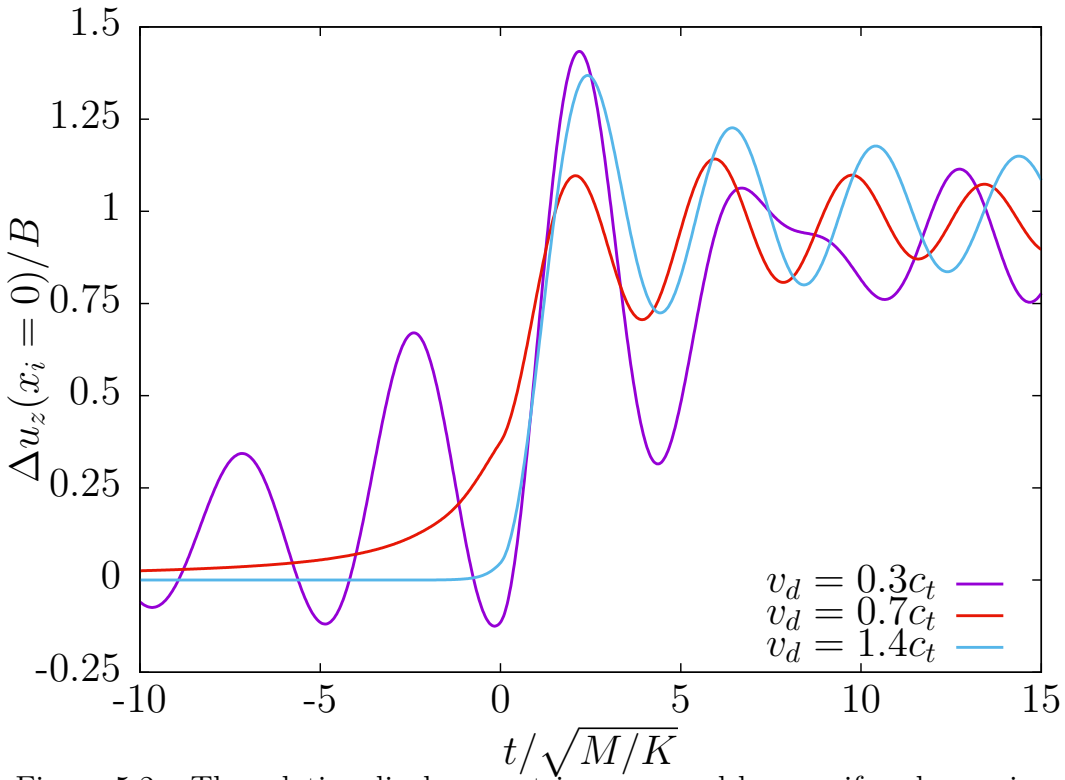


Figure 5.2: The relative displacement jump caused by a uniformly moving screw dislocation with velocity v_d in the simple cubic model as computed from Eqn.(3.54). Note the resonance for $v_d = 0.3c_t$. *Reproduced with permission (CC4.0) from [25].*

dislocation behaviour: as the dislocation passes $x_i = 0$, $\Delta u_z(x_i)$ jumps from 0 to B, around which it oscillates with decreasing amplitude. The initial overshoot increases with increasing v_d and plateaus at $1.4B$. Finally, contrary to continuum model predictions (cf. section 2.2) nothing extra-ordinary is seen to occur for $v_d = c_t$.

The simple cubic lattice dynamics model was compared with an MD simulation in an identical arrangement, where atomic rows interacted through

a quartic interaction potential

$$U^q(u_{z,ij}) = \frac{Ka^2}{2}\left(\left(\frac{u_{z,ij}}{a} \bmod 1\right)^2 - 2\left(\frac{u_{z,ij}}{a} \bmod 1\right)^4\right) \tag{5.2}$$

such that $U^q(x) = U^q(x + na)$ for $n \in \mathbb{Z}$ (cf. Fig.(5.1)). A simple cubic lattice was constructed comprising 100 by 100 atoms along x and y axes, and just 1 atom along z with periodic boundary conditions in this direction. Free boundary conditions were used in the other two directions. A homogeneous shear stress $\sigma_{yz} = 13\sigma_{th}/20$ was applied to the lattice, where $\sigma_{th} = Ka/(3\sqrt{3})$ is the theoretical shear strength, and the lattice was relaxed. Then a screw dislocation was injected by instantaneously displacing the lattice planes $y = 50a$ and $y = 51a$ by $\pm a/2\,\hat{\mathbf{z}}$ respectively for $x < 50a$. Subsequently, the MD simulation was run in the NVE ensemble whilst maintaining the uniform driving stress σ_{yz} and was stopped before the fastest travelling lattice waves emanating from the dislocation reached the box boundary. The dislocations were observed to reach their terminal velocity in just a few time units ($\sqrt{M/K}$) after their injection, in agreement with [124]. Furthermore, the velocity was observed to be almost perfectly uniform, confirming that the Peierls barrier is negligible in the pure glide regime.

Fig.(5.3) shows the observed $\Delta u_z(t)$ along the glide plane for $v_d = 0.72c_t$. It can be seen that at early times ($t < 35$ in Fig.(5.3a) the glide plane profile is exactly what one would expect for a propagating dislocation: $\Delta u_z = 0$ before and $\Delta u_z \approx B$ behind the dislocation. However, over time the initial

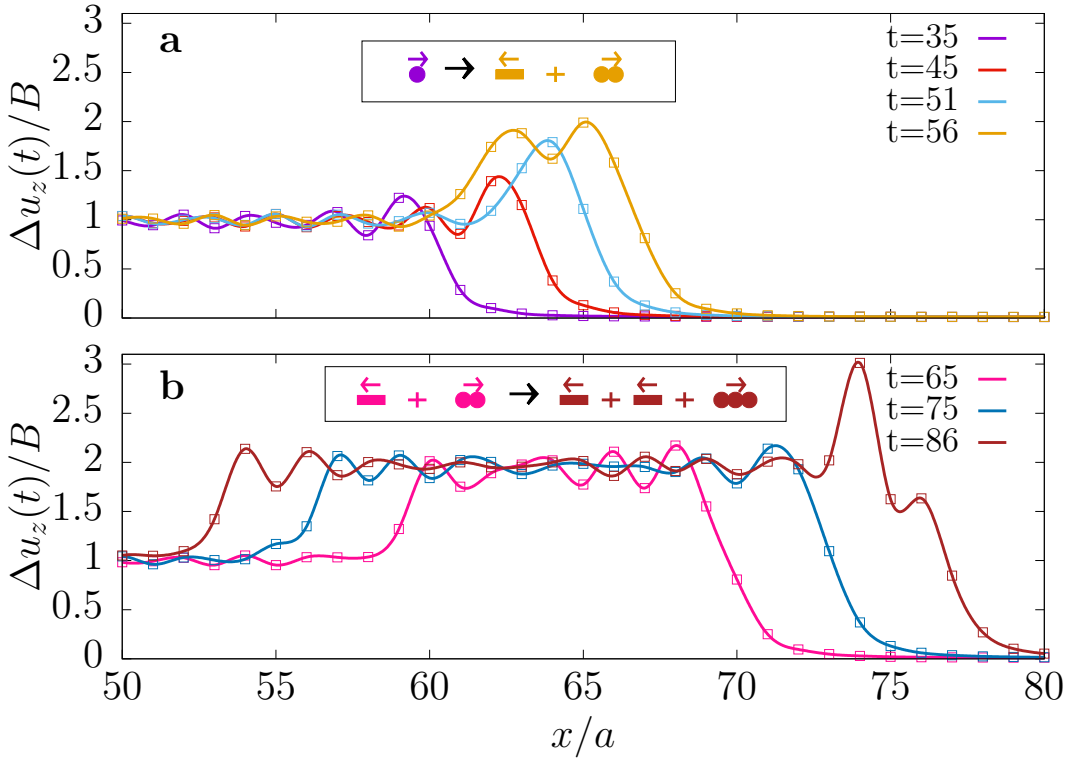


Figure 5.3: $\Delta u_z(t)$ on the glide plane as observed in the MD with quartic interaction potential U^q at different times expressed in units of $\sqrt{M/K}$. A single dislocations is injected at $x = 50a$ at $t = 0$ and travels to the right. The first kinematic generation event is shown in a), followed by the second event in b). Their associated dislocation reactions are shown in the top insets where circles and rectangles represent screw dislocations of opposite handedness and the above them indicate the directions of travel. *Reproduced with permission (CC4.0) from [25].*

overshoot increases in magnitude which builds up to a critical point at which the dislocation causes a relative displacement jump of $2B$. This necessarily gives rise to a displacement jump of $-B$ behind the initial dislocation which can be seen to propagate in the opposite direction to the original dislocation. This is a kinematic generation mechanism [6] with dislocation reaction equation $B \Rightarrow 2B + -B$, represented in the top inset of Fig.(5.3) and mentioned in section 2.2.4. Following this initial generation event, the dislocations propagate until the same mechanism produces another kinematic generation event, shown in Fig.(5.3). It is clear that these are only the first two kinematic generation events of a subsequent cascade.

From the lattice dynamics model above we can explain this kinematic generation mechanism as follows: At critical dislocation velocities, Δu_z exceeds $1.5B$ which will result in the kinematic generation mechanism discussed above. In the MD this point is reached more easily compared to the lattice dynamics model as the stiffness decreases with increasing separation between atoms. This shows that the lattice models can be considered to be a limiting case: if the overshoot goes beyond $1.5B$ in the lattice model, it is likely that this mechanism is accessible in a real crystal.

5.2 Uniformly moving dislocations in real crystals.

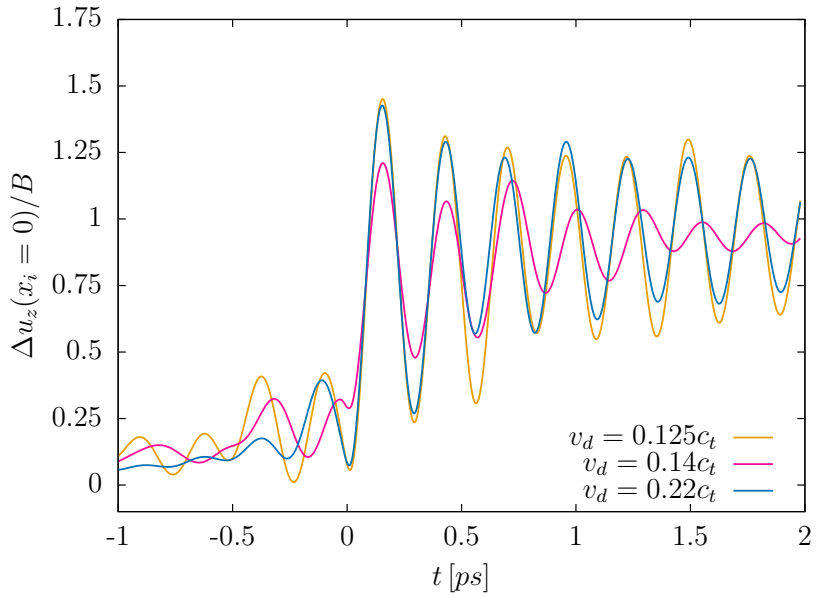
Now, we will investigate the uniform motion of both screw and edge dislocations in more realistic metals, described using modern MD interaction potentials [154, 155]. For BCC tungsten, we will first discuss the lattice model results derived from Eqn.(3.54) and then compare these to equivalent MD simulations. For FCC aluminium, only lattice model results will be presented. In particular, gliding screw and edge dislocations with dislocation line along the z-axis and travelling with speed v_d along the x-axis will be treated.

5.2.1 Gliding dislocations in tungsten

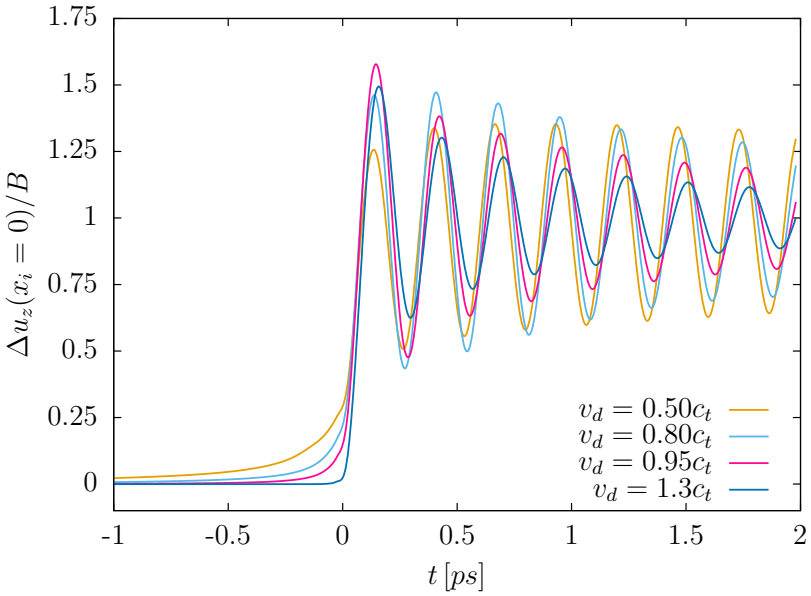
First, let us focus on the lattice dynamics model of a uniformly moving screw with Burgers vector $(0, 0, B)$ in a BCC tungsten crystal [155] with orientation such that the [1 1 1] crystal direction is aligned with the z-axis of the simulation box. Eqn.(3.54) was solved for this topology and the results may be found in Figs.(5.4) and (5.5). Note that the shear wave speeds c_t cited here are merely taken as reference values, calculated from the interaction potentials' C_{44} elastic constants [154, 155], ignoring its direction dependence in real crystals [64]. For future reference, $c_t = 2.85$ km/s was used for tungsten and $c_t = 3.45$ km/s for aluminium.

From Figs.(5.4) and (5.5), two observations may be made. Firstly, comparing Figs.(5.4a) and (5.5a), it is clear that the orientation of the lattice seems to have a significant impact on $\Delta u_z(t)$. This seems to contradict previous claims that the cut plane orientation is irrelevant for Volterra dislocations (cf. section 4.2 and [55]). However, this only holds for static properties of dislocations: it is clear that the dynamic properties should change given that the Kanzaki force magnitudes do depend on the orientation of the crystal as discussed in section 4.2.

Secondly, we may discern two distinct velocity regimes. For velocities above $\sim 0.3c_t$ (Figs.(5.4b) and (5.5b)), $\Delta u_z(t)$ behaves as one would intuitively suspect for a screw dislocation. Far ahead of the dislocation, the displacement jump is small but grows as the screw approaches. As the dislocation passes, the displacement jump initially overshoots B but over time converges to this value. It is clear that if the initial overshoot exceeds $1.5B$, dislocation motion becomes unstable as the kinematic generation mechanism discussed in the previous section may start to act. At lower speeds, $\Delta u_z(t)$ shows clear signs of resonance as it oscillates wildly as can be seen most clearly in Fig.(5.5a). This corresponds to the resonances in the dislocation–lattice interactions observed for screw dislocations in simple cubic lattices discussed in section 5.1 and in the literature [108–110, 113]. It is evident that dislocation motion at speeds that excite this instability are unstable too, given the magnitude of the oscillations they generate. Again, nothing of note occurs at $v_d = c_t$.

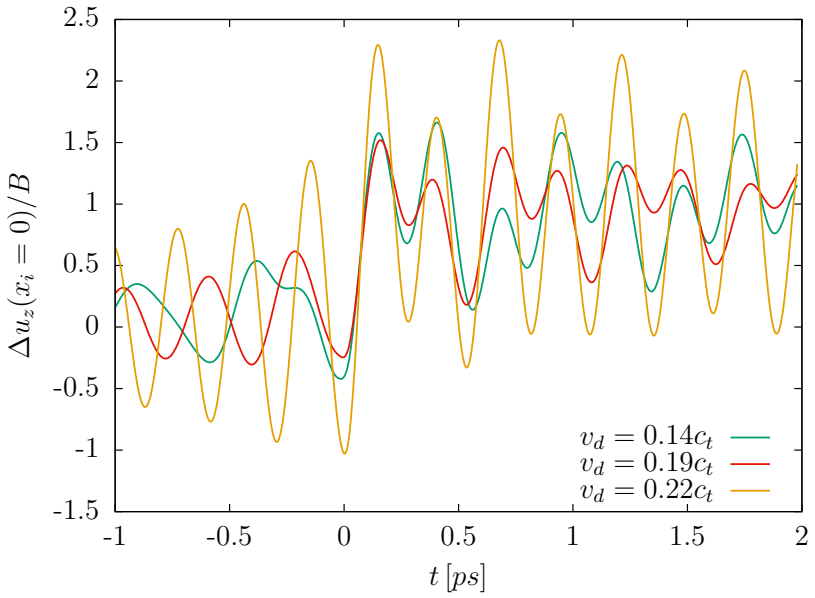


(a) Low velocity resonances

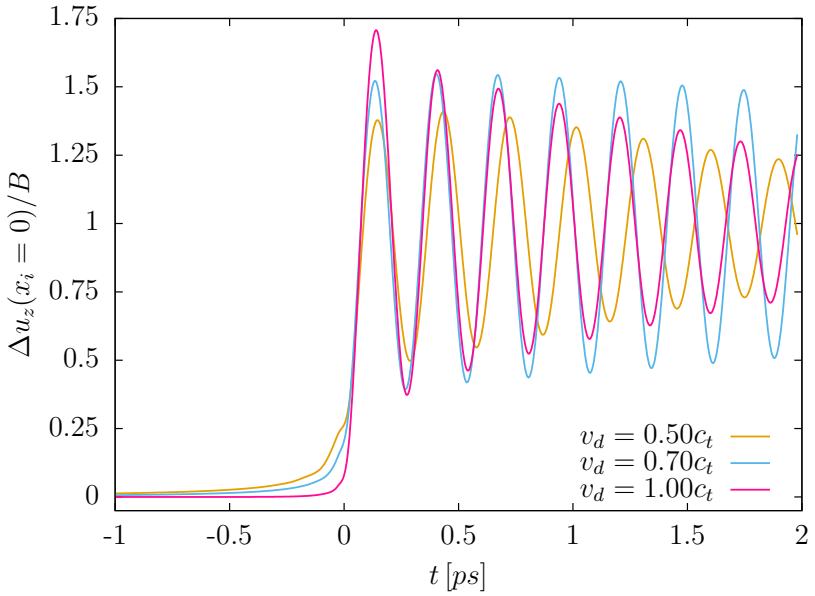


(b) High velocity instabilities

Figure 5.4: Observed $\Delta u_z(t)$ derived from Eqn.(3.54) for a screw dislocation with $\boldsymbol{B} = (0, 0, B)$ and $\boldsymbol{v_d} = (v_d, 0, 0)$ in BCC tungsten [155] with Cartesian axes aligned with the $[\bar{1}\,0\,1], [1\,\bar{2}\,1]$ and $[1\,1\,1]$ crystal directions respectively.



(a) Low velocity resonances.



(b) High velocity instabilities.

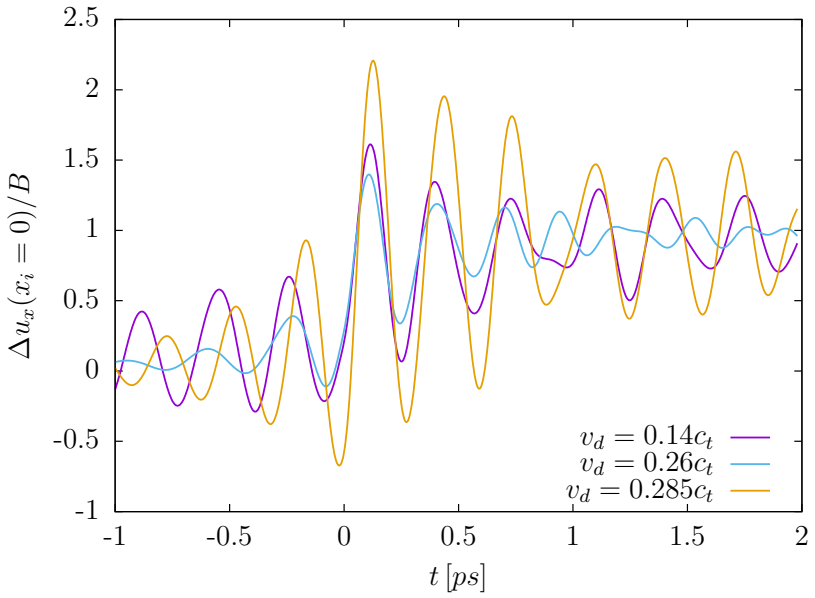
Figure 5.5: Same plot as Fig.(5.4), the only difference being that the Cartesian axes are now aligned with the $[\bar{1}\,2\,\bar{1}]$, $[\bar{1}\,0\,1]$ and $[1\,1\,1]$ crystal directions respectively. The dependence of $\Delta u_z(t)$ on crystal orientation is particularly evident upon comparison of Figs.(5.4a) and (5.5a).

Similar observations and remarks hold for uniformly moving edge dislocations with Burgers vector $(B, 0, 0)$ in the same BCC tungsten [155] crystal; results are shown in Figs.(5.6) and (5.7). More specifically, the dependence of crystal orientation is recovered. Furthermore, the potential instabilities for slow moving dislocations, due to resonances with the lattice vibrations, and faster ones, due to the initial overshoot magnitude exceeding $1.5B$, may be discerned.

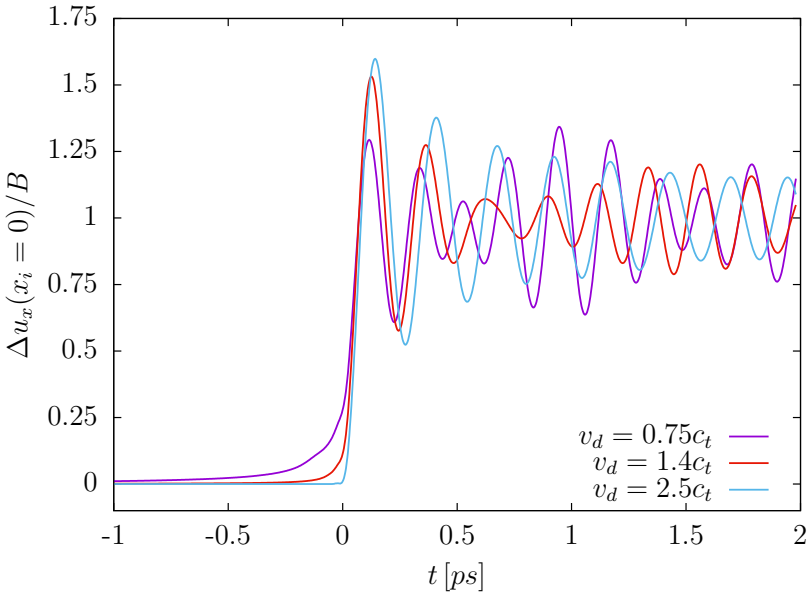
We[3] have compared the tungsten lattice dynamics model to an equivalent MD simulation of a uniformly moving screw dislocation, employing LAMMPS[4] [164] and the same embedded atom interatomic potential for BCC W [155]. A $1/2\langle 1\,1\,1\rangle$ screw dislocation gliding along $x = [1\,1\,\bar{2}]$ was initially inserted by displacing the perfect lattice atoms according to the displacement field predicted by elasticity using Atomsk [167], in a box of dimensions $80\times50\times30$ unit cells with $x = [1\,1\,\bar{2}]$,$y = [1\,\bar{1}\,0]$ $z = [1\,1\,1]$ subject to periodic boundary conditions. The system was then equilibrated using a conjugate gradient minimisation to recover the 0K dislocation structure [164, 168], and then thermalised in the NVT ensemble for 10ps to the target temperature. Subsequently the MD simulation was run in the NVE ensemble by applying a constant force in the z direction on the first two top and bottom atomic layers (cf. [143, 150]). To prevent overheating due to the applied loads, the second and third layers were thermalised in the NVT ensemble throughout

[3]More specifically, the MD simulations discussed in the remainder of this section and presented in Fig.(5.8) were performed by BGL.

[4]http://lammps.sandia.gov

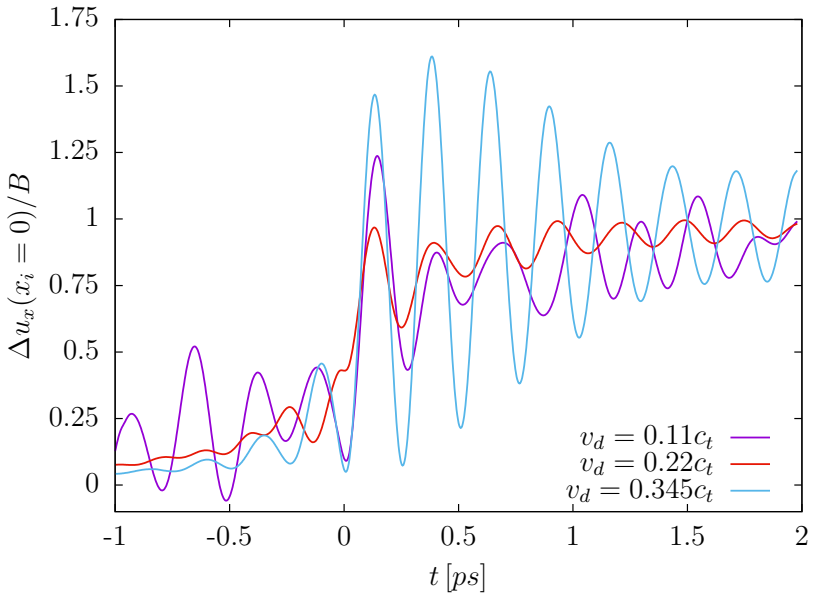


(a) Low velocity resonances.

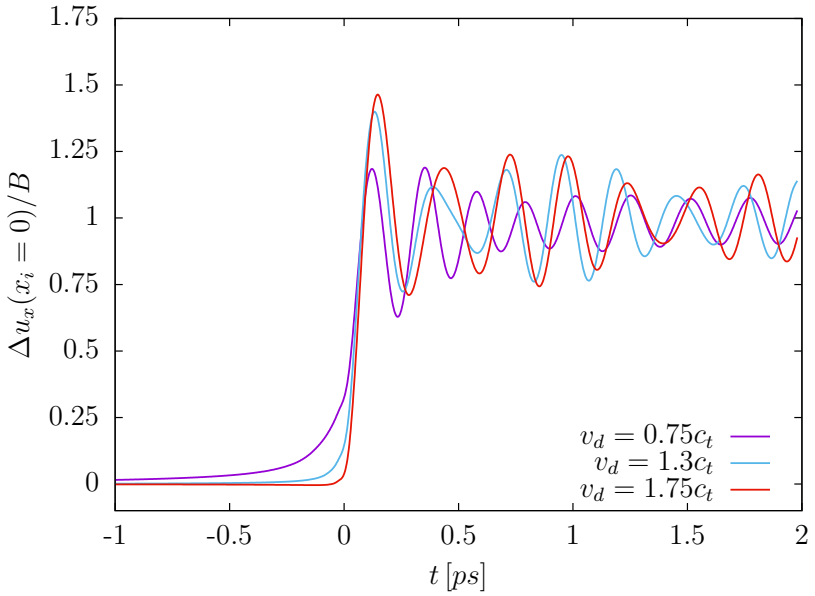


(b) High velocity instabilities

Figure 5.6: Observed $\Delta u_x(t)$ derived from Eqn.(3.54) for an edge dislocation with $\boldsymbol{B} = (B, 0, 0)$ and $\boldsymbol{v_d} = (v_d, 0, 0)$ in BCC tungsten [155] with Cartesian axes aligned with the $[1\,1\,1], [\bar{1}\,0\,1]$ and $[1\,\bar{2}\,1]$ crystal directions respectively.



(a) Low velocity resonances.



(b) High velocity instabilities.

Figure 5.7: Same plot as Fig.(5.6), the only difference being that the Cartesian axes are now aligned with the $[1\,1\,1], [\bar{1}\,2\,\bar{1}]$ and $[\bar{1}\,0\,1]$ crystal directions respectively. Again, the dependence of $\Delta u_x(t)$ on crystal orientation is particularly evident upon comparison of Figs.(5.6a) and (5.7a).

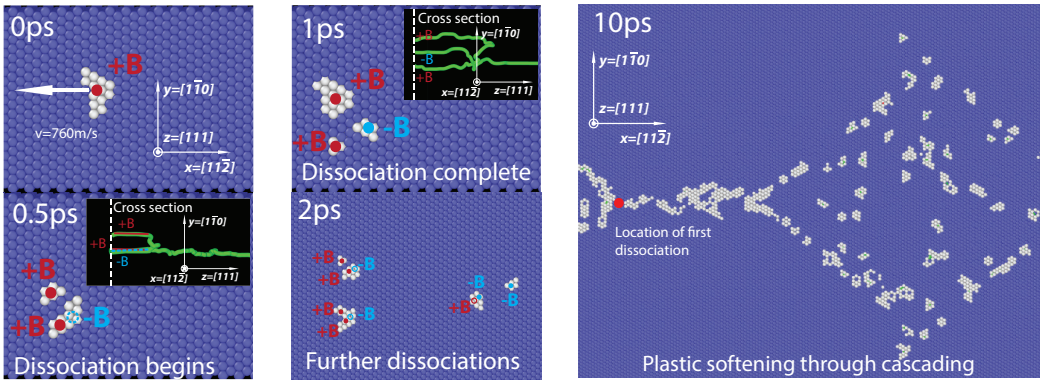


Figure 5.8: Snaphsot of the kinematic generation dissociation process observable in MD simulations of BCC W at 125K. The dislocation positions were found using the DXA algorithm [165] as implemented in Ovito [166]. White shaded particles indicate regions of considerable disregistry. Figure produced by BGL. *Reproduced with permission (CC4.0) from [25].*

(cf.[168]). As can be seen in the series of snapshots in Fig.(5.8), upon reaching a velocity of 709.74 ± 356.84m/s at an external load of around 250MPa, the original dislocation was seen to dissociate into a $+2B$ and a $-1B$ dislocation on different $\{1\,1\,2\}$ planes. This kinematic generation mechanism was observed for target temperatures of of 10K, 50K, 125K, 298K, and 450K and was solely dependent on the dislocation reaching the target critical velocity of $\approx 0.27c_t$. It is clear that this velocity has to be sustained for a duration in the region of 1 ps to give the generation mechanism time to act. This is in good agreement with the $v_d = 0.22c_t$ resonance determined from the tungsten lattice dynamics model (cf. Fig.(5.5a)). Further dissociations resulted in a cascade and substantial plastic softening of the system as shown in Fig.(5.8). The cascade is accompanied by dissipation of energy from the

dislocation cores as heat. Thus, kinematic generation offers a feasible onset mechanism for adiabatic shear banding in loading regimes where dislocation speeds are large [169].

5.2.2 Gliding dislocations in aluminium

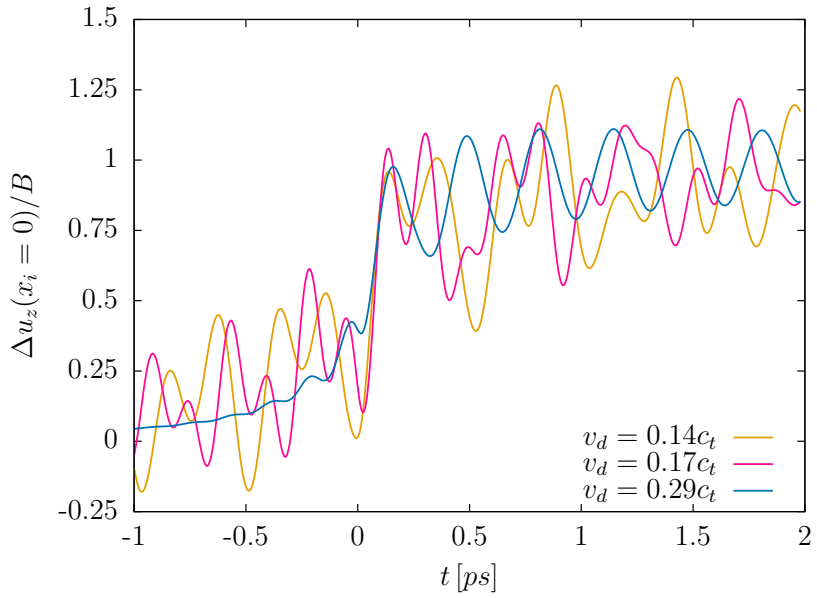
The lattice dynamics results obtained from Eqn.(3.54) for FCC aluminium [154] are displayed in Figs.(5.9) and (5.10). It is immediately clear that both the low and high velocity instabilities are much less pronounced in comparison with the tungsten results discussed in the previous section. For the edge in the high velocity region, the largest initial overshoot was observed to be only $1.11B$ as can be seen in Fig.(5.10b). This is in clear contrast with the equivalent tungsten result from Fig.(5.7b). Despite this, it is still possible that aluminium possesses the same instabilities as tungsten as the lattice model may be considered to be a conservative estimate of the oscillation magnitudes of the displacement jump (cf. section 5.1).

Although the strong material dependence of the instability is an interesting observation in itself, it is debatable whether the lattice dynamics model culminating in Eqn.(3.54) is adequate to describe gliding dislocations in aluminium. In FCC metals, dislocations tend to dissociate into partials [6]. This is in no way captured in the lattice model but is a considerable source of additional complexity as the partials that make up the gliding dislocation will interact themselves and give rise to a whole host of additional physical processes. These in turn put the uniform motion assumption - at the very

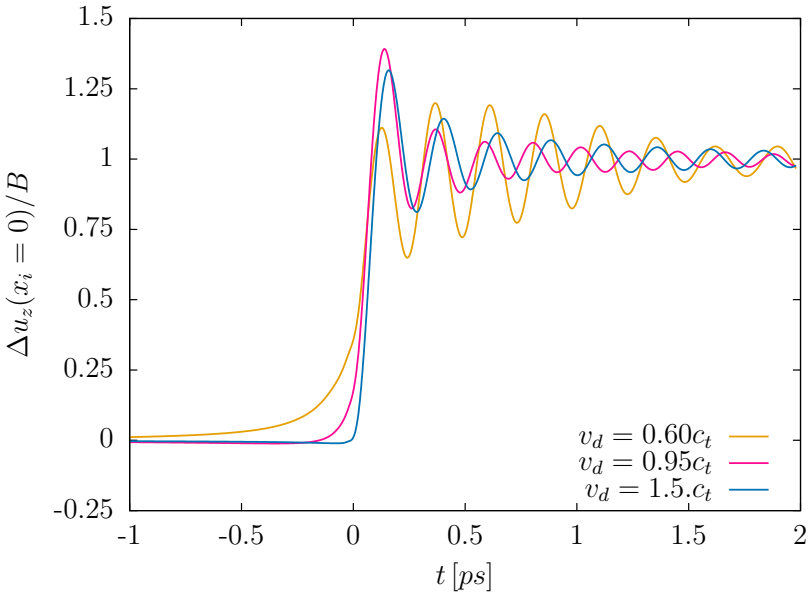
core of the lattice model discussed in this thesis - under pressure. Therefore, no attempt to compare the results of this lattice model with equivalent MD simulations will be made here. It is clear that delving further into these concerns should be the subject of potential future work. We will return to this point in chapter 6.

5.3 Revisiting kinematic generation and supersonic dislocations

The resonances uncovered by the lattice models discussed in the previous chapters were found to be an onset mechanism for kinematic generation. This has direct consequences with regards to the existence of supersonic dislocations although this discussion was purposefully avoided in the exposition of the results in sections 5.1 and 5.2. To accelerate dislocations beyond the speed of sound, it is likely they will have to pass through instabilities. These affect the motion of the dislocation qualitatively in one of two ways depending on the duration of the kinematic generation mechanism. If the dislocation is accelerated beyond the resonant velocity region quicker than the kinematic generation mechanism needs to act, the instability will be avoided. On the other hand, if the dislocation's acceleration is too small it may get trapped: At resonance the kinetic energy of atoms in the dislocation core will rise and be converted into the generation of dislocation pairs. The repetition of this process will prevent the dislocation from accelerating through the resonance.

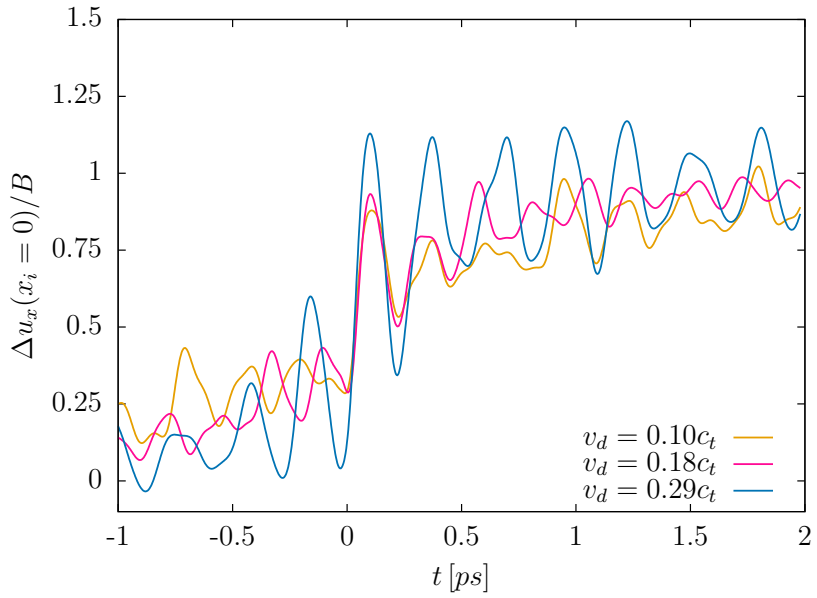


(a) Low velocity resonances.

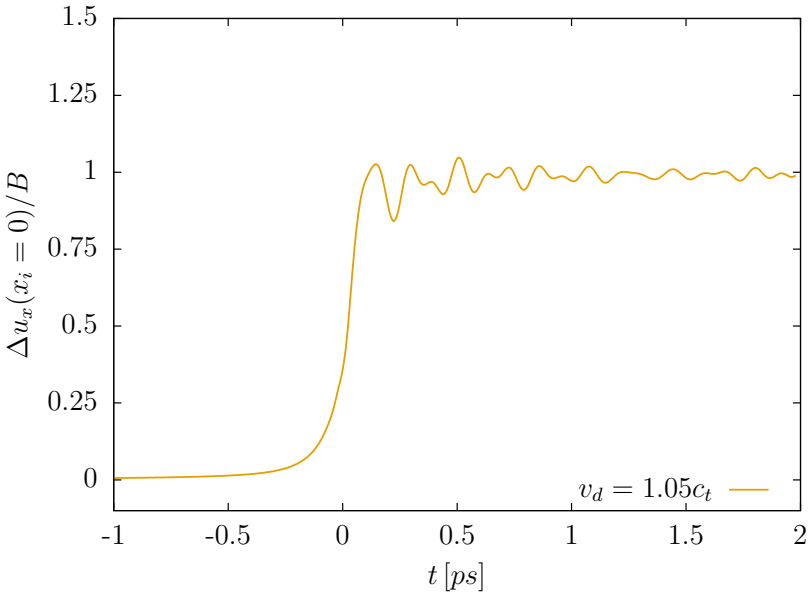


(b) High velocity instabilities

Figure 5.9: Observed $\Delta u_z(t)$ derived from Eqn.(3.54) for a screw dislocation with $\boldsymbol{B} = (0, 0, B)$ and $\boldsymbol{v_d} = (v_d, 0, 0)$ in FCC aluminium [154] with Cartesian axes aligned with the $[1\,\bar{2}\,1], [1\,1\,1]$ and $[\bar{1}\,0\,1]$ crystal directions respectively.



(a) Low velocity resonances.



(b) High velocity behaviour

Figure 5.10: Observed $\Delta u_x(t)$ derived from Eqn.(3.54) for an edge dislocation with $\boldsymbol{B} = (B, 0, 0)$ and $\boldsymbol{v_d} = (v_d, 0, 0)$ in FCC aluminium [154] with Cartesian axes aligned with the $[\bar{1}\,0\,1], [1\,\bar{2}\,1]$ and $[1\,1\,1]$ crystal directions respectively.

This argument for the existence of a hard barrier for dislocation motion is remarkably similar to arguments brought forward from continuum models and the kinematic generation of edge dislocations at the Rayleigh wave speed [6] (cf. section 2.2.4).

Thus, kinematic generation of dislocations is an avoidable barrier to supersonic dislocation motion, which depends on the time available for the mechanism to act. For example, injecting dislocations [44] at supersonic speeds avoids this instability completely. However, it does render dislocation motion beyond them highly dependent on how the instabilities were surpassed. This may explain why despite the numerous MD simulations available in the literature [142, 143, 146, 148–150] there is still no generally accepted dislocation mobility law at high dislocation speeds.

Whether there is sufficient time for a dislocation avalanche to develop will become an additional consideration in larger scale dislocation dynamics simulations [58, 63, 98] and in producing continuum plastic flow rules [170–172]. The velocities at which we observe kinematic generation are much lower than previously thought which will have implications for deformation processes at moderate strain rates, such as adiabatic shear banding [21], dynamic fracture [22, 23], and in describing the Hugoniot state under ramp and shock loading [24]. This extends the relevance of kinematic generation to many industrially relevant processes such as machining [7], forging [8], and wear [20].

The resonances are purely a consequence of the radiation that emerges

due to the periodic breaking and making of bonds across the cut plane as the dislocation moves through the crystal. This is why the instabilities are absent in continuum models. Furthermore, the qualitative agreement between the lattice dynamics models and their equivalent MD simulations in determining the resonant dislocation velocity suggests that the detail of the dislocation core structure is of secondary importance since the former do not include a core description and the latter do.

6 Conclusions & future work

I began this thesis by introducing the fundamental question I would be addressing: *How do high speed dislocations move through a crystalline material?* It was immediately clear that finding the final answer to this rather broad question was probably overly ambitious. However, in the process I was able to provide a plausible explanation for a phenomenon that so far has received little attention in the literature: the existence of instabilities due to resonances in the atomic interactions between the dislocation core and the lattice.

Historically, the dynamics of high speed dislocations has been approached from two distinct points of view. One emphasises the linearly elastic part of the problem using continuum models. In contrast, the other approaches the problem from an atomic scale perspective and emphasises the importance of the dislocation core and its interaction with the crystalline lattice. Unfortunately, disagreements between these intrinsically different approaches have been the topic of many debates in the field, as discussed in the extensive literature study of chapter 2. In this review, I argued that lattice dynamics models strike a useful balance between continuum models and molecular dynamics methods. On the one hand, the qualitative results derived from continuum scale works were shown to be highly dependent on the assumed core model used within them. Furthermore, all these continuum models of

fast moving dislocations failed to capture the *phonon drag* of a dislocation accurately, again due to a lack of appropriate atomistic detail. As explained in section 2.3, this was particularly problematic as this drag term was shown to be the dominant term in dislocation *mobility laws*. These two shortcomings of continuum models strongly suggested that capturing the atomic scale interactions between the dislocation and the lattice in more detail was essential in describing gliding dislocations. Modern MD simulations seemed to provide the obvious solution to this conundrum as they capture the required atomic interactions in great detail. The hope they provided was short lived however as a homogeneous physical picture of high speed dislocations did not emerge from the many MD investigations performed on this topic. As a case in point, we still can not provide *the* mobility law for a particular dislocation topology in a particular metal. Thus, I concluded from the literature study that lattice dynamics models may provide the required atomistic detail to address the high speed dislocation dynamics problem whilst maintaining a level of transferability that allows the qualitative features associated with gliding dislocations to be investigated in general terms.

Subsequently, in chapter 3 the theoretical foundations of the lattice dynamics method were laid out. In particular, the lattice Green's function was derived and it was shown how this could be combined with a Kanzaki type source term to describe the uniform motion of dislocations in a harmonic lattice. Chapter 4 discussed the computational methodology by which the equations from chapter 3 may be translated into a modern lattice dynamics

code.

Then, the motion of a uniformly moving screw dislocation in a simple cubic lattice was discussed in section 5.1. Firstly, the lattice model confirmed the absence of limiting velocities for dislocation motion, suggesting that the persistence of them in continuum models is an artefact of the oversimplified $\omega = ck$ dispersion relation embedded in them. In addition, the lattice dynamics results demonstrated the existence of two types of potential instabilities. At low velocities, below $\sim 0.3c_t$, resonant velocities were shown to exist at which the particles around the glide plane oscillated vigorously as the dislocation passed. At high velocities, the expected displacement jump behaviour was observed: small far ahead of the dislocation and oscillating around a Burgers vector magnitude B far behind. However, in the transient between these two limits an initial overshoot was observed to approach $1.5B$ for velocities of the order of c_t. It was demonstrated in MD simulations of a comparable system that this was the onset for a kinematic generation mechanism for screw dislocations travelling with speeds around $0.72c_t$.

These observations were largely confirmed for gliding edge and screw dislocations in BCC tungsten (cf. section 5.2). For this case however, the MD results seemed to suggest that the low velocity resonance was responsible for the spawning of new dislocations, ultimately causing a cascade. The confirmation of the kinematic generation of screw dislocations in a real crystal due to an instability as uncovered in the equivalent lattice model extended the applicability of the simple cubic results to more realistic systems. Fur-

thermore, since the dislocation—lattice resonance was excited at velocities below the shear wave speed of the material, this indicated that kinematic generation may play a larger role than previously thought in loading regimes where dislocations speeds are large. Finally, it was explained how this instability may have implications for the existence of a limiting velocity for dislocations as it provides a strong energy dissipation mechanism by spawning new dislocations. This account for the existence of a limiting velocity was remarkably similar to a previous explanation from continuum models for gliding edges travelling at the Rayleigh wave speed (cf. section 2.2.4) but the atomistic nature of the onset mechanism, valid for both edges and screws, and the speeds were crucially different. However, the full picture is more complicated as a dislocation travelling at a resonant velocity only spawns new dislocation pairs if it remains in this velocity range at least as long as the activation time of the kinematic generation mechanism.

The presented lattice model aluminium results seemed less clear, demonstrating the strong material dependence of the tungsten findings mentioned above. Namely, the dislocation–lattice resonance was a lot less pronounced as the oscillation magnitudes of the displacement jump were noticeably smaller compared to the equivalent tungsten results. Furthermore, due to the dissociation of dislocations into partials in FCC materials, it was asked whether the lattice model of uniformly moving dislocations is applicable in this case. Despite this, it is feasible that a resonance in the dislocation–lattice interaction exists which may give rise to instabilities. Whether these express

themselves with the same kinematic generation mechanism as observed for tungsten remains the subject for future work. It is interesting to note that the lattice model seems to work best for the motion of screw dislocations in BCC lattices, which is poorly understood compared to the motion of edge and screws in FCC metals [99].

Future work building on the results presented here could address the strong material dependence brought out by the tungsten and aluminium results. The idea presented in this thesis that resonances in the atomic interactions between a gliding dislocation and the lattice give rise to an instability is rather general and may apply to other metals as well. Fundamentally, this instability is caused by a drastic increase in kinetic energy of the particles near the core of a dislocation travelling at a resonant velocity. For tungsten, it was clear that this provided the energetic pathway for the spawning of additional dislocations. However, this localised excess of kinetic energy may result in a host of other phenomena such as localised twinning, point defect creation or homogeneous nucleation to just name a couple. The intricacies involved in distinguishing all these different phenomena are clearly beyond the reach of the lattice dynamics models discussed here.

A more general further investigation would be to study the effect of more realistic dislocation topologies. Here, only straight edge and screw dislocations were studied but it would be instructive to extend this to the dynamics of dislocation loops, effectively increasing the dimensionality of the problem from 2 to 3. From previous theoretical works [119–121], it is known that in

3-dimensional systems dislocations may resonate with the lattice vibrations at particular velocities as well, although the resonances are weaker.

To conclude, let us address what the significance is of all these findings for the formulation of dislocation mobility laws. Firstly, the mere existence of instabilities in the motion of dislocations in real metals, as demonstrated in chapter 5 for tungsten, certainly increases the complexity of the problem. In order to account for them, mobility laws have to be made time dependent as the behaviour of dislocations beyond resonant velocities is dependent on *how* the instability was surpassed. Secondly, the mobility law should allow for the generation of new dislocations to account for the kinematic generation mechanism that may be activated at resonant velocities. Again, this introduces explicit time dependence in the mobility law as the competition between the time the kinematic generation mechanism needs to act and the time spent in the resonant region needs to be accounted for. However, given that we currently do not yet have an overview of all the phenomenological pieces that should go in the puzzle that a high speed dislocation mobility law is, exact quantitative attempts to formulate one may be premature.

Bibliography

[1]J. Nelson, *The physics of solar cells* (Imperial College Press, London, 2003).

[2]A. K. Suri, N. Krishnamurthy, and I. S. Batra, "Materials issues in fusion reactors", J. Phys. Conf. Ser. **208**, 012001 (2010).

[3]K. Dutta and S. De, "Smart responsive materials for water purification: an overview", J. Mater. Chem. A **5**, 22095–22112 (2017).

[4]R. C. Reed, *The Superalloys: Fundamentals and Applications* (Cambridge University Press, Cambridge, 2006).

[5]A. Cottrell, *An Introduction to metallurgy*, red. by Institute of Materials, 2nd edition (Institute of Materials, London, 1995).

[6]J. P. Hirth and J. Lothe, *Theory of dislocations*, Reprint of 2nd edition (Krieger Publishing Company, 1992).

[7]T. Childs, K. Maekawa, T. Obikawa, and Y. Yamane, *Metal machining: theory and applications* (Arnold, 2000).

[8]W. Hosford and R. Caddell, *Metal Forming: Mechanics and Metallurgy* (Cambridge University Press, 2011).

[9]D. Hull and D. J. Bacon, *Introduction to dislocations*, red. by D. J. Bacon, 5th (Elsevier Butterworth Heineman, Amsterdam London, 2011).

[10]G. I. Taylor, "The Mechanism of Plastic Deformation of Crystals. Part I. Theoretical", Proc. R. Soc. Lond. Math. Phys. Eng. Sci. **145**, 362–387 (1934).

[11]E. Orowan, "Zur Kristallplastizität. III", Z. Phys. **89**, 634–659 (1934).

[12]M. Polanyi, "Über eine Art Gitterstörung, die einen Kristall plastisch machen könnte", Z. Phys. **89**, 660–664 (1934).

[13]R. Peierls, "The size of a dislocation", Proc. Phys. Soc. Lond. **52**, 34–37 (1940).

[14]T. D. Swinburne, S. L. Dudarev, S. P. Fitzgerald, M. R. Gilbert, and A. P. Sutton, "Theory and simulation of the diffusion of kinks on dislocations in bcc metals", Phys. Rev. B **87** (2013) 10.1103/PhysRevB.87.064108.

[15]T. D. Swinburne, S. L. Dudarev, and A. P. Sutton, "Classical mobility of highly mobile crystal defects", Phys. Rev. Lett. **113**, 215501 (2014).

[16]F. C. Frank, "On the Equations of Motion of Crystal Dislocations", Proc. Phys. Soc. Sect. A **62**, 131 (1949).

[17]J. D. Eshelby, "Uniformly moving dislocations", Proc. Phys. Soc. Sect. A **62**, 307 (1949).

[18]B. Gurrutxaga-Lerma, "The role of the mobility law of dislocations in the plastic response of shock loaded pure metals", Model. Simul. Mater. Sci. Eng. **24**, 065006 (2016).

[19]R. J. Amodeo and N. M. Ghoniem, "Dislocation dynamics. I. A proposed methodology for deformation micromechanics", Phys. Rev. B **41**, 6958–6967 (1990).

[20]R. Aghababaei, T. Brink, and J.-F. Molinari, "Asperity-Level Origins of Transition from Mild to Severe Wear", Phys. Rev. Lett. **120** (2018) 10.1103/PhysRevLett.120.186105.

[21]B. Dodd and Y. Bai, *Adiabatic Shear Localization: Frontiers and Advances* (Elsevier, 2012).

[22]L. B. Freund, *Dynamic Fracture Mechanics*, Cambridge Monographs on Mechanics (Cambridge University Press, 1990).

[23]V. Rajan and W. Curtin, "Crack tip blunting and cleavage under dynamic conditions", J. Mech. Phys. Solids **90**, 18–28 (2016).

[24]M. A. Meyers, *Dynamic Behavior of Materials* (John Wiley, Hoboken, NJ, 1994).

[25]J. Verschueren, B. Gurrutxaga-Lerma, D. S. Balint, A. P. Sutton, and D. Dini, "Instabilities of High Speed Dislocations", Phys. Rev. Lett. **121** (2018) 10.1103/PhysRevLett.121.145502.

[26]H. Kanzaki, "Point defects in face-centred cubic lattice—I distortion around defects", J. Phys. Chem. Solids **2**, 24–36 (1957).

[27]H. Kanzaki, "Point defects in face-centred cubic lattice-II X-ray scattering effects", J. Phys. Chem. Solids **2**, 107–114 (1957).

[28]A. J. Rosakis, "Cracks Faster than the Shear Wave Speed", Science **284**, 1337–1340 (1999).

[29]E. Faran and D. Shilo, "Twin motion faster than the speed of sound", Phys. Rev. Lett. **104**, 155501 (2010).

[30]V. Nosenko, S. Zhdanov, and G. Morfill, "Supersonic Dislocations Observed in a Plasma Crystal", Phys. Rev. Lett. **99** (2007) 10.1103/PhysRevLett.99.025002.

[31]W. G. Johnston and J. J. Gilman, "Dislocation Velocities, Dislocation Densities, and Plastic Flow in Lithium Fluoride Crystals", J. Appl. Phys. **30**, 129 (1959).

[32]D. F. Stein and J. R. Low, "Mobility of Edge Dislocations in Silicon-Iron Crystals", J. Appl. Phys. **31**, 362 (1960).

[33]W. F. Greenman, T. Vreeland, and D. S. Wood, "Dislocation Mobility in Copper", J. Appl. Phys. **38**, 3595–3603 (1967).

[34]D. P. Pope, T. Vreeland, and D. S. Wood, "Mobility of Edge Dislocations in the Basal-Slip System of Zinc", J. Appl. Phys. **38**, 4011–4018 (1967).

[35]J. A. Gorman, D. S. Wood, and T. Vreeland, "Mobility of Dislocations in Aluminum", J. Appl. Phys. **40**, 833–841 (1969).

[36]M. Kleintges, R. Labusch, H. G. Brion, and P. Haasen, "Measurement of dislocation velocities in Cu-Al single crystals—I", Acta Metall. **25**, 1247–1255 (1977).

[37]H. Ney, R. Labusch, and P. Haasen, "Measurement of dislocation velocities in Cu-Al single crystals—II", Acta Metall. **25**, 1257–1269 (1977).

[38]T. Mura, *Micromechanics of defects in solids*, 2nd, rev. ed., Mechanics of elastic and inelastic solids (Kluwer Academic Publishers/Martinus Nijhoff, Dordrecht, 1991).

[39]V. Volterra, "Sur l'équilibre des corps élastiques multiplement connexes", Ann. Sci. Éc. Norm. Supér. **24**, 401–517 (1907).

[40]M. Weingarten, "Sulle superficie di disontinuità nella teoria della elasticità dei corpi solidi", 5th ser. **10**, 57 (1901).

[41]J. Frenkel, "Zur Theorie der Elastizitätsgrenze und der Festigkeit kristallinischer Körper", Z. Phys. **37**, 572–609 (1926).

[42]J. M. Burgers, "Some considerations on the fields of stress connected with dislocations in a regular crystal lattice. I", Proc. Kon. Ned. Akad. Wetenschap. **42**, 293–325 (1939).

[43]J. M. Burgers, "Some considerations on the fields of stress connected with dislocations in a regular crystal lattice. II", Proc. Kon. Ned. Akad. Wetenschap. **42**, 378–399 (1939).

[44]P. Gumbsch and H. Gao, "Dislocations Faster than the Speed of Sound", Science **283**, 965–968 (1999).

[45]E. Oren, E. Yahel, and G. Makov, "Dislocation kinematics: a molecular dynamics study in Cu", Model. Simul. Mater. Sci. Eng. **25**, 025002 (2017).

[46]H. Gao, Y. Huang, P. Gumbsch, and A. J. Rosakis, "On radiation-free transonic motion of cracks and dislocations", J. Mech. Phys. Solids **47**, 1941–1961 (1999).

[47]X. Markenscoff, "On "radiation-free" states in transient motion of dislocations", Appl. Phys. Lett. **78**, 440 (2001).

[48]A. Einstein, "Zur Elektrodynamik bewegter Körper", Ann. Phys. **322**, 891–921 (1905).

[49]J. D. Eshelby, "The Equation of Motion of a Dislocation", Phys. Rev. **90**, 248–255 (1953).

[50]J. Weertman and J. Weertman, *Dislocations in solids / Vol.3, Moving dislocations*, red. by F. R. N. Nabarro (North-Holland Publishing Co, Amsterdam Oxford New York, 1980).

[51]J. P. Hirth, H. M. Zbib, and J. Lothe, "Forces on high velocity dislocations", Model. Simul. Mater. Sci. Eng. **6**, 165 (1998).

[52]J. D. Jackson, *Classical electrodynamics*, 3rd edition (Wiley, New York, 1999).

[53]L. C. Evans, *Partial differential equations*, 2nd edition (American Mathematical Society, Providence, R.I., 2010).

[54]J. E. Marsden, T. J. R. Hughes, and D. E. Carlson, "Mathematical Foundations of Elasticity", J. Appl. Mech. **51**, 946 (1984).

[55]B. Gurrutxaga-Lerma and J. Verschueren, "Elastic models of dislocations based on atomistic Kanzaki forces", Phys. Rev. B **98** (2018) 10.1103/PhysRevB.98.134104.

[56]M. Lazar, G. A. Maugin, and E. C. Aifantis, "Dislocations in second strain gradient elasticity", Int. J. Solids Struct. **43**, 1787–1817 (2006).

[57]F. C. Frank, "On slip bands as a consequence of the dynamic behaviour of dislocations", in *Report of the Conference on Strength of Solids* (Physical Society, London, 1948), p. 46.

[58]B. Gurrutxaga-Lerma, D. S. Balint, D. Dini, D. E. Eakins, and A. P. Sutton, "The Role of Homogeneous Nucleation in Planar Dynamic Discrete Dislocation Plasticity", J. Appl. Mech. **82**, 071008 (2015).

[59]D. Milathianaki, S. Boutet, G. J. Williams, A. Higginbotham, D. Ratner, A. E. Gleason, M. Messerschmidt, M. M. Seibert, D. C. Swift, P. Hering, J. Robinson, W. E. White, and J. S. Wark, "Femtosecond Visualization of Lattice Dynamics in Shock-Compressed Matter", Science **342**, 220–223 (2013).

[60]E. N. Hahn, S. Zhao, E. M. Bringa, and M. A. Meyers, "Supersonic Dislocation Bursts in Silicon", Sci. Rep. **6** (2016) 10.1038/srep26977.

[61]J. A. Y. Young Vandersall and B. D. Wirth, "Supersonic dislocation stability and nano-twin formation at high strain rate", Philos. Mag. **84**, 3755–3769 (2004).

[62]E. M. Bringa, K. Rosolankova, R. E. Rudd, B. A. Remington, J. S. Wark, M. Duchaineau, D. H. Kalantar, J. Hawreliak, and J. Belak, "Shock deformation of face-centred-cubic metals on subnanosecond timescales", Nat. Mater. **5**, 805–809 (2006).

[63]M. A. Shehadeh, E. M. Bringa, H. M. Zbib, J. M. McNaney, and B. A. Remington, "Simulation of shock-induced plasticity including homogeneous and heterogeneous dislocation nucleations", Appl. Phys. Lett. **89**, 171918 (2006).

[64]J. D. Achenbach, *Wave propagation in elastic solids* (North-Holland, Amsterdam London, 1973).

[65]J. Weertman, "Possibility of the Existence of Attractive Forces Between Dislocations of Like Sign", Phys. Rev. **119**, 1871–1872 (1960).

[66]J. Weertman, "Fast Moving Edge Dislocations on the (111) Plane in Anisotropic Face-Centered-Cubic Crystals", J. Appl. Phys. **33**, 1631–1635 (1962).

[67]A. Van Hull and J. Weertman, "Fast Moving Edge Dislocations in Various Face-Centered-Cubic Metals", J. Appl. Phys. **33**, 1636–1637 (1962).

[68]J. Weertman, "Coalescence Energy of Two Moving Dislocations of Like Sign", J. Appl. Phys. **37**, 4925–4927 (1966).

[69]B. Gurrutxaga-Lerma, D. S. Balint, D. Dini, and A. P. Sutton, "Elastodynamic image forces on dislocations", Proc. R. Soc. Lond. Math. Phys. Eng. Sci. **471**, 20150433 (2015).

[70]J. D. Eshelby, "Supersonic dislocations and dislocations in dispersive media", Proc. Phys. Soc. Sect. B **69**, 1013 (1956).

[71]F. R. N. Nabarro, "Dislocations in a simple cubic lattice", Proc. Phys. Soc. Lond. **59**, 256–272 (1947).

[72]J. Weertman, "Uniformly Moving Transonic and Supersonic Dislocations", J. Appl. Phys. **38**, 5293 (1967).

[73]D. N. Blaschke, E. Mottola, and D. L. Preston, "On the velocity dependence of the dislocation drag coefficient from phonon wind", Tech. Rep. LA-UR-16-24559, Los Alamos Natl. Lab. (2018) `http://www.osti.gov/servlets/purl/1434423/`.

[74]D. N. Blaschke, "Velocity dependent dislocation drag from phonon wind and crystal geometry", J. Phys. Chem. Solids **124**, 24–35 (2019).

[75]J. Weertman, "Dislocations in uniform motion on slip or climb planes having periodic force laws", Math. Theory Dislocations, edited by T. Mura, 178–202 (1969).

[76]P. Rosakis, "Supersonic Dislocation Kinetics from an Augmented Peierls Model", Phys. Rev. Lett. **86**, 95–98 (2001).

[77]L. B. Freund, "Wave motion in an elastic solid due to a nonuniformly moving line load", Q. Appl. Math. **30**, 271–281 (1972).

[78]L. B. Freund, "The Response of an Elastic Solid to Nonuniformly Moving Surface Loads", J. Appl. Mech. **40**, 699–704 (1973).

[79]X. Markenscoff, "The transient motion of a nonuniformly moving dislocation", J. Elast. **10**, 193–201 (1980).

[80]X. Markenscoff and R. J. Clifton, "The nonuniformly moving edge dislocation", J. Mech. Phys. Solids **29**, 253–262 (1981).

[81]R. Clifton and X. Markenscoff, "Elastic precursor decay and radiation from nonuniformly moving dislocations", J. Mech. Phys. Solids **29**, 227–251 (1981).

[82]X. Markenscoff and L. Ni, "The transient motion of a dislocation with a ramp-like core", J. Mech. Phys. Solids **49**, 1603–1619 (2001).

[83]X. Markenscoff and S. Huang, "Analysis for a screw dislocation accelerating through the shear-wave speed barrier", J. Mech. Phys. Solids **56**, 2225–2239 (2008).

[84]S. Huang and X. Markenscoff, "Is Intersonic Dislocation Motion Possible? Singularity Analysis for an Edge Dislocation Accelerating through the Shear Wave Speed Barrier", Exp. Mech. **49**, 219–224 (2009).

[85]M. Lazar, "The gauge theory of dislocations: a uniformly moving screw dislocation", Proc. R. Soc. Math. Phys. Eng. Sci. **465**, 2505–2520 (2009).

[86]Y.-P. Pellegrini, "Dynamic Peierls-Nabarro equations for elastically isotropic crystals", Phys. Rev. B **81** (2010) `10.1103/PhysRevB.81.024101`.

[87]X. Markenscoff, "Comment on "Dynamic Peierls-Nabarro equations for elastically isotropic crystals"", Phys. Rev. B **83** (2011) `10.1103/PhysRevB.83.056101`.

[88]Y.-P. Pellegrini, "Reply to "Comment on 'Dynamic Peierls-Nabarro equations for elastically isotropic crystals' "", Phys. Rev. B **83** (2011) 10.1103/PhysRevB.83.056102.

[89]Y.-P. Pellegrini, "Screw and edge dislocations with time-dependent core width: From dynamical core equations to an equation of motion", J. Mech. Phys. Solids **60**, 227–249 (2012).

[90]Y.-P. Pellegrini, "Equation of motion and subsonic-transonic transitions of rectilinear edge dislocations: A collective-variable approach", Phys. Rev. B **90** (2014) 10.1103/PhysRevB.90.054120.

[91]L. Pillon, C. Denoual, and Y.-P. Pellegrini, "Equation of motion for dislocations with inertial effects", Phys. Rev. B **76** (2007) 10.1103/PhysRevB.76.224105.

[92]Y.-P. Pellegrini and M. Lazar, "On the gradient of the Green tensor in two-dimensional elastodynamic problems, and related integrals: Distributional approach and regularization, with application to nonuniformly moving sources", Wave Motion **57**, 44–63 (2015).

[93]Y.-P. Pellegrini, "Uniformly-moving non-singular dislocations with ellipsoidal core shape in anisotropic media", (2018) arXiv:1808.10272.

[94]A. W. Sáenz, "Uniformly Moving Dislocations in Anisotropic Media", J. Ration. Mech. Anal. **2**, 83–98 (1953).

[95]R. Bullough and B. A. Bilby, "Uniformly moving dislocations in anisotropic media", Proc. Phys. Soc. B **67**, 615 (1954).

[96]A. N. Stroh, "Steady State Problems in Anisotropic Elasticity", J. Math. Phys. **41**, 77–103 (1962).

[97]L. J. Teutonico, "Uniformly Moving Dislocations of Arbitrary Orientation in Anisotropic Media", Phys. Rev. **127**, 413–418 (1962).

[98]V. V. Bulatov and W. Cai, *Computer simulations of dislocations*, red. by W. Cai (Oxford University Press, Oxford, 2006).

[99]W. Cai and V. V. Bulatov, "Mobility laws in dislocation dynamics simulations", Mater. Sci. Eng. A **387-389**, 277–281 (2004).

[100]J. Verschueren, B. Gurrutxaga-Lerma, D. Balint, D. Dini, and A. Sutton, "The injection of a screw dislocation into a crystal: Atomistics vs. continuum elastodynamics", J. Mech. Phys. Solids **98**, 366–389 (2017).

[101]P. P. Gillis, J. J. Gilman, and J. W. Taylor, "Stress dependences of dislocation velocities", Philos. Mag. **20**, 279–289 (1969).

[102]P. P. Gillis and J. Kratochvil, "Dislocation acceleration", Philos. Mag. J. Theor. Exp. Appl. Phys. **21**, 425–432 (1970).

[103]V. K. Tewary, "Green-function method for lattice statics", Adv. Phys. **22**, 757–810 (1973).

[104]N. W. Ashcroft, *Solid state physics*, red. by N. D. Mermin (Saunders College, Philadelphia, 1977).

[105]A. A. Maradudin, "Some effects of point defects on the vibrations of crystal lattices", Rep. Prog. Phys. **28**, 331–380 (1965).

[106]A. A. Maradudin, "Screw dislocations and discrete elastic theory", J. Phys. Chem. Solids **9**, 1–20 (1959).

[107]L. L. Boyer and J. R. Hardy, "Lattice statics applied to screw dislocations in cubic metals", Philos. Mag. **24**, 647–671 (1971).

[108]W. Atkinson and N. Cabrera, "Motion of a Frenkel—Kontorowa Dislocation in a One-Dimensional Crystal", Phys. Rev. **138**, A763–A766 (1965).

[109]V. Celli and N. Flytzanis, "Motion of a Screw Dislocation in a Crystal", J. Appl. Phys. **41**, 4443 (1970).

[110]S. Ishioka, "Uniform Motion of a Screw Dislocation in a Lattice", J. Phys. Soc. Jpn. **30**, 323–327 (1971).

[111]V. Celli, N. Flytzanis, and S. Crowley, "Analysis of the displacement field of a moving dislocation in a crystal", J. Phys. Chem. Solids **37**, 1125–1133 (1976).

[112]N. E. Glass, "A lattice-dynamics model of an oscillating screw dislocation", J. Phys. **44**, 741–753 (1983).

[113]J. A. Caro and N. Glass, "A lattice-dynamics model of the interaction of a dislocation with point defects", J. Phys. **45**, 1337–1345 (1984).

[114]J. Frenkel and T. Kontorova, "On the theory of plastic deformation and twinning", Ph. Z. Sowjetunion **13**, 1–10 (1938).

[115]S. Crowley, N. Flytzanis, and V. Celli, "Dislocation-phonon interaction", J. Phys. Chem. Solids **41**, 63–67 (1980).

[116]S. Ramos de Debiaggi and A. Caro, "Phonons radiated by moving dislocations in disordered alloys", J. Phys. **48**, 1499–1504 (1987).

[117]N. Flytzanis and V. Celli, "Motion of a screw dislocation in a crystal at finite temperature", J. Appl. Phys. **43**, 3301 (1972).

[118]T. D. Swinburne and S. L. Dudarev, "Phonon drag force acting on a mobile crystal defect: Full treatment of discreteness and nonlinearity", Phys. Rev. B **92** (2015) 10.1103/PhysRevB.92.134302.

[119]D. Rogula, "Influence of spatial acoustic dispersion on dynamical properties of dislocations. I.", Bull. Acad. Pol. Sci., Sér. sci. techn. **13**, 337 (1965).

[120]D. Rogula, "Influence of spatial acoustic dispersion on the dynamic properties of dislocations. II", Bull. Acad. Pol. Sci., Sér. sci. techn. **14**, 159 (1966).

[121]D. Rogula, "Kinematic resonances in periodic structures", Proc. Vibr. Probl. (Warsaw) **3**, 215 (1967).

[122]V. A. Al'shitz and V. L. Indenbom, "Dynamic dragging of dislocations", Sov. Phys. Usp. **18**, 21 (1975).

[123]S. Ishioka, "Steady Motion of a Dislocation in a Lattice", J. Phys. Soc. Jpn. **34**, 462–469 (1973).

[124]H. Koizumi, H. O. K. Kirchner, and T. Suzuki, "Lattice wave emission from a moving dislocation", Phys. Rev. B **65** (2002) 10.1103/PhysRevB.65.214104.

[125]N. Flytzanis, S. Crowley, and V. Celli, "High velocity dislocation motion and interatomic force law", J. Phys. Chem. Solids **38**, 539–552 (1977).

[126]Y. Y. Earmme and J. H. Weiner, "Can Dislocations be Accelerated through the Sonic Barrier?", Phys. Rev. Lett. **31**, 1055–1057 (1973).

[127]Y. Y. Earmme and J. H. Weiner, "Breakdown phenomena in high-speed dislocations", J. Appl. Phys. **45**, 603–609 (1974).

[128]S. Ishioka, "Stress field around a high speed screw dislocation", J. Phys. Chem. Solids **36**, 427–430 (1975).

[129]J. H. Weiner and M. Pear, "Breakdown in high-speed edge dislocation motion", Philos. Mag. **31**, 679–688 (1975).

[130]D. Frenkel and B. Smit, *Understanding molecular simulation : from algorithms to applications*, 2nd (Academic Press, San Diego London, 2002).

[131]J. A. Moriarty, V. Vitek, V. V. Bulatov, and S. Yip, "Atomistic Simulations of Dislocations and Defects", J. Comput.-Aided Mater. Des. **9**, 99–132 (2002).

[132]V. Vitek, "Core structure of screw dislocations in body-centred cubic metals: relation to symmetry and interatomic bonding", Philos. Mag. **84**, 415–428 (2004).

[133]M. S. Daw and M. I. Baskes, "Semiempirical, Quantum Mechanical Calculation of Hydrogen Embrittlement in Metals", Phys. Rev. Lett. **50**, 1285–1288 (1983).

[134]M. W. Finnis and J. E. Sinclair, "A simple empirical N-body potential for transition metals", Philos. Mag. A **50**, 45–55 (1984).

[135]G. J. Ackland and R. Thetford, "An improved N-body semi-empirical model for body-centred cubic transition metals", Philos. Mag. A **56**, 15–30 (1987).

[136]Y. Mishin, D. Farkas, M. J. Mehl, and D. A. Papaconstantopoulos, "Interatomic potentials for monoatomic metals from experimental data and ab initio calculations", Phys. Rev. B **59**, 3393 (1999).

[137]Q. Li and S.-Q. Shi, "Dislocation jumping over the sound barrier in tungsten", Appl. Phys. Lett. **80**, 3069 (2002).

[138]D. Mordehai, Y. Ashkenazy, I. Kelson, and G. Makov, "Dynamic properties of screw dislocations in Cu: A molecular dynamics study", Phys. Rev. B **67** (2003) 10.1103/PhysRevB.67.024112.

[139]A. Carpio and L. L. Bonilla, "Discrete models of dislocations and their motion in cubic crystals", Phys. Rev. B **71** (2005) 10.1103/PhysRevB.71.134105.

[140]J. Marian and A. Caro, "Moving dislocations in disordered alloys: Connecting continuum and discrete models with atomistic simulations", Phys. Rev. B **74** (2006) 10.1103/PhysRevB.74.024113.

[141]D. Mordehai, I. Kelson, and G. Makov, "Nonplanar core and dynamical behavior of screw dislocations in copper at high velocities", Phys. Rev. B **74** (2006) 10.1103/PhysRevB.74.184115.

[142]Z. Jin, H. Gao, and P. Gumbsch, "Energy radiation and limiting speeds of fast moving edge dislocations in tungsten", Phys. Rev. B **77** (2008) 10.1103/PhysRevB.77.094303.

[143]H. Tsuzuki, P. S. Branicio, and J. P. Rino, "Accelerating dislocations to transonic and supersonic speeds in anisotropic metals", Appl. Phys. Lett. **92**, 191909 (2008).

[144]Z. Q. Wang and I. J. Beyerlein, "Stress orientation and relativistic effects on the separation of moving screw dislocations", Phys. Rev. B **77** (2008) 10.1103/PhysRevB.77.184112.

[145]G. Monnet and D. Terentyev, "Structure and mobility of the 1/2<111>{112} edge dislocation in BCC iron studied by molecular dynamics", Acta Mater. **57**, 1416–1426 (2009).

[146]H. Tsuzuki, P. S. Branicio, and J. P. Rino, "Molecular dynamics simulation of fast dislocations in copper", Acta Mater. **57**, 1843–1855 (2009).

[147]S. Queyreau, J. Marian, M. R. Gilbert, and B. D. Wirth, "Edge dislocation mobilities in bcc Fe obtained by molecular dynamics", Phys. Rev. B **84** (2011) 10.1103/PhysRevB.84.064106.

[148]C. J. Ruestes, E. M. Bringa, R. E. Rudd, B. A. Remington, T. P. Remington, and M. A. Meyers, "Probing the character of ultra-fast dislocations", Sci. Rep. **5**, 16892 (2015).

[149]J. Cho, J.-F. Molinari, and G. Anciaux, "Mobility law of dislocations with several character angles and temperatures in FCC aluminum", Int. J. Plast. **90**, 66–75 (2017).

[150]D. L. Olmsted, L. G. Hector Jr, W. A. Curtin, and R. J. Clifton, "Atomistic simulations of dislocation mobility in Al, Ni and Al/Mg alloys", Model. Simul. Mater. Sci. Eng. **13**, 371–388 (2005).

[151]H. Koizumi and H. O. K. Kirchner, "Energy flow around a moving dislocation", IOP Conf. Ser. Mater. Sci. Eng. **3**, 012028 (2009).

[152]J. Schiøtz, K. W. Jacobsen, and O. H. Nielsen, "Kinematic generation of dislocations", Philos. Mag. Lett. **72**, 245–250 (1995).

[153]L. A. Zepeda-Ruiz, A. Stukowski, T. Oppelstrup, and V. V. Bulatov, "Probing the limits of metal plasticity with molecular dynamics simulations", Nature **550**, 492–495 (2017).

[154]X.-Y. Liu, F. Ercolessi, and J. B. Adams, "Aluminium interatomic potential from density functional theory calculations with improved stacking fault energy", Model. Simul. Mater. Sci. Eng. **12**, 665–670 (2004).

[155]M.-C. Marinica, L. Ventelon, M. R. Gilbert, L. Proville, S. L. Dudarev, J. Marian, G. Bencteux, and F. Willaime, "Interatomic potentials for modelling radiation defects and dislocations in tungsten", J. Phys. Condens. Matter **25**, 395502 (2013).

[156]E. N. Economou, *Green's functions in quantum physics*, 3rd (Springer, Berlin, 2006).

[157]C. J. Isham, *Lectures on quantum theory : mathematical and structural foundations* (Imperial College Press, London, 1995).

[158]R. Burridge and L. Knopoff, "Body force equivalents for seismic dislocations", Bull. Seismol. Soc. Am. **54**, 1875–1888 (1964).

[159]J. D. Eshelby, "The Determination of the Elastic Field of an Ellipsoidal Inclusion, and Related Problems", Proc. R. Soc. Math. Phys. Eng. Sci. **241**, 376–396 (1957).

[160]A. I. Markushevich, *Theory of functions of a complex variable*, Vol. I (American Mathematical Soc., Providence, RI, 2005).

[161]G. J. Ackland, M. C. Warren, and S. J. Clark, "Practical methods in *ab initio* lattice dynamics", J. Phys. Condens. Matter **9**, 7861–7872 (1997).

[162]S. Baroni, S. de Gironcoli, A. Dal Corso, and P. Giannozzi, "Phonons and related crystal properties from density-functional perturbation theory", Rev. Mod. Phys. **73**, 515–562 (2001).

[163]E. Hayward, C. Deo, B. P. Uberuaga, and C. N. Tomé, "The interaction of a screw dislocation with point defects in bcc iron", Philos. Mag. **92**, 2759–2778 (2012).

[164]S. Plimpton, "Fast Parallel Algorithms for Short Range Molecular Dynamics", J. Comp. Phys. **117**, 42 (1995).

[165]A. Stukowski, V. V. Bulatov, and A. Arsenlis, "Automated identification and indexing of dislocations in crystal interfaces", Model. Simul. Mater. Sci. Eng. **20**, 085007 (2012).

[166]A. Stukowski, "Visualization and analysis of atomistic simulation data with OVITO–the Open Visualization Tool", Model. Simul. Mater. Sci. Eng. **18**, 015012 (2010).

[167]P. Hirel, "Atomsk: A tool for manipulating and converting atomic data files", Comput. Phys. Commun. **197**, 212–219 (2015).

[168]M. R. Gilbert, S. Queyreau, and J. Marian, "Stress and temperature dependence of screw dislocation mobility in α -Fe by molecular dynamics", Phys. Rev. B **84** (2011) 10.1103/PhysRevB.84.174103.

[169]R. Armstrong and W. Elban, "Temperature rise at a dislocation pile-up breakthrough", Mater. Sci. Eng. A **122**, L1–L3 (1989).

[170]E. Orowan, "Problems of plastic gliding", Proc. Phys. Soc. **52**, 8 (1940).

[171]R. A. Austin and D. L. McDowell, "A dislocation-based constitutive model for viscoplastic deformation of fcc metals at very high strain rates", Int. J. Plast. **27**, 1–24 (2011).

[172]Z. Zhang, D. E. Eakins, and F. P. Dunne, "On the formation of adiabatic shear bands in textured HCP polycrystals", Int. J. Plast. **79**, 196–216 (2016).

List of Figures

2.1 Schematic representation in three steps of the kinematic generation of edge dislocations as accounted for by continuum works [6]. The coloured arrows represent the forces the dislocations exert on one another where the directions are key and magnitudes approximate. The vectors labelled F_A represent the forces on B and C due to A, and similarly for F_B and F_C. Step 1 shows an edge dislocation A travelling with a speed above the Rayleigh wave speed of the material which may generate two nascent edge dislocations of opposite sign (B and C), shown in step 2. From the mutual interactions between the dislocations represented in stage 2, it can be seen that this results in the final configuration consisting of a single dislocation and a bound dislocation pair travelling in opposite directions. 28

2.2 Comparison of various inertial terms in mobility laws with a Rosakis [76] (a and b) or Taylor [101, 102] (c and d) drag force for an edge dislocation accelerating from rest in aluminium. 1 ps (a and c) later, the difference in mobility due to the differnt intertial terms can still be distinguished but at 10 ps (b and d) the dislocation's mobility is completely dominated by its drag component. *Reproduced with permission (CC3.0) from [18].* . . . 40

2.3 Dislocation mobility law derived for uniformly moving screw dislocation in a simple cubic lattice dynamics model with nearest neighbour interactions. *Reproduced with permission, (c) (1971) The Physical Society of Japan* [110]. 42

2.4 Observed average dislocation velocity for edge dislocations in MD simulations of tungsten [134, 135]. Solid circles indicate stable dislocation motion whereas open circles mark the average velocities at which the observed motion was unstable varied significantly throughout the simulation. *From [44]. Reprinted with permission from AAAS.* 47

3.1 Schematic representing a uniformly moving screw dislocation propagating in a simple cubic lattice with velocity v_d. *Reproduced with permission (CC4.0) from [25].* 66

4.1 Magnitude of the F_z Kanzaki forces across the cut surface for a $1/2\langle 1\,1\,1\rangle$ screw dislocation in BCC tungsten [155]. Note that the Kanzaki forces are the fictional forces that generate the required displacement discontinuity across the glide plane in an harmonic lattice. They should not be mistaken for the physical forces between the particles in the real lattice. *Reproduced with permission (CC4.0) from [55].* 78

5.1 The quartic interaction potential U^q from Eqn.(5.2) as used in the square lattice MD simulation. It is compared to the harmonic potential U^h assumed in lattice dynamics models (cf. Eqn.(5.1)) and the cosinusoidal potential $U^c \propto 1-\cos(2\pi u/a)$ used in [124]. Note that all potentials assume periodic boundary conditions $U(x) = U(x+n)$ for $n \in \mathbb{N}$. Furthermore, the interaction constant K was scaled such that the theoretical shear strengths of all potentials are equal. 82

5.2 The relative displacement jump caused by a uniformly moving screw dislocation with velocity v_d in the simple cubic model as computed from Eqn.(3.54). Note the resonance for $v_d = 0.3c_t$. *Reproduced with permission (CC4.0) from [25].* 83

5.3 $\Delta u_z(t)$ on the glide plane as observed in the MD with quartic interaction potential U^q at different times expressed in units of $\sqrt{M/K}$. A single dislocations is injected at $x = 50a$ at $t = 0$ and travels to the right. The first kinematic generation event is shown in a), followed by the second event in b). Their associated dislocation reactions are shown in the top insets where circles and rectangles represent screw dislocations of opposite handedness and the above them indicate the directions of travel. *Reproduced with permission (CC4.0) from [25].* 85

5.4 Observed $\Delta u_z(t)$ derived from Eqn.(3.54) for a screw dislocation with $\boldsymbol{B} = (0, 0, B)$ and $\boldsymbol{v_d} = (v_d, 0, 0)$ in BCC tungsten [155] with Cartesian axes aligned with the $[\bar{1}\,0\,1]$, $[1\,\bar{2}\,1]$ and $[1\,1\,1]$ crystal directions respectively. 89

5.5 Same plot as Fig.(5.4), the only difference being that the Cartesian axes are now aligned with the $[\bar{1}\,2\,\bar{1}]$, $[\bar{1}\,0\,1]$ and $[1\,1\,1]$ crystal directions respectively. The dependence of $\Delta u_z(t)$ on crystal orientation is particularly evident upon comparison of Figs.(5.4a) and (5.5a). 90

5.6 Observed $\Delta u_x(t)$ derived from Eqn.(3.54) for an edge dislocation with $\boldsymbol{B} = (B, 0, 0)$ and $\boldsymbol{v_d} = (v_d, 0, 0)$ in BCC tungsten [155] with Cartesian axes aligned with the $[1\,1\,1]$, $[\bar{1}\,0\,1]$ and $[1\,\bar{2}\,1]$ crystal directions respectively. 92

5.7 Same plot as Fig.(5.6), the only difference being that the Cartesian axes are now aligned with the $[1\,1\,1]$, $[\bar{1}\,2\,\bar{1}]$ and $[\bar{1}\,0\,1]$ crystal directions respectively. Again, the dependence of $\Delta u_x(t)$ on crystal orientation is particularly evident upon comparison of Figs.(5.6a) and (5.7a). 93

5.8 Snaphsot of the kinematic generation dissociation process observable in MD simulations of BCC W at 125K. The dislocation positions were found using the DXA algorithm [165] as implemented in Ovito [166]. White shaded particles indicate regions of considerable disregistry. Figure produced by BGL. *Reproduced with permission (CC4.0) from [25].* 94

5.9 Observed $\Delta u_z(t)$ derived from Eqn.(3.54) for a screw dislocation with $\boldsymbol{B} = (0, 0, B)$ and $\boldsymbol{v_d} = (v_d, 0, 0)$ in FCC aluminium [154] with Cartesian axes aligned with the $[1\,\bar{2}\,1]$, $[1\,1\,1]$ and $[\bar{1}\,0\,1]$ crystal directions respectively. 97

5.10 Observed $\Delta u_x(t)$ derived from Eqn.(3.54) for an edge dislocation with $\boldsymbol{B} = (B, 0, 0)$ and $\boldsymbol{v_d} = (v_d, 0, 0)$ in FCC aluminium [154] with Cartesian axes aligned with the $[\bar{1}\,0\,1]$, $[1\,\bar{2}\,1]$ and $[1\,1\,1]$ crystal directions respectively. 98

A Publications resulting from this work

- J. Verschueren, B. Gurrutxaga-Lerma, D. S. Balint, D. Dini, and A. P. Sutton, "The injection of a screw dislocation into a crystal: Atomistics vs. continuum elastodynamics", J. Mech. Phys. Solids **98**, 366-389 (2017) 10.1016/j.jmps.2016.10.004

- J. Verschueren, B. Gurrutxaga-Lerma, D. S. Balint, A. P. Sutton, and D. Dini, "Instabilities of High Speed Dislocations", Phys. Rev. Lett. **121** (2018) 10.1103/PhysRevLett.121.145502.

- B. Gurrutxaga-Lerma and J. Verschueren, "Elastic models of dislocationsbased on atomistic Kanzaki forces", Phys. Rev. B **98** (2018) 10.1103/PhysRevB.98.134104

B Copyright permissions

Journal of the Physical Society of Japan (JPSJ)
Permission to Reproduce Figures/Tables

74-049

December 4, 2018

Dear Jonas Verschueren

The Physical Society of Japan gives you permission to reproduce the following material(s) in print and digital version.

Reproduce from:

Title: Uniform Motion of a Screw Dislocation in a Lattice

Authors: Shunya Ishioka

Journal of the Physical Society of Japan

Vol. 30 No. 2 (1971) Page/Article ID pp. 323-327

Material to be used: Figure 4

Reproduce to:

Title: PhD Thesis, Instabilities of high speed dislocations

Publisher: Imperial College London

Month and Year of Publication: Expected February 2019

Hidetoshi Nishimori
hairperson of the Publication Committee of
the Physical Society of Japan

The Physical Society of Japan
5F, 2-31-22 Yushima, Bunkyo-ku, Tokyo 113-0034, JAPAN
TEL +81-3-3816-6206 FAX +81-3-3816-6206 permission@jps.or.jp

THE AMERICAN ASSOCIATION FOR THE ADVANCEMENT OF SCIENCE LICENSE TERMS AND CONDITIONS

Dec 11, 2018

This Agreement between Imperial College London -- Jonas Verschueren ("You") and The American Association for the Advancement of Science ("The American Association for the Advancement of Science") consists of your license details and the terms and conditions provided by The American Association for the Advancement of Science and Copyright Clearance Center.

License Number	4481260394574
License date	Dec 03, 2018
Licensed Content Publisher	The American Association for the Advancement of Science
Licensed Content Publication	Science
Licensed Content Title	Dislocations Faster than the Speed of Sound
Licensed Content Author	Peter Gumbsch,Huajian Gao
Licensed Content Date	Feb 12, 1999
Licensed Content Volume	283
Licensed Content Issue	5404
Volume number	283
Issue number	5404
Type of Use	Thesis / Dissertation
Requestor type	Scientist/individual at a research institution
Format	Print and electronic
Portion	Figure
Number of figures/tables	1
Order reference number	
Title of your thesis / dissertation	Instabilities of high speed dislocations
Expected completion date	Feb 2019
Estimated size(pages)	120
Requestor Location	Imperial College London Exhibition Road London, SW7 2AZ

	United Kingdom Attn: Imperial College London
Billing Type	Invoice
Billing Address	Imperial College London Exhibition Road London, United Kingdom SW7 2AZ Attn: Imperial College London
Total	**0.00 GBP**

Terms and Conditions

American Association for the Advancement of Science TERMS AND CONDITIONS
Regarding your request, we are pleased to grant you non-exclusive, non-transferable permission, to republish the AAAS material identified above in your work identified above, subject to the terms and conditions herein. We must be contacted for permission for any uses other than those specifically identified in your request above.
The following credit line must be printed along with the AAAS material: "From [Full Reference Citation]. Reprinted with permission from AAAS."
All required credit lines and notices must be visible any time a user accesses any part of the AAAS material and must appear on any printed copies and authorized user might make.
This permission does not apply to figures / photos / artwork or any other content or materials included in your work that are credited to non-AAAS sources. If the requested material is sourced to or references non-AAAS sources, you must obtain authorization from that source as well before using that material. You agree to hold harmless and indemnify AAAS against any claims arising from your use of any content in your work that is credited to non-AAAS sources.
If the AAAS material covered by this permission was published in Science during the years 1974 - 1994, you must also obtain permission from the author, who may grant or withhold permission, and who may or may not charge a fee if permission is granted. See original article for author's address. This condition does not apply to news articles.
The AAAS material may not be modified or altered except that figures and tables may be modified with permission from the author. Author permission for any such changes must be secured prior to your use.
Whenever possible, we ask that electronic uses of the AAAS material permitted herein include a hyperlink to the original work on AAAS's website (hyperlink may be embedded in the reference citation).
AAAS material reproduced in your work identified herein must not account for more than 30% of the total contents of that work.
AAAS must publish the full paper prior to use of any text.
AAAS material must not imply any endorsement by the American Association for the Advancement of Science.
This permission is not valid for the use of the AAAS and/or Science logos.
AAAS makes no representations or warranties as to the accuracy of any information contained in the AAAS material covered by this permission, including any warranties of
merchantability or fitness for a particular purpose.
If permission fees for this use are waived, please note that AAAS reserves the right to charge for reproduction of this material in the future.
Permission is not valid unless payment is received within sixty (60) days of the issuance of this permission. If payment is not received within this time period then all rights granted herein shall be revoked and this permission will be considered null and void.
In the event of breach of any of the terms and conditions herein or any of CCC's Billing and Payment terms and conditions, all rights granted herein shall be revoked and this permission will be considered null and void.
AAAS reserves the right to terminate this permission and all rights granted herein at its discretion, for any purpose, at any time. In the event that AAAS elects to terminate this permission, you will have no further right to publish, publicly perform, publicly display, distribute or otherwise use any matter in which the AAAS content had been included, and all fees paid hereunder shall be fully refunded to you. Notification of termination will be sent to the contact information as supplied by you during the request process and termination shall be

immediate upon sending the notice. Neither AAAS nor CCC shall be liable for any costs, expenses, or damages you may incur as a result of the termination of this permission, beyond the refund noted above.
This Permission may not be amended except by written document signed by both parties.
The terms above are applicable to all permissions granted for the use of AAAS material. Below you will find additional conditions that apply to your particular type of use.

FOR A THESIS OR DISSERTATION

If you are using figure(s)/table(s), permission is granted for use in print and electronic versions of your dissertation or thesis. A full text article may be used in print versions only of a dissertation or thesis.
Permission covers the distribution of your dissertation or thesis on demand by ProQuest / UMI, provided the AAAS material covered by this permission remains in situ.
If you are an Original Author on the AAAS article being reproduced, please refer to your License to Publish for rules on reproducing your paper in a dissertation or thesis.

FOR JOURNALS:

Permission covers both print and electronic versions of your journal article, however the AAAS material may not be used in any manner other than within the context of your article.

FOR BOOKS/TEXTBOOKS:

If this license is to reuse figures/tables, then permission is granted for non-exclusive world rights in all languages in both print and electronic formats (electronic formats are defined below).
If this license is to reuse a text excerpt or a full text article, then permission is granted for non-exclusive world rights in English only. You have the option of securing either print or electronic rights or both, but electronic rights are not automatically granted and do garner additional fees. Permission for translations of text excerpts or full text articles into other languages must be obtained separately.
Licenses granted for use of AAAS material in electronic format books/textbooks are valid only in cases where the electronic version is equivalent to or substitutes for the print version of the book/textbook. The AAAS material reproduced as permitted herein must remain in situ and must not be exploited separately (for example, if permission covers the use of a full text article, the article may not be offered for access or for purchase as a stand-alone unit), except in the case of permitted textbook companions as noted below.
You must include the following notice in any electronic versions, either adjacent to the reprinted AAAS material or in the terms and conditions for use of your electronic products: "Readers may view, browse, and/or download material for temporary copying purposes only, provided these uses are for noncommercial personal purposes. Except as provided by law, this material may not be further reproduced, distributed, transmitted, modified, adapted, performed, displayed, published, or sold in whole or in part, without prior written permission from the publisher."
If your book is an academic textbook, permission covers the following companions to your textbook, provided such companions are distributed only in conjunction with your textbook at no additional cost to the user:

- Password-protected website
- Instructor's image CD/DVD and/or PowerPoint resource
- Student CD/DVD

All companions must contain instructions to users that the AAAS material may be used for non-commercial, classroom purposes only. Any other uses require the prior written permission from AAAS.
If your license is for the use of AAAS Figures/Tables, then the electronic rights granted herein permit use of the Licensed Material in any Custom Databases that you distribute the electronic versions of your textbook through, so long as the Licensed Material remains within the context of a chapter of the title identified in your request and cannot be downloaded by a user as an independent image file.
Rights also extend to copies/files of your Work (as described above) that you are required to provide for use by the visually and/or print disabled in compliance with state and federal laws.
This permission only covers a single edition of your work as identified in your request.

FOR NEWSLETTERS:

Permission covers print and/or electronic versions, provided the AAAS material reproduced as permitted herein remains in situ and is not exploited separately (for example, if permission covers the use of a full text article, the article may not be offered for access or for purchase as a stand-alone unit)

FOR ANNUAL REPORTS:

Permission covers print and electronic versions provided the AAAS material reproduced as permitted herein

remains in situ and is not exploited separately (for example, if permission covers the use of a full text article, the article may not be offered for access or for purchase as a stand-alone unit)

FOR PROMOTIONAL/MARKETING USES:

Permission covers the use of AAAS material in promotional or marketing pieces such as information packets, media kits, product slide kits, brochures, or flyers limited to a single print run. The AAAS Material may not be used in any manner which implies endorsement or promotion by the American Association for the Advancement of Science (AAAS) or Science of any product or service. AAAS does not permit the reproduction of its name, logo or text on promotional literature.

If permission to use a full text article is permitted, The Science article covered by this permission must not be altered in any way. No additional printing may be set onto an article copy other than the copyright credit line required above. Any alterations must be approved in advance and in writing by AAAS. This includes, but is not limited to, the placement of sponsorship identifiers, trademarks, logos, rubber stamping or self-adhesive stickers onto the article copies.

Additionally, article copies must be a freestanding part of any information package (i.e. media kit) into which they are inserted. They may not be physically attached to anything, such as an advertising insert, or have anything attached to them, such as a sample product. Article copies must be easily removable from any kits or informational packages in which they are used. The only exception is that article copies may be inserted into three-ring binders.

FOR CORPORATE INTERNAL USE:

The AAAS material covered by this permission may not be altered in any way. No additional printing may be set onto an article copy other than the required credit line. Any alterations must be approved in advance and in writing by AAAS. This includes, but is not limited to the placement of sponsorship identifiers, trademarks, logos, rubber stamping or self-adhesive stickers onto article copies.

If you are making article copies, copies are restricted to the number indicated in your request and must be distributed only to internal employees for internal use.

If you are using AAAS Material in Presentation Slides, the required credit line must be visible on the slide where the AAAS material will be reprinted

If you are using AAAS Material on a CD, DVD, Flash Drive, or the World Wide Web, you must include the following notice in any electronic versions, either adjacent to the reprinted AAAS material or in the terms and conditions for use of your electronic products: "Readers may view, browse, and/or download material for temporary copying purposes only, provided these uses are for noncommercial personal purposes. Except as provided by law, this material may not be further reproduced, distributed, transmitted, modified, adapted, performed, displayed, published, or sold in whole or in part, without prior written permission from the publisher." Access to any such CD, DVD, Flash Drive or Web page must be restricted to your organization's employees only.

FOR CME COURSE and SCIENTIFIC SOCIETY MEETINGS:

Permission is restricted to the particular Course, Seminar, Conference, or Meeting indicated in your request. If this license covers a text excerpt or a Full Text Article, access to the reprinted AAAS material must be restricted to attendees of your event only (if you have been granted electronic rights for use of a full text article on your website, your website must be password protected, or access restricted so that only attendees can access the content on your site).

If you are using AAAS Material on a CD, DVD, Flash Drive, or the World Wide Web, you must include the following notice in any electronic versions, either adjacent to the reprinted AAAS material or in the terms and conditions for use of your electronic products: "Readers may view, browse, and/or download material for temporary copying purposes only, provided these uses are for noncommercial personal purposes. Except as provided by law, this material may not be further reproduced, distributed, transmitted, modified, adapted, performed, displayed, published, or sold in whole or in part, without prior written permission from the publisher."

FOR POLICY REPORTS:

These rights are granted only to non-profit organizations and/or government agencies. Permission covers print and electronic versions of a report, provided the required credit line appears in both versions and provided the AAAS material reproduced as permitted herein remains in situ and is not exploited separately.

FOR CLASSROOM PHOTOCOPIES:

Permission covers distribution in print copy format only. Article copies must be freestanding and not part of a course pack. They may not be physically attached to anything or have anything attached to them.

FOR COURSEPACKS OR COURSE WEBSITES:
These rights cover use of the AAAS material in one class at one institution. Permission is valid only for a single semester after which the AAAS material must be removed from the Electronic Course website, unless new permission is obtained for an additional semester. If the material is to be distributed online, access must be restricted to students and instructors enrolled in that particular course by some means of password or access control.
FOR WEBSITES:
You must include the following notice in any electronic versions, either adjacent to the reprinted AAAS material or in the terms and conditions for use of your electronic products: "Readers may view, browse, and/or download material for temporary copying purposes only, provided these uses are for noncommercial personal purposes. Except as provided by law, this material may not be further reproduced, distributed, transmitted, modified, adapted, performed, displayed, published, or sold in whole or in part, without prior written permission from the publisher."
Permissions for the use of Full Text articles on third party websites are granted on a case by case basis and only in cases where access to the AAAS Material is restricted by some means of password or access control. Alternately, an E-Print may be purchased through our reprints department (brocheleau@rockwaterinc.com).
REGARDING FULL TEXT ARTICLE USE ON THE WORLD WIDE WEB IF YOU ARE AN 'ORIGINAL AUTHOR' OF A SCIENCE PAPER
If you chose "Original Author" as the Requestor Type, you are warranting that you are one of authors listed on the License Agreement as a "Licensed content author" or that you are acting on that author's behalf to use the Licensed content in a new work that one of the authors listed on the License Agreement as a "Licensed content author" has written.
Original Authors may post the 'Accepted Version' of their full text article on their personal or on their University website and not on any other website. The 'Accepted Version' is the version of the paper accepted for publication by AAAS including changes resulting from peer review but prior to AAAS's copy editing and production (in other words not the AAAS published version).
FOR MOVIES / FILM / TELEVISION:
Permission is granted to use, record, film, photograph, and/or tape the AAAS material in connection with your program/film and in any medium your program/film may be shown or heard, including but not limited to broadcast and cable television, radio, print, world wide web, and videocassette.
The required credit line should run in the program/film's end credits.
FOR MUSEUM EXHIBITIONS:
Permission is granted to use the AAAS material as part of a single exhibition for the duration of that exhibit. Permission for use of the material in promotional materials for the exhibit must be cleared separately with AAAS (please contact us at permissions@aaas.org).
FOR TRANSLATIONS:
Translation rights apply only to the language identified in your request summary above.
The following disclaimer must appear with your translation, on the first page of the article, after the credit line: "This translation is not an official translation by AAAS staff, nor is it endorsed by AAAS as accurate. In crucial matters, please refer to the official English-language version originally published by AAAS."
FOR USE ON A COVER:
Permission is granted to use the AAAS material on the cover of a journal issue, newsletter issue, book, textbook, or annual report in print and electronic formats provided the AAAS material reproduced as permitted herein remains in situ and is not exploited separately
By using the AAAS Material identified in your request, you agree to abide by all the terms and conditions herein.
Questions about these terms can be directed to the AAAS Permissions department permissions@aaas.org.
Other Terms and Conditions:
v 2

Questions? customercare@copyright.com or +1-855-239-3415 (toll free in the US) or +1-978-646-2777.